1506
UNIVERSITÀ
DEGLI STUDI
DI URBINO
CARLO BO

DEPARTMENT OF BIOMOLECULAR SCIENCES

PhD Course in Life Sciences, Health and Biotechnology

Biochemical and Pharmacological Sciences and Biotechnology

XXXIII cycle

Fine-tuning of intracellular redox state by pro-glutathione molecules modulates the cellular immune/inflammatory response to infections: *in vivo* and *in vitro* studies

SSD: BIO/13

Supervisor:
Dr. Alessandra Fraternale

PhD student:
Dr. Carolina Zara

ACADEMIC YEAR 2019/2020

GENERAL INTRODUCTION

Redox state

The term "redox state" has been utilized historically to indicate the ratio of the oxidized and reduced form of a specific redox couple [1]. However, cells are complex structures and, for this reason, Shafer and Buettner suggested the use of the term "redox environment". According to their definition, "the redox environment of a linked set of redox couples as found in a biological fluid, organelle, cell, or tissue is the summation of the products of the reduction potential and reducing the capacity of the linked redox couples present" [2]. However, in this work I will refer to "redox state" because it is the most commonly used term.

The functioning of many cellular components may be dependent on the cellular redox state; therefore, it is crucial to maintain correct redox homeostasis [3][4]. This is also important for the proper functioning of the immune system. When an infection occurs (caused by bacteria, or virus), cells respond by activating all of the mechanisms aimed to kill the pathogen, including the production of several reactive oxygen/nitrogen species (ROS/RNS) with the goal to eliminate the non-self. ROS and RNS can affect/modulate the redox-sensitive mechanisms implicated in the immune/inflammatory response, so it is crucial that the redox state is under cellular control; otherwise, a malfunction could lead to many oxidative stress-related diseases [5].

Oxidative stress

The definition of oxidative stress was first formulated by Sies in 1985 [6] as "a disturbance in the prooxidant-antioxidant balance in favor of the former". This disturbance can be caused by the presence of the so-called reactive oxygen species (ROS), which are derived from oxygen, an obligate component of eukaryotic organisms. These species can be present in free-radical form, like the superoxide anion ($O_2^{\cdot-}$) and the hydroxyl radical ($^{\cdot}OH$), or as chemically stable molecules, like hydrogen peroxide (H_2O_2). In addition to ROS, other molecules that have an impact on oxidative stress are reactive nitrogen species (RNS). The RNS system includes different compounds like peroxynitrite ($ONOO^-$) and the free-radical nitric oxide ($NO^{\cdot}$) [6]. Giles et al. proposed an additional group of redox-active molecules termed reactive sulfur species (RSS), which "are redox-active sulfur compounds formed under conditions of oxidative stress that may be capable of initiating oxidation reactions" [7]. However, these species are synthesized also under non-oxidative conditions. RSS comprehend different forms of cysteine and methionine, and some low-molecular-mass compounds such as glutathione, thioredoxin, or mycothiol [8]. Although all these molecules have been historically considered harmful agents for cells at high concentrations, recent evidence showed that at moderate/low concentrations they can function as secondary signaling molecules [9], bringing to the updated concept of oxidative stress as "an imbalance between oxidants and antioxidants in favor of the oxidants, leading to a disruption of redox signaling and control and/or molecular damage" [6].

ROS/RNS production

The generation of reactive oxygen and nitrogen species (ROS, and RNS) in the cells is due to both endogenous and exogenous sources. The main ROS source is mitochondria, where adenosine triphosphate (ATP) is generated. Its generation depends on the electron transport chain (ETC), which needs O_2; part of this

molecular oxygen is incompletely metabolized and converted into O_2^- by complex I and III of the ETC [10]. The enzyme NADPH oxidase (NOX), which catalyzes the transport of one electron to oxygen from cytosolic NADPH, is another important ROS source. Of the seven isoforms of NOX, NOX4 is the only known form to produce H_2O_2 instead of O_2^- [11]. Another important cellular organelle that generates ROS is the endoplasmic reticulum (ER). One of the ER's main roles is to promote correct protein folding by forming disulfide bonds, which is ensured by the maintaining of an oxidized environment [12]. Other ROS sources can be microsomes and peroxisomes, which primarily generate H_2O_2, cytochrome c oxidase, and xanthine oxidase [13]. The production of these reactive species is one of the major mechanisms to fight and kill pathogens by cells of the immune system, such as neutrophils and macrophages. The RNS $NO^{\cdot}$ is synthesized from L-arginine in the presence of molecular oxygen through a reaction catalyzed by the nitric oxide synthase (NOS) [14]. There are several known isoforms of this enzyme, such as the neuronal NOS (nNOS), endothelial NOS (eNOS), and the inducible NOS (iNOS) that can be induced by pro-inflammatory cytokines [15]. Nitric oxide can react with O_2^- to generate $ONOO^-$ [16]. Exogenous sources of ROS and RNS are irradiation (e.g. UV irradiation, γ irradiation), drugs, and atmospheric pollutants [17].

Oxidative damage

ROS and RNS have been historically considered harmful agents for cells because they can react with important cellular structures, like lipids, proteins, and DNA. These modifications could cause damages to these structures, leading to their dysfunction and oxidative stress-related diseases, such as inflammation, neurodegenerative diseases, and cancers [5].

High concentrations of ROS/RNS can lead to lipid oxidation, which causes lipid peroxidation and oxysterol formation. The former is a radical chain reaction, that consists of three major steps: initiation, propagation, and termination [18]. Briefly, a polyunsaturated fatty acid (PUFA) can be attacked by a free radical molecule (initiation) producing an unstable fatty acid radical ($L^{\cdot}$) that in turn reacts with a molecule of oxygen. The product of this reaction is a peroxyl-fatty acid radical ($LOO^{\cdot}$), which can continue the cycle by reacting with another PUFA (propagation) or stop it by reacting with another radical molecule or with an antioxidant able to break the cycle (e.g., Vitamin E) (termination). This chain reaction mechanism can lead to a loss of membrane components and to the formation of reactive end products, like malondialdehyde (MDA), 4-hydroxy-2-nonenal (HNE), acrolein, and isoprostanes, which can cause further damage to protein and DNA [5]. The reactive end products have been investigated, especially HNE and MDA that were found to easily react with proteins ad DNA and to be highly toxic molecules [19]. Furthermore, MDA is a stable compound used as a biomarker for oxidative stress [20]. In addition to lipid peroxidation, there may be the oxidation of cholesterol caused by specific enzymatic reactions to generate oxysterols. This reaction can be caused either by cytochrome P451 or by non-specific reactions that involve ROS and RNS. Oxysterols are physiologically produced as intermediates in the cholesterol catabolism, but when in excess they can be involved in many diseases (e.g., neurodegenerative diseases and cancers) [21]. It is interesting to note that oxidative stress appears to both induce the formation of oxysterols and to be induced by their presence [22]. All these reactions will eventually

lead to a loss of membrane properties where lipids and cholesterol are mainly localized, and their reactive end products can consequently damage other molecules.

Besides lipids, proteins can also be modified by oxidative stress. Protein damages may cause dysfunction in the cellular activity which in turn may lead to the development of diseases, like chronic inflammatory diseases (cancer, atherosclerosis, ischemia), aging, and age-related neurodegenerative disorders (Alzheimer's disease) [5]. Proteins can be subject to modification on their amino-acid side chains. ROS mainly cause sulfur oxidation of cysteine and methionine, protein hydroxides, and carbonyl derivatives, while RNS induce protein nitration. It is important to note that these protein modifications are mostly irreversible and that damaged proteins, such as carbonylated proteins, are marked for their degradation by proteasomes, and once escaped from degradation they can form high-molecular-weight aggregates that accumulate with age [23]. Carbonylated proteins can be valid biomarkers of oxidative stress because carbonylation is more difficult to be induced compared to the SH oxidation of cysteine and methionine, and they can also be a sign of disease-derived protein dysfunction [24]. Protein oxidative modifications are not always harmful to cells, in fact, this is an important step of protein folding inside the endoplasmic reticulum (ER), in which intra and intermolecular disulfide bonds are introduced [8].

DNA oxidation causes instability and decay of the genome. The most susceptible base to oxidative damage is guanine, which undergoes the major mutagenic lesion is 8-oxo-7,8-dihydroguanine. This mutation is characterized by the pairing of guanine with adenine rather than with cytosine, thus generating transversion mutation after replication [25]. RNA can also be subject to oxidation; for example, the oxidation of microRNA-184 results in the blocking of the translation of anti-apoptotic factors, such as Bcl-xL [26].

Protective antioxidant systems

Under physiological conditions, cells maintain redox homeostasis by the production and elimination of ROS and RNS. To prevent oxidative damages and maintain redox homeostasis, the cells have evolved enzymatic or non-enzymatic antioxidant systems. Enzymatic antioxidants include superoxide dismutase (SOD), glutathione reductase (GR), catalase, and glutathione peroxidase (GPX); while the non-enzymatic antioxidants are thiol molecules, like reduced glutathione (GSH), thioredoxin (Trx), and glutaredoxin (Grx) which take part to thiol-disulfide exchange reactions [3].

SOD catalyzes the dismutation of $O_2^{\cdot-}$ to oxygen and H_2O_2 [4]. This enzyme is present in different cellular compartments, and in different isoforms. SOD1 (CuZnSOD) is present in the cytoplasm, SOD2 (MnSOD) is found in mitochondria, and SOD4 in the extracellular matrix [27]. The H_2O_2 produced is then converted into $H_2O + O_2$ by catalase, which is a heme-based enzyme found in the peroxisome [28]. In addition to this pathway, hydrogen peroxide can be converted into not harmful molecules via the conversion of GSH to oxidized glutathione (GSSG), catalyzed by GPX [29]. GSH, that will be discussed in paragraph "Glutathione", is the most important low molecular weight antioxidant synthesized in cells. The Trx system consists of thioredoxin reductase (TrxR), and Trx, in which TrxR activity is to reduce the oxidized form of Trx [4]. To date, two Trxs isoforms have been identified, Trx1 (cytosolic), and Trx2 (mitochondrial), and three TrxRs isoforms, TrxR1

(cytosolic), TrxR2 (mitochondrial), and thioredoxin glutathione reductase (TGR) [30]. The Grx system also functions to reduce protein disulfides; their oxidized form is reduced by GSH. To date, four Grxs isoforms have been discovered, Grx1, Grx2, Grx3, and Grx5 [31].

Intracellular redox-sensitive pathways

Although ROS are mainly associated with cell damage caused by irreversible oxidation of proteins, lipids, and nucleic acids, low concentrations of ROS play a crucial role in the response and adaptation to local and overall stress conditions. Redox-regulated proteins are the first to respond to changes in the intracellular redox state and induce initial steps to protect against oxidants, repair cellular damage, and restore the redox homeostasis. Those proteins contain highly specific cysteine residues which can undergo reversible oxidative modifications, causing conformational and functional switch of the protein [32]. Oxidative modifications can consist of the oxidation of cysteine residues on proteins, which translate into the formation of reactive sulfenic acid (-SOH). This acid can react with cysteines and form disulfide bonds (-S-S-), or it can be further oxidized and form sulfinic ($-SO_2H$) or sulfonic ($-SO_3H$) acid [33]. These redox oxidations are mostly reversible by reducing systems, like thioredoxin and peroxiredoxin, and this is because these modifications have important roles in the redox signaling [34]. Overproduction of ROS may contribute to altering these redox-sensitive pathways, which could, in turn, lead to the onset of several diseases, such as cancer, neurodegeneration, atherosclerosis, and diabetes, and also to aging [35]. There are many cellular redox-sensitive pathways, in which several phosphatases are often involved, and the presence of ROS causes their oxidation and subsequent inactivation, leading to an impairment in the phosphatase activity [3][36]. Moreover, each pathway is not isolated from the other, in fact, there is a crosstalk between them; for this reason, their correct activation and inactivation are fundamental for the prevention of diseases [4]. Here are described some of these pathways.

Nrf2 – Nuclear factor erythroid 2-related factor 2 (Nrf2) is a basic leucine zipper transcription factor, that under basal conditions is bound to the dimeric inhibitory protein Kelch-like ECH-associated protein 1 (Keap1) in the cytosol [37]. Keap1 is an adaptor of the Cul3-based E3-ubiquitin ligase complex that polyubiquitinates Nrf2 for proteasomal degradation [38]. Keap1 possesses cysteine residues that under stress conditions (ROS, electrophiles) are oxidized; the result is the dissociation of Nrf2 from Keap1 and its nuclear translocation. Once in the nucleus, Nrf2 forms a complex with Maf proteins (Maf-F, Maf-g, and Maf-K), which binds to the antioxidant response element (ARE) [39]. The effects of Nrf2 can be dual: on the one hand, it can regulate the production of ROS/RNS by controlling the transcription of certain enzymes, such as superoxide dismutase (SOD), and iNOS; on the other hand, it can lead to the transcription of enzymes involved in the antioxidant response, such as catalase (CAT), and enzymes involved in the GSH synthesis, such as GCL [4]. (Figure 1).

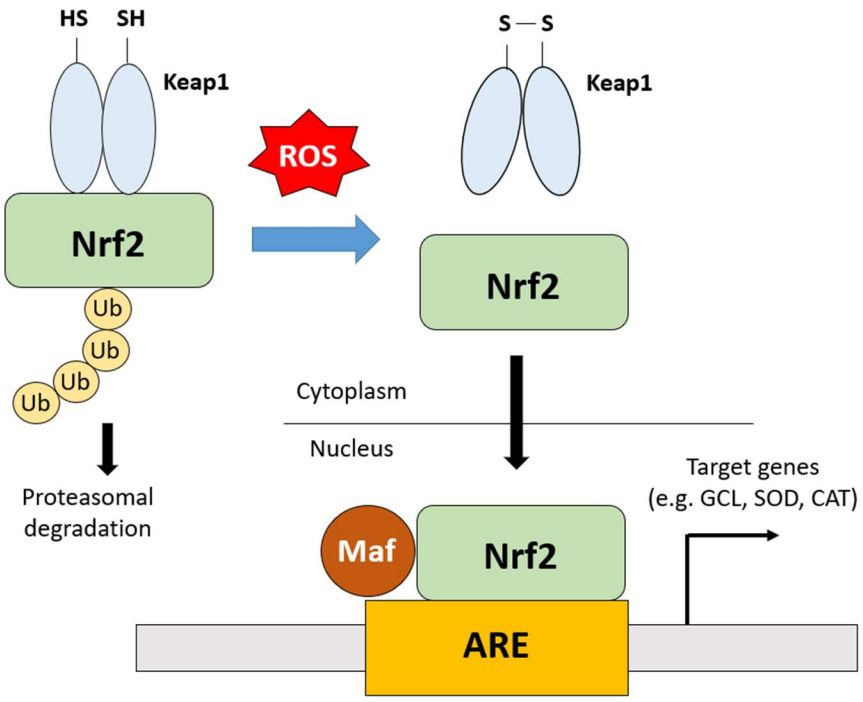

Figure 1 Nrf2 activation by ROS. ROS cause the oxidation of Keap1 cysteines, leading to its conformational change. Keap1 dissociates from Nrf2, which is now free to translocate into the nucleus. Here it creates a complex with the Maf protein and binds to the antioxidant response element (ARE) to induce the transcription of several enzymes, such as glutamate-cysteine ligase (GCL), superoxide dismutase (SOD), and catalase (CAT).

NF-kB – Nuclear factor-kappa B (NF-kB) represents a family that consists of five transcription factors (p65, Rel B, c-Rel, p52, and p50). Under non-stress conditions, it is sequestered in the cytosol by the binding of the inhibitor of kappa B (IkB) [40]. In the presence of stress stimuli (e.g. cytokines, toll-like receptor (TLR) ligands), the IkB kinase (IKK) is activated and phosphorylates IkB, which dissociates from NF-kB, and is subsequently ubiquitinated and degraded. NF-kB is now free to translocate to the nucleus, where it binds to specific DNA promoter regions [41]. NF-kB, as a redox-sensitive factor, is a target activated by ROS and is involved in the inflammatory response (e.g. pro-inflammatory cytokines, such as TNF-α, IL-6, and IL-1β). Interestingly, a severe increase of ROS could lead to a different effect, which is the inactivation of NF-kB and subsequently cell death [3]. The binding of activated NF-kB and DNA requires the reduced form of the transcription factor; in fact, the oxidation of some NF-kB cysteines could lead to the binding inability [42] (Figure 2).

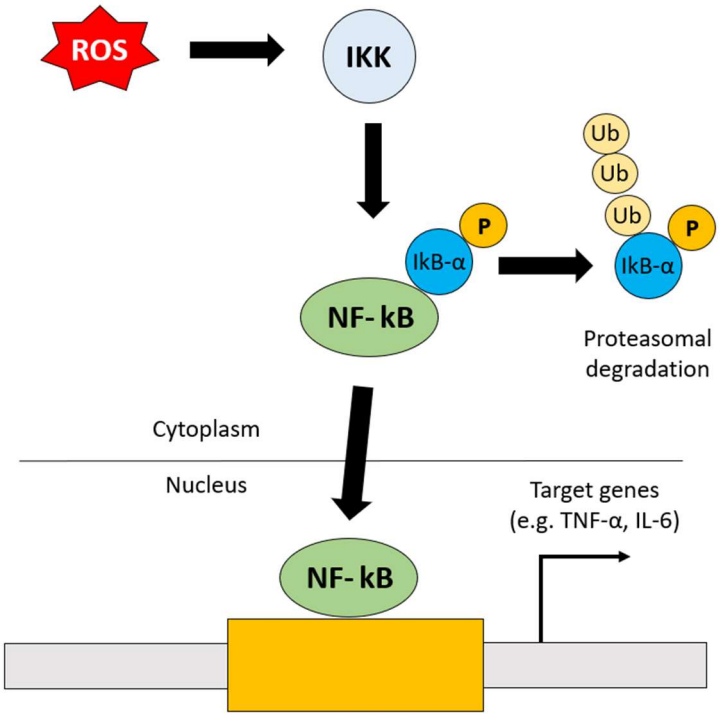

Figure 2 NF-kB activation by ROS. ROS activates the IkB kinase (IKK), which in turn phosphorylates IkB-α. This phosphorylation causes the dissociation of IkB-α from NF-kB, which is now free to translocate into the nucleus and to bind to the DNA. NF-kB induces the transcription of factors involved in the inflammation, such as pro-inflammatory cytokines (e.g. TNF-α and IL-6).

MAPK – The mitogen-activated protein kinase (MAPK) is a family that consists mainly of the extracellular regulated kinases (ERK1/2), the Jun N-terminal kinase (JNK), and the p38 kinase (p38). These factors operate in cascades of sequential phosphorylation that are regulated by different kinases (MAPKKK, and MAPKK), which in turn phosphorylate the MAPK [33]. The outcomes of these pathways can be different: ERK1/2 activation brings to cell survival; while JNK and p38, also known as stress-activated protein kinases (SAPKs), promote cell death (i.e. necrosis, and apoptosis) [43]. It is known that ERK1/2 can be activated by oxidative stress [44]; in fact, its cascade initiates when ROS cause the activation of the growth-factor receptor, which is a tyrosine kinase receptor, that in turn activates Ras. This factor recruits Raf (MAPKKK), which in turn activates MEK1/2 (MAPKK), and ERK1/2 (MAPK) [45]. This pathway is involved in cellular survival by regulating the BCL-2 pro-survival activity [46], and in inflammation by modulating the production of inflammatory cytokines (increased production of TNF-α, IL-1β, and IL-10, and decreased production of IL-12) [47]. SAPKs can be activated by multiple stimuli: ligands, such as lipopolysaccharide (LPS), and hormones, cytokines, and many other stresses [48]. Their activation results in pro-inflammatory cytokines production, and apoptosis. The apoptosis-regulating signal kinase 1 (ASK1) is an important redox sensor for the initiation of the SAPKs signaling cascade. ASK1 phosphorylates MKK4/7 and MKK3/6 to induce the activation of JNK and p38, respectively [48]. Under non-stress conditions, ASK1 is inactive because of its binding to the thioredoxin (Trx). When oxidative stress occurs, the cysteines present on both Trx and ASK1

are oxidized and the bond can not be formed [49]. The active form of ASK1, in turn, phosphorylates MKK4/7 and MKK3/6 which phosphorylate JNK and p38 (Figure 3).

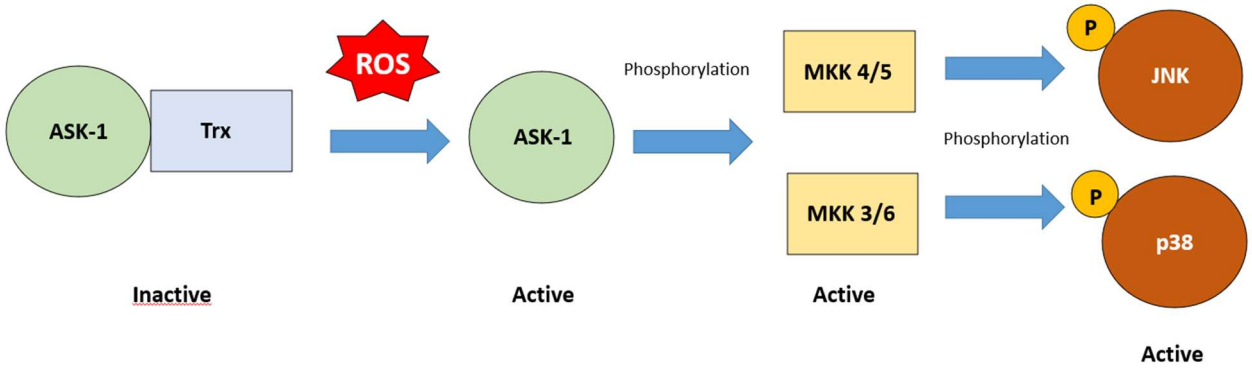

Figure 3 MAPK activation by ROS. ROS induce the dissociation of Trx from the initiator of the stress-activated protein kinases (SAPKs) signaling cascade, apoptosis-regulating signal kinase 1 (ASK-1). ASK-1 phosphorylates and activates MKK 4/5 and MKK 3/6, which in turn phosphorylate and activate JNK and p38 respectively. Their activation leads to the production of pro-inflammatory cytokines, such as TNF-α, and IL1β.

PI3K/Akt – The phosphoinositide 3-kinase (PI3K), involved in cell proliferation and survival [50], consists of two subunits, the catalytic (p110) and the regulatory (p85). The activation of this pathway starts when various growth factors, cytokines, and hormones bind to the receptor tyrosine kinase (RTK), causing the bound of PI3K by its p85 subunit, or by the insulin receptor substrate (IRS) protein [51]. Activated PI3K catalyzes the conversion of phosphatidylinositol 4,5-bisphosphate (PIP2) to the second messenger phosphatidylinositol 3,4,5-triphosphate (PIP3), which subsequently recruits to the plasma membrane proteins that contain pleckstrin homology (PH) domain, such as Akt [52]. This pathway is negatively regulated by the activity of the Phosphatase and TENsin homolog (PTEN), which dephosphorylates PIP3 back to PIP2 [53]. Oxidative stress can regulate the PI3K/Akt pathway. In fact, PTEN is normally active when is present in the reduced form, which is promoted by the protective activity of the NADPH/Trx system [54]. The oxidative inactivation of PTEN results in sustained activation of the PI3K/Akt signaling [55]. The outcomes are the synthesis of anti-apoptotic proteins, such as Bcl-2, the inhibition of ASK1 and SAPKs, and the activation of the NF-kB cascade [3][56] (Figure 4).

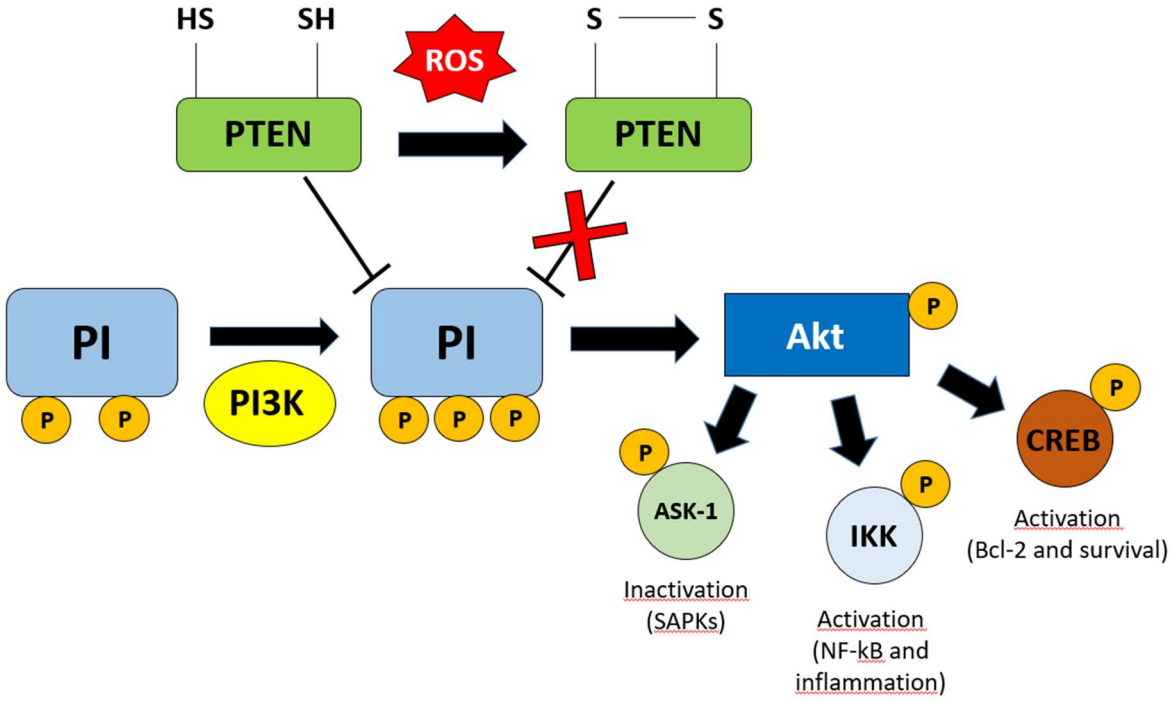

Figure 4 PI3K promotes the activation by ROS. ROS oxidize and inactivate the phosphatase PTEN, which leads to the incapacity of dephosphorylating PIP3 to PIP2. Therefore, the activity of PI3K, which phosphorylates PIP2 to PIP3, is not counteracted. PIP3 recruits Akt, which in turn inactivates the apoptosis-regulating signal kinase 1 (ASK-1) inhibiting SAPKs action; while it activates both the IkB kinase (IKK) and therefore the NF-kB pathway, and the cyclic AMP response element-binding protein (CREB) promoting cell survival.

Glutathione

Glutathione (GSH) is a tripeptide, γ-glutamylcysteinglycine (Figure 5), widely distributed in mammalian cells and tissues, in plants, and most microorganisms [57]. It was discovered by De Rey Pailhade in 1888 during his studies in extracts of yeast, and he called it "Philothion" [58]. It is the most abundant non-protein thiol of the cells, with a concentration that ranges between 1-10 mM, with the liver as the main reservoir [59]. Inside the cells, the GSH is mostly present in the cytosol (90%), where its synthesis occurs, followed by mitochondria (10%), and the endoplasmic reticulum (ER) (small percentage) [60]. It is present in the reduced form, GSH, and in the oxidized form, GSSG [61]. The latter consists of two GSH molecules bound by a disulfide bond, and its concentration is less than 1% of GSH [60]. GSH structure and function as an antioxidant were established by Sir Hopkins in 1922 [62].

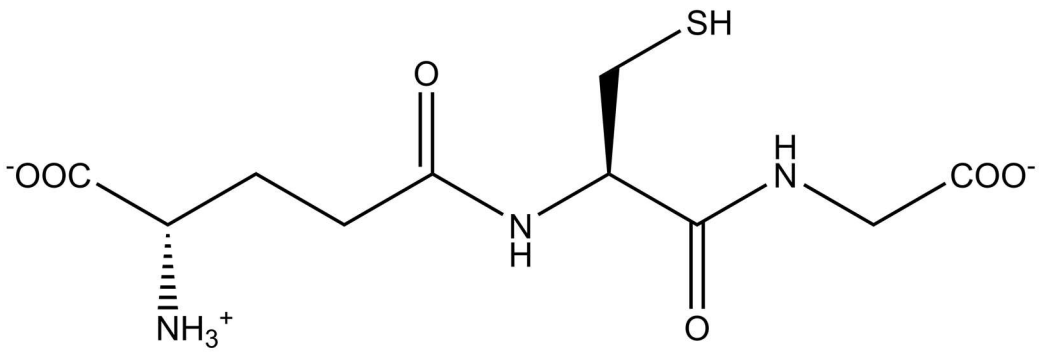

Figure 5 GSH chemical structure.

GSH synthesis

GSH is synthesized from the amino acids glycine, cysteine, and glutamate in the cytosol, and its de novo synthesis involves two ATP-requiring enzymatic steps [63][64].

The first step (Figure 6) is catalyzed by the enzyme glutamate-cysteine ligase (GCL), which produces γ-glutamylcysteine by forming an amide bond between the γ-carboxyl group of glutamate and the amino group of cysteine. This enzyme is a heterodimer, formed by a heavy or catalytic (GCLc), and a light or modifier (GCLm) subunit. The former exhibits the catalytic activity and is regulated by the presence of GSH via negative feedback; the latter is enzymatically inactive but regulates the functioning of the GCLc. In fact, it lowers the Km of GCL for glutamate and raises the Ki for GSH, which means that GCL is more efficient and less subject to inhibition by GSH [65]. Oxidative stress may enhance the activation of the enzyme, even without changing the expression of GCL [66]. Under physiological conditions, GCL is mostly inactive [60]; moreover, its functionality depends on the presence of cysteine which is considered the rate-limiting enzyme [64].

The second step (Figure 6) in GSH synthesis is catalyzed by the glutathione synthase (GS), which is composed of two identical subunits and is not inhibited by GSH [67]. GS is present in higher concentration than GCL, and overexpression of the enzyme does not translate in an increase of GSH concentration [68]; however, the presence of GS has an important role in determining GSH synthesis for example under stressful conditions, such as in response to surgical traumas [60].

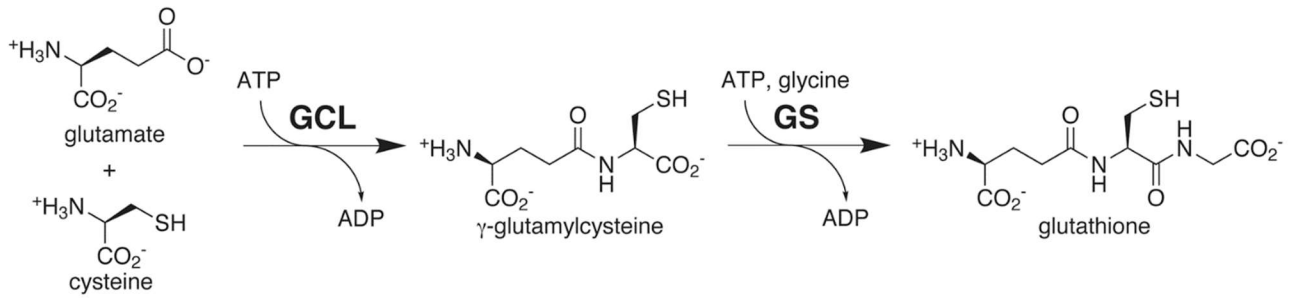

Figure 6 Enzymes involved in the de novo synthesis of GSH.

GSH degradation

The structure of GSH is characterized by the presence of γ-bond between glutamate and cysteine, which makes the tripeptide resistant to hydrolysis from peptidases [69]. For a long time, it has been thought that the degradation of GSH was possible only outside of the cells because the only known enzyme able to break the γ-bond was the γ-glutamyltranspeptidase (GGT or γ-GT) [70]. GGT is located on the plasma membrane and it is implicated in the γ-glutamyl cycle. This enzyme transports GSH outside of the cell in the form of the dipeptide cysteynilglycine and the γ-glutamyl moiety, which is then transferred to an amino acid to form γ-glu-aa [71]. The dipeptide is the substrate of a dipeptidase on the plasma membrane and is broken down into cysteine and glycine. Cysteine is then taken up by the cell and the majority is used to form GSH [58]. γ-glu-aa, on the other hand, is transported back inside the cell and separated from the amino acid; the free glutamate can be used for GSH synthesis [58].

Recently, an intracellular pathway of GSH degradation catalyzed by the ChaC enzyme family was discovered [72]. The mammalian ChaC1 was discovered as a protein upregulated during the Unfolded Protein Response (UPR) caused by ER stress [73], and it was shown to be able to break the γ-bond between glutamate and cysteine because of its γ-glutamylcyclotransferase activity [72]. Chac1 is able to exclusively act on reduced GSH, by forming the dipeptide cysteynilglycine and 5-oxoproline, while GSSG is not affected by its activity [74].

GSH functions

GSH is involved in various cellular functions, which can be categorized into two main reactions: conjugation, and reduction [75]. The first group of reactions is involved in the metabolism of xenobiotics, where GSH is conjugated with the exogenous compounds by the activity of the enzyme glutathione-S-transferase (GST) [58]. The resulted conjugates can be excreted from the cells [75]. The second group of reactions explains its antioxidant activity and includes the GSH itself and several enzymes involved in the intracellular defense against oxidative stress. This mechanism is composed of GSH itself and several enzymes, such as glutathione peroxidase (GPx), GST, and glutathione reductase (GR) [76]. GPx and GST, which not only have conjugating activity, are implicated in the reduction of peroxides, while GR is involved in the conversion of GSSG in two molecules of GSH [77]. Moreover, GSH is involved in the maintenance of the sulfhydryl groups of proteins in the reduced state. It is known that the redox state of proteins regulates different intracellular pathways and that the cysteine residues in the active sites can be easily oxidized [78].

Recent evidence has shown that GSH has a broader activity, in addition to the scavenging one. In fact, GSH deficiency has been described as an important mechanism contributing to the pathogenesis and outcomes of several infections (both viral and bacterial), [79][80].

GSH in infections and inflammation

Alterations of the redox state are common during infections. The consequent modulation of the many intracellular redox-sensitive pathways affects the ability of the cells to cope with pathogens by modifying both

the innate and the adaptive immune response [79]. GSH has many important roles in the immune response. Antigen-presenting cells (APCs) need the tripeptide in order to correctly processing the antigen; in fact, the endocytosed proteins must undergo a process of denaturation/unfolding, and the rate-limiting-step seems to be the reduction of disulfide bonds [81]. This antigen processing seems to be correlated with GSH content; indeed, if it is present in APCs at low concentrations the process is defective [82], while high concentrations of GSH promote the capacity to present the antigen [83]. APCs, like macrophages, can influence the differentiation of T helper cells (Th) in Th1 (cellular immunity) and Th2 (humoral immunity) according to the secreted cytokines; thus, the redox state of APCs is important to mount a proper immune response against pathogens [84]. Macrophages with a decreased GSH content were found to produce less IL-12, which in turn inhibit the Th1 differentiation in a murine model [84], while elevated GSH concentrations induced by pro-GSH molecules were found to increase IL-12 secretion associated with a Th1 response [85].

Many viruses are known to alter the intracellular redox state versus a more oxidized, often characterized by GSH depletion, with the aim to make the cellular environment favorable to an efficient virus cycle. For this reason, GSH has been proposed as an effective antiviral molecule, and its capacity to hinder the replication of different viruses has been described. For example, GSH can inhibit NF-kB activation induced by HIV [86], or influenza virus-induced apoptosis resulting in a reduced spread of the virus [87]. Another interesting mechanism could be the ability to inhibit the proper folding and stabilization of viral proteins, like the maturation of the glycoprotein hemagglutinin of the influenza virus in the endoplasmic reticulum (ER) of the host [88]. In this regard, it is known that viruses don't have the biosynthetic machinery to translate their genome and to produce their structural proteins, thus they take advantage of the host's protein biosynthetic machinery associated with the ER [89]. The ER is important for the correct folding of proteins, which includes the disulfide bond formation that is important for the protein maturation and stability and to do that the ER lumen is characterized by a low GSH/GSSG ratio [90]. The ER redox state is fundamental for the correct functioning of the protein disulfide isomerase (PDI), which exerts oxidoreductase and redox-regulated chaperone activities. In fact, PDI leads to the formation, isomerization, and reduction of disulfide bonds, and it has also an important role in the degradation of misfolded proteins [91]. As a redox-dependent protein, PDI needs a correct ratio between GSH and GSSG to function properly, otherwise, alterations in the disulfide bond formation could occur, leading to misfolded protein.

The GSH depletion caused by viruses leads to the activation of the NF-kB pathway, which is normally considered as an important factor of the innate immune response against pathogens, promoting viral replication, as said above [92]. GSH has the ability to inhibit NF-kB activation at many levels; as a scavenger it can eliminate oxidants, it can prevent the activation of IKK by inhibiting the kinase, it can interfere with the translocation of activated NF-kB, and it can inhibit the binding of NF-kB to the DNA. However, it is important to remember that this pathway is involved in the immediate early step of immune activation, so in order to promote a correct immune response, the NF-kB pathway can not be completely suppressed [93]. In fact, the outcome is the inflammatory response, which brings to the production of various cytokines and chemokines that have the role to activate the immune response and viral clearance [94].

Although an effective anti-viral immune response is necessary for viral elimination, an exaggerated response can be harmful. In particular, pro-inflammatory cascades have a fundamental role in the pathogenesis of lung damage in respiratory virus infections, such as influenza virus, and other diseases, such as Cystic Fibrosis (CF). Redox regulation of inflammatory cytokine production induced by *Pseudomonas aeruginosa* (P. aeruginosa), which is the most common chronic infection in CF, has been one of the topics of my thesis work [95]. This disease is characterized by a lack/malfunction of the cystic fibrosis transmembrane regulator channel (CFTR) [96], and also by an altered redox state in the CF lung which is translated in a decreased concentration of GSH with respect to healthy lung [97][98]. Furthermore, CF lung has an impaired mucociliary clearance, which means that an eventual P. aeruginosa infection in the lung would not be prevented/resolved properly [99]. Normally, an increase of ROS production leads to the activation of the redox-sensitive inflammatory pathways, such as NF-kB that is considered fundamental for the immune response, and for the production of several inflammatory cytokines, like IL-6, TNF-α [100]; however, CF is characterized by unresolved infection and hyperinflammation, with basal high ROS levels and increased pro-inflammatory cytokines. This alteration leads to increased oxidative stress and impairment of the intracellular pathways involved in the immune response against pathogens [101].

Besides viral infections, bacteria could also invade the cellular host, such as macrophages, and put in place mechanisms aimed to manipulate the cellular immune signaling pathways to survive [102]. It is known that macrophages could be a bacterial reservoir and that the bacterial infection could alter the redox state and in turn influence the antibacterial pathways of the host [103]. One example is represented by infection of *Mycobacterium tuberculosis*, which is an opportunistic intracellular pathogen able to persist in the macrophage host by inhibiting the killing mechanisms, especially in patients with acquired immune deficiency syndrome (AIDS) [104]. Treatments aimed to increase intracellular GSH levels could influence bacterial survival and replication for three reasons. First, mycobacteria do not produce GSH, but they synthesize mycothiol as a regulator of reduction and oxidation reactions [105]. Therefore, the exposure of this bacterium to high concentrations of GSH could imbalance its redox state and bring to growth inhibition. Second, it is thought that GSH could have evolved in higher eukaryotes as a precursor of antibiotics before the emergence of cellular immunity [106]. Third, the tripeptide is a precursor of GSNO, which may represent one of the most important active forms of NO as an antimicrobial agent [107].

Many diseases, in which GSH alterations have been described, are characterized by impairment in the cellular immune/inflammatory response, and the replenishment/increase of GSH levels, by GSH itself or GSH-boosting drugs, could be considered as a useful approach to modulate the pathways involved in the immune response.

Pro-GSH molecules

Replenishment or augmentation of intracellular GSH concentration can be achieved by treatment with pro-GSH molecules [108]. The use of GSH as it is, in fact, is not ideal because it has a short half-life in plasma (<3 min), and is unable to cross the cell membrane; therefore, high doses of GSH would be required to achieve

therapeutic value [109]. For these reasons, several pro-GSH molecules have been designed and used to increase the levels of the tripeptide more easily. For the synthesis of these molecules, different approaches can be followed; it is possible to administer GSH-conjugates to facilitate the passage of the tripeptide across the membrane, such as GSH esters [110]; another potential way is to give GSH precursors, such as the rate-limiting amino acid cysteine, in the form of N-acetylcysteine (NAC) [111] and β-mercaptoethylamine (cysteamine, MEA) [112].

NAC, a precursor of L-cysteine, is widely used in clinical treatments and is recognized by the World Health Organization (WHO). This drug is useful in the treatment of paracetamol overdose [113] and is recognized by the FDA as a mucolytic [114]. NAC can act as an antioxidant via several mechanisms. It can exert an indirect effect by providing cysteine, useful to GSH synthesis; a direct effect against oxidant species; a reducing effect on the sulfhydryl group of protein [115]. For these reasons, NAC has been considered a beneficial drug able to counteract oxidative stress, which is a common characteristic of many diseases [116]. NAC, in fact, is used in several clinical treatments, like neurological disorders [117], substance abuse disorders [118], Alzheimer's disease [119], asthma [120], influenza [121]; moreover, because of its ability to break bacterial biofilms, it can be used as an adjuvant microbial drug that could improve antibiotic permeability [122]. However, the use of NAC has some limitations since in order to activate the synthesis of GSH the cells must have undamaged enzymatic machinery.

MEA is an aminothiol used in the treatment of the rare disease cystinosis that was approved by the FDA in 1994 [122]. Cystinosis is characterized by a redox alteration that affects GSH content in favor of its oxidized form, GSSG [123]. The effects of MEA had been studied in the cystinosis model, and the results obtained by *in vitro* studies in proximal tubular epithelial cells showed that this molecule was able to increase GSH levels. The GSH-boosting drug of MEA is presumably linked to its capacity to reduce cystine, the oxidized form of cysteine, in cysteine [124]. Because of its ability to restore GSH and its antioxidant properties, MEA could be used in diseases hallmarked by a damaging oxidative environment. Furthermore, it had been demonstrated that MEA has a synergistic effect when used with the antimalarial artemisinin-derivatives, suggesting a broader effect of this molecule [125].

I-152

I-152 is a pro-GSH molecule composed of NAC and MEA linked together by an amide bond; this molecule enters the cells where it is first deacetylated on the MEA moiety and subsequently hydrolyzed to release NAC and MEA [126]. I-152 was synthesized for the first time in 2001 by Oiry et al., and the main goal was to obtain a potent antioxidant molecule able to pass across the cellular plasma membrane and increase GSH intracellular content by taking advantage of the two GSH parent drugs (i.e. NAC and MEA) [127]. The pro-GSH activity of I-152 was reviewed by our research group as reported in Chapter 1 where we collected old and more recent data that can be summarized as follows:

- in primary human monocyte-derived macrophages (MDMs) I-152 (i.e. 10 μM – 1 mM) can increase the intracellular content of GSH (old data);

- in murine macrophage RAW 264.7 cell line and macrophages obtained from the peritoneal cavity of mice low concentrations of I-152 (not higher than 1 mM) can increase GSH content, while high concentrations of I-152 (i.e. 10 and 20 mM), caused a GSH depletion but provided a large amount of thiol species, such as I-152, NAC, MEA, and cysteine (old data);
- in GSH-experimentally depleted RAW 264.7 cells I-152, at low concentrations (i.e. 0.1 and 0.5 mM), replenishes GSH (recent data);
- *in vivo* I-152 can deliver NAC and MEA in several mouse organs (recent data);
- *in vivo* I-152 can restore GSH whose content was depleted by the retroviral complex LP-BM5. Moreover, I-152 immunomodulatory activity towards antigens was demonstrated in different animal models. Ova-sensitized and Tat-immunized mice pre-treated with I-152 showed a shift to a Th1 immune response involving splenocyte IFN-gamma production and higher levels of IL-12 in circulation [128][129]. Moreover, in a murine model of AIDS, a correlation between GSH deficiency and a prevalent Th2 immune response was established; in the same animals, I-152 treatment was found to restore a balanced Th1/Th2 response [129][130] (old data).

Structure of the thesis

The thesis is divided into 5 chapters. Every chapter is introduced by a brief paragraph explaining what the chapter contains. While the chapters 1-3 report papers which have been already published, the chapters 4 and 5 describe results which have not been yet published.

The References of the section "General introduction" and of the Chapters 4 and 5 can be found in the section "References" at the end of the thesis.

Aim of the study

The study was aimed to modulate intracellular redox-sensitive pathways to hinder directly the pathogen (like in the case of *Mycobacterium avium*), whose survival depends on the thiol-based redox metabolism which is fundamental to maintain a reducing environment to preserve cellular homeostasis, especially from ROS, and antibiotics, and indirectly by modulating the host's immune/inflammatory response to the pathogen. Furthermore, it was investigated whether the redox state could play a role in immune/antiviral response by modulating folding and secretion of immunoglobulins.

Alteration of redox state was induced by I-152 whose pro-GSH capacity had already been demonstrated, but the metabolism and the mechanism by which it increases intracellular GSH levels had not been studied in depth. In this thesis, one of the aims was also to deepen this aspect.

CHAPTER 1

Chapter 1 – This chapter consists of a review where the pro-GSH activity of I-152 is discussed.

Original article published in Nutrients
Volume 11, Issue 6, 2020, 1291

nutrients

MDPI

Review

Boosting GSH Using the Co-Drug Approach: I-152, a Conjugate of *N*-acetyl-cysteine and β-mercaptoethylamine

Rita Crinelli [1], Carolina Zara [1], Michaël Smietana [2], Michele Retini [1], Mauro Magnani [1] and Alessandra Fraternale [1,*]

[1] Department of Biomolecular Sciences, University of Urbino Carlo Bo, 61029 Urbino, Italy; rita.crinelli@uniurb.it (R.C.); c.zara@campus.uniurb.it (C.Z.); michele.retini@uniurb.it (M.R.); mauro.magnani@uniurb.it (M.M.)

[2] Institut des Biomolécules Max Mousseron, Université de Montpellier UMR 5247 CNRS, ENSCM, 34095 Montpellier, France; michael.smietana@umontpellier.fr

* Correspondence: alessandra.fraternale@uniurb.it; Tel.: +39-0722-305243

Received: 12 April 2019; Accepted: 5 June 2019; Published: 7 June 2019

Abstract: Glutathione (GSH) has poor pharmacokinetic properties; thus, several derivatives and biosynthetic precursors have been proposed as GSH-boosting drugs. I-152 is a conjugate of *N*-acetyl-cysteine (NAC) and *S*-acetyl-β-mercaptoethylamine (SMEA) designed to release the parent drugs (i.e., NAC and β-mercaptoethylamine or cysteamine, MEA). NAC is a precursor of L-cysteine, while MEA is an aminothiol able to increase GSH content; thus, I-152 represents the very first attempt to combine two pro-GSH molecules. In this review, the in-vitro and in-vivo metabolism, pro-GSH activity and antiviral and immunomodulatory properties of I-152 are discussed. Under physiological GSH conditions, low I-152 doses increase cellular GSH content; by contrast, high doses cause GSH depletion but yield a high content of NAC, MEA and I-152, which can be used to resynthesize GSH. Preliminary in-vivo studies suggest that the molecule reaches mouse organs, including the brain, where its metabolites, NAC and MEA, are detected. In cell cultures, I-152 replenishes experimentally depleted GSH levels. Moreover, administration of I-152 to C57BL/6 mice infected with the retroviral complex LP-BM5 is effective in contrasting virus-induced GSH depletion, exerting at the same time antiviral and immunomodulatory functions. I-152 acts as a pro-GSH agent; however, GSH derivatives and NAC cannot completely replicate its effects. The co-delivery of different thiol species may lead to unpredictable outcomes, which warrant further investigation.

Keywords: glutathione; pro-glutathione molecules; co-drug; antiviral activity; immunomodulation; *N*-acetyl-cysteine; cysteamine

1. Introduction

Glutathione (GSH) is the most powerful antioxidant molecule within cells performing a variety of functions that go beyond its protective activity against reactive oxygen species (ROS). Indeed, in its reduced form, GSH not only acts as a scavenger of ROS and as a substrate for antioxidant enzymes, but also promotes drug detoxification [1]. Moreover, by controlling the redox potential, GSH modulates many redox-sensitive proteins within signaling pathways [2]. Notably, GSH itself can be conjugated to the cysteines of proteins in a process known as *S*-glutathionylation. It is widely accepted that thiol redox transitions cause changes in protein activity, abundance, localization, and interaction with other macromolecules [3]. These properties of GSH may at least partially explain its ability to stimulate cell proliferation and act as an immunomodulator, although research in this field is still limited.

Alterations in GSH levels may be transient in response to an oxidative insult, or they may become chronic under conditions of prolonged oxidation and/or dysfunction/deficiency of the enzymes involved in GSH synthesis/degradation. Inborn errors in GSH metabolism include those arising from defective γ-glutamyl-cysteine ligase and glutathione transferase which are the most frequently occurring disorders [4]. Conversely, examples of acquired GSH deficiency include mitochondrial diseases, cystic fibrosis, and many viral/microbial infections [5,6]. In the last few decades, the number of pathologies found to be associated with low GSH levels has risen rapidly, prompting researchers to consider GSH and its derivatives as possible therapeutic agents. Cellular GSH concentration can be affected by the exogenous administration of GSH or GSH-boosting drugs, such as glutathione esters and GSH biosynthetic precursors, which have been used to overcome the poor pharmacokinetic properties of GSH [7,8]. GSH and *N*-acetylcysteine (NAC) have also been used in the co-drug approach as bioconjugates of several therapeutics employed in the treatment of neurodegenerative diseases [9]. In this context, the use of I-152 marks the very first attempt to combine two pro-GSH molecules into one to potentiate both the cellular uptake and to improve the biopharmaceutical properties of the parent drugs.

In this review, the design, metabolism and ability of I-152 to affect GSH levels are discussed. Moreover, the antiviral and immunomodulatory properties of I-152 in light of its GSH-boosting activity are also summarized.

2. I-152 Design and Synthesis

I-152 is a conjugate of NAC and *S*-acetyl-β-mercaptoethylamine (SMEA) linked together by an amide bond. The molecule was synthesized by Oiry et al., in 2001 using commercially available *N*-acetyl-*S*-trityl–L-cysteine and *S*-acetylcysteamine hydrochloride [10]. Experiments performed in cell-free extracts have shown that this compound is deacetylated to the corresponding dithiol derivative, which may be responsible for the in-situ release of NAC and MEA [10] (Figure 1).

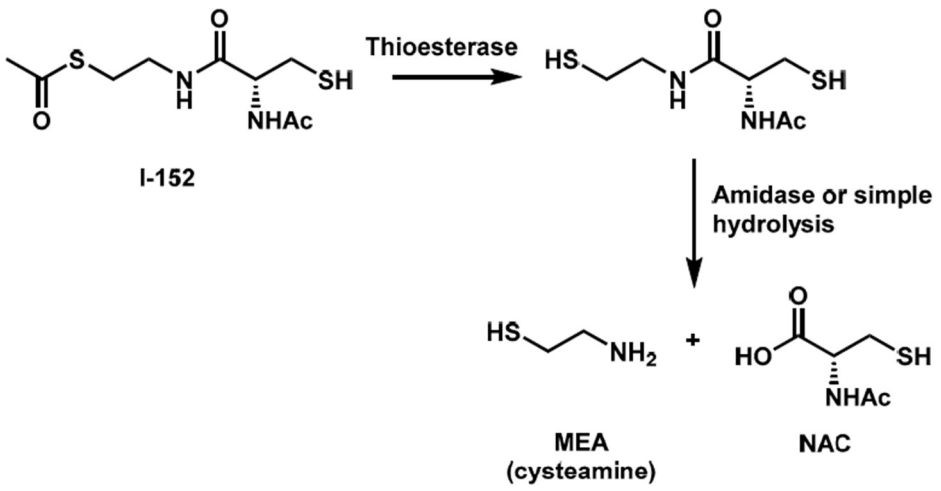

Figure 1. Chemical structure and proposed metabolism of I-152. NAC, *N*-acetyl-cysteine; MEA, β-mercaptoethylamine or cysteamine.

In an attempt to enhance the lipophilic properties of the molecule, a series of I-152 analogues carrying different *S*-acyl groups on the MEA moiety and *S*-acylation of the free thiol group were subsequently synthesized by the same team [11]. In terms of pro-GSH activity, the potency of the molecules increased with the presence of the free thiol group. By contrast, the presence of an R-radical on the MEA moiety had no significant effects.

The initial aim of combining NAC and MEA was to design a new potent antioxidant molecule able to liberate two potential pro-GSH compounds after metabolic conversion. NAC is the *N*-acetyl derivative of the natural amino acid L-cysteine; thus, it is a direct precursor of glutathione. NAC has long been used therapeutically as a well-tolerated and safe medication for the treatment of various

pathologies, including paracetamol intoxication and cystic fibrosis. Its efficacy as an antioxidant has been demonstrated in a wide range of clinical settings where oxidation is tightly linked to GSH deficiency, given that NAC is a poor direct antioxidant [12]. Although NAC was designed to facilitate membrane permeability, it has been suggested that its pharmacological activity might rely on the reduction of plasma cystine to cysteine which then enters the cells and sustains glutathione synthesis [13]. NAC-induced cytoprotection and the NAC signal transduction pathway are not well understood. Recent evidence suggests that NAC may modulate antioxidant pathways by increasing the expression of miR-141 regulating Keap1/Nrf2 signaling, at least under conditions in which the miRNA is downregulated [14]. β-mercaptoethylamine (MEA) or cysteamine is a product of the constitutive degradation of Coenzyme A. It derives from the cleavage of pantetheine to form MEA and pantothenate (vitamin B5). In mammalian cells, MEA can be oxidized to hypotaurine and taurine by aminothiol dioxygenase [15]. The thiol cysteamine can be oxidized into the disulfide cystamine depending on the local redox environment. Both forms have been used in clinical and experimental settings; however, in most cases their specific role in the observed biological effects was not understood. High intracellular levels of GSH are probably sufficient to reduce cystamine to cysteamine; thus, it has been proposed that most of the effects of cystamine may be mediated by its reduced form [16]. On the other hand, there is evidence that cysteamine has the propensity to form disulfides in vivo, suggesting that cysteamine-containing disulfides such as cystamine may normally be present along with cysteamine in mammalian tissue under physiological conditions [17]. Cysteamine can perform a wide range of functions acting as a cystine-depleting agent, pro-GSH molecule, enzyme inhibitor, and gene expression modulator. Interestingly, many of these activities are thought to rely on thiol/disulfide exchange reactions between cystamine/cysteamine and susceptible protein cysteine sulfhydryl groups in a process called cysteaminylation [17]. Cysteamine, in the form of cysteamine bitartrate (Cystagon), has been approved by the Food and Drug Administration (FDA) for the clinical treatment of nephropathic cystinosis acting as a cystine-depleting agent by forming cysteine-cysteamine mixed disulfides [18]. Recent studies suggest that cysteamine may have several other potential therapeutic applications beyond cystinosis, including the treatment of neurodegenerative diseases and cancer. Indeed, cysteamine/cystamine is an efficient inhibitor of transglutaminase and caspase 3 which play a pivotal role in mutant Huntington protein processing [19]. Other proteins whose activity has been reported to be affected by cysteamine/cystamine treatment are protein kinase C and metalloproteinases, important drug targets in cancer progression and metastasis [20,21]. More poorly understood are the mechanisms mediating the pro-GSH activity of cysteamine and its oxidized form. Cysteamine treatment of normal and cystinotic cells has been shown to increase GSH content. However, the authors claimed that the increase of cysteine levels resulting from cystine reduction can only partially explain elevated GSH levels [22]. The ability of cystamine and, less potently, of cysteamine to activate the Nrf2 antioxidant pathway was shown by Calkins et al., in astrocytes [23]. Cystamine-mediated activation of Nrf2 was found to be inversely correlated with the GSH content of the culture and the increase in GSH levels was shown to be dependent on de novo synthesis. Unfortunately, experiments performed with Nrf2 knockout cells revealed that the cystamine-induced GSH increase was Nrf2-independent. Hence, cystamine-induced GSH up-regulation seems to involve other yet-unknown mechanism(s).

3. I-152: Metabolism and Effects on GSH Levels

The ability of I-152 to increase basal intracellular GSH content was evaluated in human and murine cellular models. In primary human monocyte-derived macrophages (MDMs) and other human cell lines, I-152 ranging from 10 μM to 1 mM was found to increase GSH content even at doses which were ineffective when NAC and MEA, alone or in equimolar combinations, were used [10]. In murine monocyte/macrophage-like cell line RAW 264.7 and macrophages obtained from the peritoneal cavity of mice, low concentrations of I-152, i.e., 1 mM, increased GSH level [24]. By contrast, high I-152 concentrations (i.e., 10 and 20 mM) caused GSH depletion but provided large quantities of

I-152 and NAC which can be used to resynthesize GSH [24]. The decrease in the GSH content at high I-152 doses has been suggested to be the consequence of a negative feedback of GSH on γ-glutamylcysteinyl synthetase, the first enzyme involved in GSH synthesis [10]. Alternatively, GSH could be depleted because of its conjugation to I-152 in a reaction catalyzed by the detoxification enzyme glutathione-*S*-tranferase (GST). Preliminary in-vitro experiments indicate that GSH could be indeed conjugated to I-152 by GST. Under the condition of GSH depletion, cysteamine could be converted into cystamine, which has been shown to inhibit γ-glutamylcysteinyl synthetase, further supporting the decrease in GSH levels [25].

Less information is available on I-152 in-vivo metabolism. Preliminary studies were performed in our laboratory to assess the distribution of I-152 and its metabolites in mouse organs after I-152 intraperitoneal injection (i.p.). GSH and cysteine levels were also measured. The analyses were performed in selected organs, i.e., the lymph nodes, brain and pancreas. The lymph nodes were chosen because it has been reported that lymphoid tissues are significantly more "reduced" than the other tissues, and that the immune response is strongly influenced by variations in the redox state [26]. In particular, some lymphocyte functions, such as DNA synthesis, are favored by high levels of GSH, while other redox-sensitive pathways are favored by low intracellular GSH. However, immunological functions in the diseases characterized by oxidative stress can be restored by cysteine or GSH supplementation [27,28]. The brain generates high levels of ROS due to its high oxygen
consumption, hence it is more susceptible to the damaging effects of ROS than other tissues [29,30].
The GSH concentration has a key role in maintaining redox balance in the central nervous system (CNS) and it is altered in neurodegenerative diseases [5,31,32] such as Alzheimer's disease (AD), Parkinson's disease (PD), amyotrophic lateral sclerosis (ALS), multiple sclerosis (MS), HIV-associated neurocognitive disorder (HAND or "NeuroAIDS"), cerebral ischemia/reperfusion injury (I/R), and traumatic brain injury (TBI) [33]. The presence of the tightly regulated blood brain barrier (BBB) represents a serious obstacle to effective treatment of CNS disorders, in fact its selective permeability prevents most bioactive molecules from entering the brain [34]. Several antioxidants, including vitamin E (the important scavenger of lipid peroxidation in the brain), vitamin C (intracellular reducing molecule), coenzyme Q10 (transporter of electrons in the electron transport chain, ETC), and NAC (acting as a precursor of GSH) have been used as therapeutic agents. Although antioxidant therapies have shown benefits in preclinical animal models, negative results have been obtained from clinical trials [30]. Moreover, in such treatments, dosage and additives as well as synergistic interactions with other antioxidants must be considered [35]. Hence, the design and development of antioxidant-based therapies for the brain require a great deal of effort [33,34,36]. Lastly, the pancreas plays a major role, along with several other organs, in GSH metabolism, as shown by the high concentration of the tripeptide, its rapid turnover rate, and the presence of high levels of various enzymes involved in GSH metabolism [37]. Therefore, the pancreas requires a great amount of cystine/cysteine for pancreatic enzymes, which is provided by glutathione (GSH). Moreover, the induction of CYP450 enzymes by xenobiotics in pancreatic acinar cells can cause a decrease in GSH content, which can affect both detoxification and pancreatic enzyme synthesis [38].

Our preliminary data indicate that I-152 can be used to deliver precursors for GSH synthesis, in the form of NAC and MEA, to different organs, including the brain (Table 1).

The presence of NAC within tissues supports the hypothesis that I-152 is able to reach the target site and release in situ the active molecules. In fact, it has been demonstrated that NAC does not pass the cell membrane, but rather reacts with cystine reducing it to cysteine, which then enters the cells and sustains GSH synthesis [13]. Hence, increased cysteine found in the organs can derive from NAC released by I-152 or by the reduction of plasma cystine to cysteine. The presence of NAC in the brain is an interesting aspect since NAC's ability to cross the BBB is disputed [40]. Hence, I-152 could be a promising pro-drug to release NAC in the brain. Interestingly, increased intracellular thiol availability did not enhance intracellular GSH with the exception of the brain, probably because these cells had normal GSH levels. Indeed, under conditions of GSH depletion, e.g., in cells treated with diethyl

maleate (DEM) [41], I-152 even at low concentrations (0.1 and 0.5 mM) exerts a GSH-replenishing effect (Figure 2).

Table 1. Thiol content in different mouse organs after i.p. administration of I-152.

Time from Injection (min)	30				240			
Thiol Species	NAC	MEA	GSH	Cysteine	NAC	MEA	GSH	Cysteine
BRAIN	+	+	=	=	/	/	↑	↑
LYMPH NODES	+	+	↓	↑	+	/	=	=
PANCREAS	+	+	=	=	/	/	=	=

CD-1 mice were i.p. injected with I-152 (30 µmol/mouse), and the thiol content was determined by HPLC [39]. (+) detectable; (/) undetectable; (↑) increased, (↓) decreased and (=) unchanged compared to control levels. NAC, *N*-acetyl-cysteine; MEA, cysteamine; GSH, reduced glutathione.

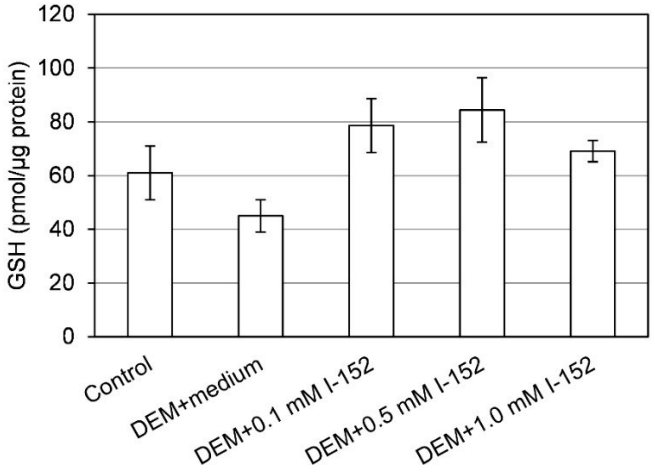

Figure 2. In-vitro replenishment of intracellular GSH by I-152. RAW 264.7 cells were treated with 6 mM diethyl maleate (DEM) for 15 min, then medium not containing I-152 (DEM+medium) or containing I-152 at different concentrations were added for 2h. Reduced glutathione (GSH) content was determined by HPLC [24]. Results represent the mean ± S.D. of two independent experiments.

The capacity of I-152 to restore the intracellular GSH content was also studied in vivo in organs of mice experimentally infected with the retroviral complex LP-BM5. This infection causes a disease with many similarities to human Acquired Immuno Deficiency Syndrome (AIDS), including GSH deficiency [42,43]. Glutathione depletion was found in most organs of LP-BM5-infected mice both in the early phases of the disease and later, in particular in the lymphoid organs, e.g., lymph nodes, known to be the site where viral loads are higher [42]. The effect of intraperitoneal administration of I-152 in infected mice is shown in Figure 3, where it can be observed that the treatment was able to re-establish the content of the tripeptide in the lymph nodes of infected mice at all the times of infection. Notably, GSSG content was unaffected by I-152 treatment [42]. Hence, as hypothesized above, I-152 could be used to increase intracellular GSH during aging and various disease states in which antioxidant defense systems can be altered leading to progressive oxidative damage and subsequent cell death and/or significant impairment of several cellular processes.

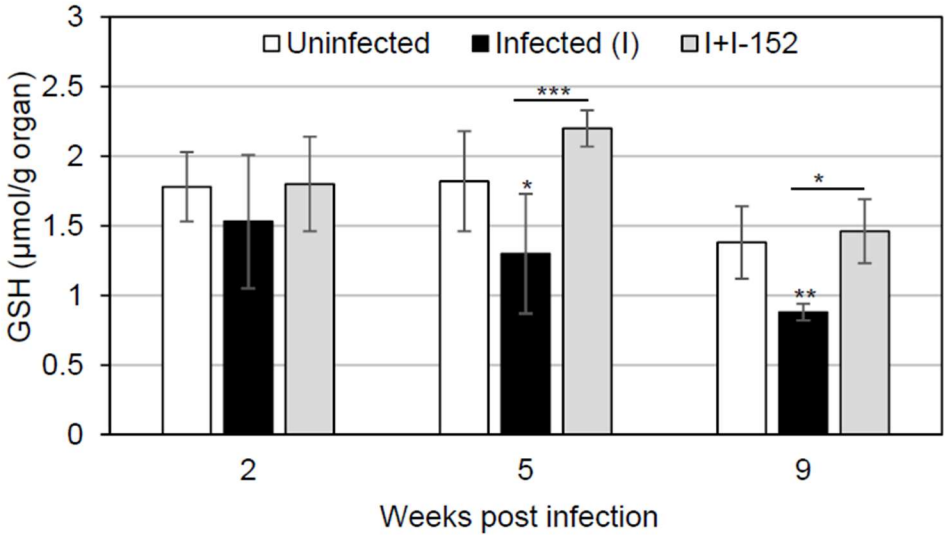

Figure 3. Replenishment of reduced glutathione (GSH) by I-152 in LP-BM5-infected mice. C57BL/6 mice were infected and treated with I-152 (30 µmol/mouse) three times a week, every other day, for a total of 9 weeks. At 2, 5 and 9 weeks after virus inoculation, GSH content in the lymph nodes was determined by HPLC [39,42]. Data are the mean ± S.D. of at least three mice. *$p < 0.05$; ** $p < 0.01$; *** $p < 0.001$ (ANOVA). [42]; (unpublished results).

4. Antiviral and Immunomodulatory Properties of I-152

GSH depletion characterizes several viral infections and associated-disease progression [44]. Numerous studies have demonstrated that the use of GSH is effective in reducing viral production in different experimental models suggesting that the administration of the tripeptide can be considered a useful strategy to hinder viral infection and infection-associated symptoms [2,28,44,45]. Due to the poor pharmacokinetic properties of GSH, high GSH concentrations are necessary to sufficiently increase its content in order to obtain an antiviral effect [7,8]. Hence, taking advantage of the GSH-replenishing capacity of I-152, antiviral effects of the molecule were explored in two retroviral infections associated with systemic and tissue decrease in the GSH content, i.e., HIV and LP-BM5 infections. In HIV-1/BaL-infected MDMs, 150 µM I-152 was able to inhibit viral replication by 90% likely interfering with both early and late steps of the virus life cycle [11]. In LP-BM5-infected mice I-152, when administered at a concentration of about 10 times lower than GSH, significantly reduced murine AIDS (MAIDS) symptoms were observed, i.e., splenomegaly and lymphadenopathy, as well as BM5d proviral DNA in spleen and lymph nodes [46]. Actually, the exact mechanisms through which I-152 can exert antiviral activity are not known. However, since I-152 treatment replenished virus-induced GSH depletion both in human MDMs [10,11] and in mouse lymphoid organs (Figure 3), it could be hypothesized that the antiviral effect observed is dependent on GSH. Indeed, GSH can inhibit the replication of viruses by different modes of action [44,45]. For example, it has been reported that administration of GSH permeable analogue GSH-C4 can interfere with the maturation of influenza virus glycoproteins modifying the activity of the host-cell protein disulphide isomerase (PDI) which is essential for the correct disulphide bond formation of viral proteins [47]. Glutathione can interfere with the entry of rhinovirus by inhibiting rhinovirus induction of intercellular adhesion molecule-1 (ICAM-1) mRNA in respiratory epithelial cells [48]. Furthermore, GSH by counteracting the action of reactive oxygen intermediates (ROI), can prevent the activation of NF-kB and HIV replication [49].

I-152 effects against HIV and LP-BM5 can be due to its direct antiviral action, but also to its immunomodulatory activity. In fact, many studies have correlated altered GSH levels with an impaired immune response, suggesting a combination of the highly active antiviral therapy with the GSH replenishment approach [50,51]. Recently, the main functions of GSH in the immune response have been reviewed [52]. Accordingly, a possible immunomodulatory role of I-152 was investigated. In particular, the role of I-152 in Th1/Th2 polarization was studied. In fact, several studies have underlined the correlation between altered GSH levels and an unbalanced Th1/Th2

immune response in favor of Th2 linked to an impaired cytokine production by antigen-presenting cells [42,50,53–56]. The immunomodulatory activity of I-152 was demonstrated in in-vitro systems where the molecule-stimulated IL-27 p28 gene expression and sustained STAT-1-mediated IRF-1 de novo synthesis [24]; moreover, in vivo, it enhanced Th1 response in ovalbumin immunized mice as well as drove Th1 immune responses and CTL activity against HIV antigens [55,56]. Finally, I-152 treatment, by inducing Th1 cytokine production, restored a balanced Th1/Th2 response in mice affected by murine AIDS [42]. Hence, the effect exerted by I-152 on MAIDS can be derived from its dual mechanisms of action: On the one hand, it can directly inhibit viral replication; on the other hand, it can re-establish a correct GSH content favoring the production of cytokines which induce the Th1 immune response (Table 2).

Table 2. Antiviral and immunomodulatory effects of I-152 in MAIDS.

DISEASE PARAMETERS	INFECTED	INFECTED+I-152	
Splenomegaly	+++	+	[42]
Lymphadenopathy	+++	+	[42]
Hypergammaglobulinemia	+++	++	[42]
Proviral DNA in lymphoid organs	+++	+	[42]
B and T cell proliferative index decrease	+++	++	[42]
Th1/Th2 unbalance in favour of Th2	+++	+	[46]

C57BL/6 mice were infected with the LP-MB5 murine leukemia virus stock and treated with I-152. +, minor; ++, moderate; +++, severe.

However, the immunomodulatory activity of I-152 could go beyond the regulation of Th1/Th2 response. In fact, I-152 treatment inhibited total IgG secretion in LP-BM5 infected mice [46] and influenced IgG1/IgG2a ratio in favor of the IgG2a subtype (unpublished results). This second effect is likely the consequence of Th1/Th2 response regulation; in fact, the induction of high IgG1 titers is considered indicative of a Th2-type immune response while high IgG2a are typical of a Th1-type response [57,58]. On the contrary, the inhibition of hypergammaglobulinemia could be the consequence of a lower viral load, but it cannot be excluded that I-152 could also directly affect plasma cell maturation and Ig folding/secretion.

One of the features characterizing murine retrovirus LP-BM5-induced MAIDS is decreased T- and B-cell responses. I-152 treatment was demonstrated to partially restore T and B cell proliferative capacity to mitogens [46]. In this context, Green et al., who had previously demonstrated that monocytic myeloid-derived suppressor cells (M-MDSCs) suppress both T and B cell responses [59,60], found that I-152 could interfere with the suppressive function of M-MDSCs (Green, personal communication). On the whole, these observations suggest that I-152 can influence different components of the immune system. Future studies aimed to shed light on the molecular mechanisms modulated by I-152 will provide further insights into the immunomodulatory activity of this pro-GSH molecule.

5. Conclusions

The data presented in this review show that I-152 is an excellent co-drug able to generate NAC and MEA which can be used to increase intracellular GSH. I-152 has been shown to regulate the intracellular GSH content differently depending on the concentration used and the pre-existing redox states; consequently, different redox-sensitive pathways could be activated or inhibited. For example, it has been reported that different concentrations of NAC cause opposite effects on the GSH/GSSG ratio and on the production of pro-inflammatory cytokines [61,62]. Moreover, pro-GSH molecules such as NAC and MEA could affect cellular processes independently of their ability to influence intracellular GSH/GSSG balance [63,64]. Furthermore, the exact mechanisms through which NAC and MEA can increase GSH levels are not yet completely understood. Preliminary experiments have shown that I-152 can influence different redox-signaling pathways linked to GSH [24] and that NAC and MEA administered alone or in combination are less efficient in raising intracellular GSH [10]. Hence, it

would be interesting to investigate all of these aspects. Moreover, such studies could yield useful information for the design and synthesis of new redox-modulating agents with improved activity.

Author Contributions: A.F. and R.C. literature search and original draft preparation. M.M., M.S., C.Z. and M.R. reviewing and editing. M.S. I-152 synthesis. A.F. and R.C. conception, design, writing, reviewing, and editing of the manuscript. M.M. funding acquisition and supervision.

Funding: This work was partially supported by grants from Urbino University; Ministero dell'Istruzione, dell'Università e della Ricerca (MIUR) (PRIN (Research Projects of National Interest) 2010-2011-prot. 2010PHT9NF_004).

Conflicts of Interest: The authors declare no conflict of interest.

References

1. Forman, H.J.; Zhang, H.; Rinna, A. Glutathione: Overview of its protective roles, measurement, and biosynthesis. *Mol. Asp. Med.* **2009**, *30*, 1–12. [CrossRef] [PubMed]
2. Aquilano, K.; Baldelli, S.; Ciriolo, M.R. Glutathione: New roles in redox signaling for an old antioxidant. *Front. Pharmacol.* **2014**, *5*, 196. [CrossRef] [PubMed]
3. Wang, Y.; Yang, J.; Yi, J. Redox sensing by proteins: Oxidative modifications on cysteines and the consequent events. *Antioxid. Redox Signal.* **2012**, *16*, 649–657. [CrossRef] [PubMed]
4. Ristoff, E.; Larsson, A. Inborn errors in the metabolism of glutathione. *Orphanet J. Rare Dis.* **2007**, *2*, 16. [CrossRef] [PubMed]
5. Ballatori, N.; Krance, S.M.; Notenboom, S.; Shi, S.; Tieu, K.; Hammond, C.L. Glutathione dysregulation and the etiology and progression of human diseases. *Biol. Chem.* **2009**, *390*, 191–214. [CrossRef]
6. Morris, D.; Khurasany, M.; Nguyen, T.; Kim, J.; Guilford, F.; Mehta, R.; Gray, D.; Saviola, B.; Venketaraman, V. Glutathione and infection. *Biochim. Biophys. Acta* **2013**, *1830*, 3329–3349. [CrossRef] [PubMed]
7. Palamara, A.T.; Brandi, G.; Rossi, L.; Millo, E.; Benatti, U.; Nencioni, L.; Iuvara, A.; Garaci, E.; Magnani, M. New synthetic glutathione derivatives with increased antiviral activities. *Antivir. Chem. Chemother.* **2004**, *15*, 83–91. [CrossRef]
8. Cacciatore, I.; Cornacchia, C.; Pinnen, F.; Mollica, A.; Di Stefano, A. Prodrug approach for increasing cellular glutathione levels. *Molecules* **2010**, *15*, 1242–1264. [CrossRef]
9. Cacciatore, I.; Baldassarre, L.; Fornasari, E.; Mollica, A.; Pinnen, F. Recent advances in the treatment of neurodegenerative diseases based on GSH delivery systems. *Oxid. Med. Cell. Longev.* **2012**, *2012*, 240146. [CrossRef]
10. Oiry, J.; Mialocq, P.; Puy, J.Y.; Fretier, P.; Clayette, P.; Dormont, D.; Imbach, J.L. NAC/MEA conjugate: A new potent antioxidant which increases the GSH level in various cell lines. *Bioorg. Med. Chem. Lett.* **2001**, *11*, 1189–1191. [CrossRef]
11. Oiry, J.; Mialocq, P.; Puy, J.Y.; Fretier, P.; Dereuddre-Bosquet, N.; Dormont, D.; Imbach, J.L.; Clayette, P. Synthesis and biological evaluation in human monocyte-derived macrophages of *N*-(*N*-acetyl-L-cysteinyl)-*S*-acetylcysteamine analogues with potent antioxidant and anti-HIV activities. *J. Med. Chem.* **2004**, *47*, 1789–1795. [CrossRef] [PubMed]
12. Rushworth, G.F.; Megson, I.L. Existing and potential therapeutic uses for *N*-acetylcysteine: The need for conversion to intracellular glutathione for antioxidant benefits. *Pharmacol. Ther.* **2014**, *141*, 150–159. [CrossRef] [PubMed]
13. Whillier, S.; Raftos, J.E.; Chapman, B.; Kuchel, P.W. Role of *N*-acetylcysteine and cystine in glutathione synthesis in human erythrocytes. *Redox Rep.* **2009**, *14*, 115–124. [CrossRef] [PubMed]
14. Wang, L.L.; Huang, Y.H.; Yan, C.Y.; Wei, X.D.; Hou, J.Q.; Pu, J.X.; Lv, J.X. *N*-acetylcysteine Ameliorates Prostatitis via miR-141 Regulating Keap1/Nrf2 Signaling. *Inflammation* **2016**, *39*, 938–947. [CrossRef] [PubMed]
15. Dominy, J.E., Jr.; Simmons, C.R.; Hirschberger, L.L.; Hwang, J.; Coloso, R.M.; Stipanuk, M.H. Discovery and characterization of a second mammalian thiol dioxygenase, cysteamine dioxygenase. *J. Biol. Chem.* **2007**, *282*, 25189–25198. [CrossRef] [PubMed]
16. Besouw, M.; Masereeuw, R.; van den Heuvel, L.; Levtchenko, E. Cysteamine: An old drug with new potential. *Drug Discov. Today* **2013**, *18*, 785–792. [CrossRef] [PubMed]

17. O'Brian, C.A.; Chu, F. Post-translational disulfide modifications in cell signaling-role of inter-protein, intra-protein, *S*-glutathionyl, and *S*-cysteaminyl disulfide modifications in signal transmission. *Free Radic. Res.* **2005**, *39*, 471–480. [CrossRef]
18. Medic, G.; van der Weijden, M.; Karabis, A.; Hemels, M. A systematic literature review of cysteamine bitartrate in the treatment of nephropathic cystinosis. *Curr. Med. Res. Opin.* **2017**, *33*, 2065–2076. [CrossRef] [PubMed]
19. Verny, C.; Bachoud-Lévi, A.C.; Durr, A.; Goizet, C.; Azulay, J.P.; Simonin, C.; Tranchant, C.; Calvas, F.; Krystkowiak, P.; Charles, P.; et al. CYST-HD Study Group. A randomized, double-blind, placebo-controlled trial evaluating cysteamine in Huntington's disease. *Mov. Disord.* **2017**, *32*, 932–936. [CrossRef]
20. Fujisawa, T.; Rubin, B.; Suzuki, A.; Patel, P.S.; Gahl, W.A.; Joshi, B.H.; Puri, R.K. Cysteamine suppresses invasion, metastasis and prolongs survival by inhibiting matrix metalloproteinases in a mouse model of human pancreatic cancer. *PLoS ONE* **2012**, *7*, e34437. [CrossRef]
21. Chu, F.; Koomen, J.M.; Kobayashi, R.; O'Brian, C.A. Identification of an inactivating cysteine switch in protein kinase Cepsilon, a rational target for the design of protein kinase Cepsilon-inhibitory cancer therapeutics. *Cancer Res.* **2005**, *65*, 10478–10485. [CrossRef] [PubMed]
22. Wilmer, M.J.; Kluijtmans, L.A.; van der Velden, T.J.; Willems, P.H.; Scheffer, P.G.; Masereeuw, R.; Monnens, L.A.; van den Heuvel, L.P.; Levtchenko, E.N. Cysteamine restores glutathione redox status in cultured cystinotic proximal tubular epithelial cells. *Biochim. Biophys. Acta* **2011**, *1812*, 643–651. [CrossRef] [PubMed]
23. Calkins, M.J.; Townsend, J.A.; Johnson, D.A.; Johnson, J.A. Cystamine protects from 3-nitropropionic acid lesioning via induction of nf-e2 related factor 2 mediated transcription. *Exp. Neurol.* **2010**, *224*, 307–317. [CrossRef] [PubMed]
24. Fraternale, A.; Crinelli, R.; Casabianca, A.; Paoletti, M.F.; Orlandi, C.; Carloni, E.; Smietana, M.; Palamara, A.T.; Magnani, M. Molecules altering the intracellular thiol content modulate NF-kB and STAT-1/IRF-1 signalling pathways and IL-12 p40 and IL-27 p28 production in murine macrophages. *PLoS ONE* **2013**, *8*, e57866. [CrossRef] [PubMed]
25. Griffith, O.W.; Larsson, A.; Meister, A. Inhibition of gamma-glutamylcysteine synthetase by cystamine: An approach to a therapy of 5-oxoprolinuria (pyroglutamic aciduria). *Biochem. Biophys. Res. Commun.* **1977**, *79*, 919–925. [CrossRef]
26. Castellani, P.; Angelini, G.; Delfino, L.; Matucci, A.; Rubartelli, A. The thiol redox state of lymphoid organs is modified by immunization: Role of different immune cell populations. *Eur. J. Immunol.* **2008**, *38*, 2419–2425. [CrossRef] [PubMed]
27. Dröge, W.; Breitkreutz, R. Glutathione and immune function. *Proc. Nutr. Soc.* **2000**, *59*, 595–600. [CrossRef] [PubMed]
28. Fraternale, A.; Brundu, S.; Magnani, M. Glutathione and glutathione derivatives in immunotherapy. *Biol. Chem.* **2017**, *398*, 261–275. [CrossRef]
29. Xiaoyuan, R.; Lili, Z.; Xu, Z.; Vasco, B.; Jun, W.; Cristina, C.; Arne, H.; Jun, L. Redox Signaling Mediated by Thioredoxin and Glutathione Systems in the Central Nervous System. *Antioxid. Redox Signal.* **2017**, *27*, 989–1010.
30. Geon, H.K.; Jieun, E.K.; Sandy, J.R.; Sujung, Y. The Role of Oxidative Stress in Neurodegenerative Diseases. *Exp. Neurobiol.* **2015**, *24*, 325–340.
31. Johnson, W.M.; Wilson-Delfosse, A.L.; Mieyal, J.J. Dysregulation of Glutathione Homeostasis in Neurodegenerative Diseases. *Nutrients* **2012**, *4*, 1399–1440. [CrossRef] [PubMed]
32. Aoyama, K.; Nakaki, T. Impaired glutathione synthesis in neurodegeneration. *Int. J. Mol. Sci.* **2013**, *14*, 21021–21044. [CrossRef] [PubMed]
33. Nowacek, A.; Kosloski, L.M.; Gendelman, H.E. Neurodegenerative disorders and nanoformulated drug development. *Nanomedicine* **2009**, *4*, 541–555. [CrossRef] [PubMed]
34. Pandey, P.K.; Sharma, A.K.; Gupta, U. Blood brain barrier: An overview on strategies in drug delivery, realistic in vitro modeling and in vivo live tracking. *Tissue Barriers* **2015**, *4*, e1129476. [CrossRef] [PubMed]
35. Sonam, K.S.; Guleria, S. Synergistic Antioxidant Activity of Natural Products. *Ann. Pharmacol. Pharm.* **2017**, *2*, 1086.
36. Bahat-Stroomza, M.; Gilgun-Sherki, Y.; Offen, D.; Panet, H.; Saada, A.; Krool-Galron, N.; Barzilai, A.; Atlas, D.; Melamed, E. A novel thiol antioxidant that crosses the blood brain barrier protects dopaminergic neurons in experimental models of Parkinson's disease. *Eur. J. Neurosci.* **2005**, *21*, 637–646. [CrossRef] [PubMed]

37. Githens, S. Glutathione metabolism in the pancreas compared with that in the liver, kidney, and small intestine. *Int. J. Pancreatol.* **1991**, *8*, 97–109.
38. Bhardwaj, P.; Yadav, R.K. Chronic pancreatitis: Role of oxidative stress and antioxidants. *Free Radic. Res.* **2013**, *47*, 941–949. [CrossRef] [PubMed]
39. Brundu, S.; Nencioni, L.; Celestino, I.; Coluccio, P.; Palamara, A.T.; Magnani, M.; Fraternale, A. Validation of a reversed-phase high performance liquid chromatography method for the simultaneous analysis of cysteine and reduced glutathione in mouse organs. *Oxid. Med. Cell. Longev.* **2016**, *2016*, 1746985. [CrossRef]
40. Hara, Y.; McKeehan, N.; Dacks, P.A.; Fillit, H.M. Evaluation of the neuroprotective potential of *N*-Acetylcysteine for revention and treatment of cognitive aging and dementia. *J. Prev. Alzheimers Dis.* **2017**, *4*, 201–206.
41. Boyland, E.; Chasseaud, L.F. Enzyme-catalysed conjugations of glutathione with unsaturated compounds. *Biochem. J.* **1967**, *104*, 95–102. [CrossRef] [PubMed]
42. Brundu, S.; Palma, L.; Picceri, G.G.; Ligi, D.; Orlandi, C.; Galluzzi, L.; Chiarantini, L.; Casabianca, A.; Schiavano, G.F.; Santi, M.; et al. Glutathione depletion is linked with Th2 polarization in mice with a retrovirus-induced immunodeficiency syndrome, murine AIDS: Role of proglutathione molecules as immunotherapeutics. *J. Virol.* **2016**, *90*, 7118–7130. [CrossRef] [PubMed]
43. Morris, D.; Guerra, C.; Donohue, C.; Oh, H.; Khurasany, M.; Venketaraman, V. Unveiling the Mechanisms for Decreased Glutathione in Individuals with HIV Infection. *Clin. Dev. Immunol.* **2012**, *2012*, 734125. [CrossRef] [PubMed]
44. Fraternale, A.; Paoletti, M.F.; Casabianca, A.; Nencioni, L.; Garaci, E.; Palamara, A.T.; Magnani, M. GSH and analogs in antiviral therapy. *Mol. Asp. Med.* **2009**, *30*, 99–110. [CrossRef] [PubMed]
45. Fraternale, A.; Paoletti, M.F.; Casabianca, A.; Oiry, J.; Clayette, P.; Vogel, J.U.; Cinatl, J., Jr.; Palamara, A.T.; Sgarbanti, R.; Garaci, E.; et al. Antiviral and immunomodulatory properties of new pro-glutathione (GSH) molecules. *Curr. Med. Chem.* **2006**, *13*, 1749–1755. [CrossRef] [PubMed]
46. Fraternale, A.; Paoletti, M.F.; Casabianca, A.; Orlandi, C.; Schiavano, G.F.; Chiarantini, L.; Clayette, P.; Oiry, J.; Vogel, J.U.; Cinatl, J., Jr.; et al. Inhibition of murine AIDS by pro-glutathione (GSH) molecules. *Antivir. Res.* **2008**, *77*, 120–127. [CrossRef] [PubMed]
47. Sgarbanti, R.; Nencioni, L.; Amatore, D.; Coluccio, P.; Fraternale, A.; Sale, P.; Mammola, C.L.; Carpino, G.; Gaudio, E.; Magnani, M.; et al. Redox regulation of the influenza hemagglutinin maturation process: A new cell-mediated strategy for anti-influenza therapy. *Antioxid. Redox Signal.* **2011**, *15*, 593–606. [CrossRef] [PubMed]
48. Papi, A.; Papadopoulos, N.G.; Stanciu, L.A.; Bellettato, C.M.; Pinamonti, S.; Degitz, K.; Holgate, S.T.; Johnston, S.L. Reducing agents inhibit rhinovirus-induced up-regulation of the rhinovirus receptor intercellular adhesion molecule-1 (ICAM-1) in respiratory epithelial cells. *FASEB J.* **2002**, *16*, 1934–1936. [CrossRef] [PubMed]
49. Schreck, R.; Rieber, P.; Baeuerle, P.A. Reactive oxygen intermediates as apparently widely used messengers in the activation of the NF-kappa B transcription factor and HIV-1. *EMBO J.* **1991**, *10*, 2247–2258. [CrossRef]
50. Ly, J.; Lagman, M.; Saing, T.; Singh, M.K.; Tudela, E.V.; Morris, D.; Anderson, J.; Daliva, J.; Ochoa, C.; Patel, N.; et al. Liposomal Glutathione Supplementation Restores TH1 Cytokine Response to Mycobacterium tuberculosis Infection in HIV-Infected Individuals. *J. Interferon Cytokine Res.* **2015**, *35*, 875–887. [CrossRef] [PubMed]
51. Cribbs, S.K.; Guidot, D.M.; Martin, G.S.; Lennox, J.; Brown, L.A. Anti-retroviral therapy is associated with decreased alveolar glutathione levels even in healthy HIV-infected individuals. *PLoS ONE* **2014**, *9*, e88630. [CrossRef] [PubMed]
52. Rodrigues, C.; Percival, S.S. Immunomodulatory Effects of Glutathione, Garlic Derivatives, and Hydrogen Sulfide. *Nutrients* **2019**, *11*, 295. [CrossRef] [PubMed]
53. Alam, K.; Ghousunnissa, S.; Nair, S.; Valluri, V.L.; Mukhopadhyay, S. Glutathione-redox balance regulates c-rel-driven IL-12 production in macrophages: Possible implications in antituberculosis immunotherapy. *J. Immunol.* **2010**, *184*, 2918–2929. [CrossRef] [PubMed]
54. Peterson, J.D.; Herzenberg, L.A.; Vasquez, K.; Waltenbaugh, C. Glutathione levels in antigen-presenting cells modulate Th1 versus Th2 response patterns. *Proc. Natl. Acad. Sci. USA* **1998**, *95*, 3071–3076. [CrossRef]
55. Fraternale, A.; Paoletti, M.F.; Dominici, S.; Caputo, A.; Castaldello, A.; Millo, E.; Brocca-Cofano, E.; Smietana, M.; Clayette, P.; Oiry, J.; et al. The increase in intra-macrophage thiols induced by new pro-GSH molecules directs the Th1 skewing in ovalbumin immunized mice. *Vaccine* **2010**, *28*, 7676–7682. [CrossRef]
56. Fraternale, A.; Paoletti, M.F.; Dominici, S.; Buondelmonte, C.; Caputo, A.; Castaldello, A.; Tripiciano, A.; Cafaro, A.; Palamara, A.T.; Sgarbanti, R.; et al. Modulation of Th1/Th2 immune responses to HIV-1 Tat by new pro-GSH

molecules. *Vaccine* **2011**, *29*, 6823–6829. [CrossRef]
57. Liu, X.; Wetzler, L.; Massari, P. The PorB porin from commensal Neisseria lactamica induces Th1 and Th2 immune responses to ovalbumin in mice and is a potential immune adjuvant. *Vaccine* **2008**, *26*, 786–796. [CrossRef]
58. Lefeber, D.J.; Benaissa-Trouw, B.; Vliegenthart, J.F.; Kamerling, J.P.; Jansen, W.T.; Kraaijeveld, K.; Harme, S. Th1-directing adjuvants increase the immunogenicity of oligosaccharide-protein conjugate vaccines protein related to Streptococcus pneumoniae type 3. *Infect. Immun.* **2003**, *71*, 6915–6920. [CrossRef]
59. Green, K.A.; Cook, W.J.; Green, W.R. Myeloid-derived suppressor cells in murine retrovirus-induced AIDS inhibit T- and B-cell responses in vitro that are used to define the immunodeficiency. *J. Virol.* **2013**, *87*, 2058–2071. [CrossRef]
60. O'Connor, M.A.; Fu, W.W.; Green, K.A.; Green, W.R. Subpopulations of M-MDSCs from mice infected by an immunodeficiency-causing retrovirus and their differential suppression of T- vs. B-cell responses. *Virology* **2015**, *485*, 263–273. [CrossRef]
61. Ohnishi, T.; Bandow, K.; Kakimoto, K.; Kusuyama, J.; Matsuguchi, T. Long-Time Treatment by Low-Dose *N*-Acetyl-L-Cysteine Enhances Proinflammatory Cytokine Expressions in LPS-Stimulated Macrophages. *PLoS ONE* **2014**, *9*, e87229. [CrossRef]
62. Dobashi, K.; Aihara, M.; Araki, T.; Shimizu, Y.; Utsugi, M.; Iizuka, K.; Murata, Y.; Hamuro, J.; Nakazawa, T.; Mori, M. Regulation of LPS induced IL-12 production by IFN-γ and IL-4 through intracellular glutathione status in human alveolar macrophages. *Clin. Exp. Immunol.* **2001**, *124*, 290–296. [CrossRef]
63. Liu, M.; Pelling, J.C.; Ju, J.; Chu, E.; Brash, D.E. Antioxidant action via p53-mediated apoptosis. *Cancer Res.* **1998**, *58*, 1723–1729.
64. Okamura, D.M.; Bahrami, N.M.; Ren, S.; Pasichnyk, K.; Williams, J.M.; Gangoiti, J.A.; Lopez-Guisa, J.M.; Yamaguchi, I.; Barshop, B.A.; Duffield, J.S.; et al. Cysteamine modulates oxidative stress and blocks myofibroblast activity in CKD. *J. Am. Soc. Nephrol.* **2014**, *25*, 43–54. [CrossRef]

CHAPTER 2

LP-BM5 infection is a syndrome characterized by lymphadenopathy, hypergammaglobulinemia, immune deficiency induced in C57BL/6 mice injected with LP-BM5 murine leukemia viruses [131][132][133][134]. This model has been already previously used to study the redox alterations induced by the virus mixture and their fallout on Th1/Th2 immune balance. [126][130]. In this work, LP-BM5 infection was considered as a model of hypergammaglobulinemia to establish a role of redox state in IgG folding/assembly and plasma cell maturation.

Original article published in Biochimica et Biophysica Acta (BBA) - Molecular Basis of Disease
Volume 1866, Issue 12, 2020, 165922
Preprint version

I-152, a supplier of *N*-acetyl-cysteine and cysteamine, inhibits immunoglobulin secretion and plasma cell maturation in LP-BM5 murine leukemia retrovirus-infected mice by affecting the unfolded protein response

Fraternale Alessandra[a], Zara Carolina[a], Di Mambro Tomas[a], Manuali Elisabetta[b], Genovese Domenica Anna[b], Galluzzi Luca[a], Diotallevi Aurora[a], Pompa Andrea[a], De Marchis Francesca[c], Ambrogini Patrizia[a], Cesarini Erica[a], Luchetti Francesca[a], Smietana Michaël[d], Green Kathy[e], Bartoccini Francesca[a], Magnani Mauro[a], Crinelli Rita[a]

[a]Department of Biomolecular Sciences, University of Urbino Carlo Bo, Via Saffi 2, 61029 Urbino, Italy

[b]Laboratory of Histopathology and Clinical Chemistry, Istituto Zooprofilattico Sperimentale dell'Umbria e delle Marche "Togo Rosati", 06126 Perugia, Italy

[c]CNR, Institute of Biosciences and Bioresources (IBBR), 06128 Perugia, Italy

[d]Institut des Biomolécules Max Mousseron, Université de Montpellier UMR 5247 CNRS, ENSCM, 34095 Montpellier, France

[e]Department of Microbiology and Immunology, Geisel School of Medicine at Dartmouth, Lebanon, New Hampshire, NH, 03766, USA

Corresponding author: Dr. Alessandra Fraternale, PhD

Department of Biomolecular Sciences, University of Urbino Carlo Bo, 61029 Urbino, Italy Phone:+39-0722-305243

email: alessandra.fraternale@uniurb.it

List of abbreviations

ABTS=2,2′-Azino-di-(3-ethylbenzothiazoline)-6-sulfonic acid) ATF6=activating transcription factor 6α (ATF6α)

BiP=binding immunoglobulin protein

CHAC1=ChaC glutathione-specific γ-glutamylcyclotransferase 1 ER=endoplasmic reticulum

GSH=reduced glutathione HRP=horseradish peroxidase IgG=immunoglobulins G

IRE1=inositol-requiring transmembrane kinase/endonuclease 1 MAIDS=murine AIDS

PC=plasma cell

PDI=protein disulfide isomerase

PERK=PKR-like endoplasmic reticulum kinase (PERK) s-XBP-1=spliced X-box-binding protein 1

UPR=unfolded protein response

ABSTRACT

Excessive production of immunoglobulins (Ig) causes endoplasmic reticulum (ER) stress and triggers the unfolded protein response (UPR). Hypergammaglobulinemia and lymphadenopathy are hallmarks of murine AIDS that develops in mice infected with the LP-BM5 murine leukemia retrovirus complex. In these mice, Th2 polarization and aberrant humoral response have been previously correlated to altered intracellular redox homeostasis. Our goal was to understand the role of the cell's redox state in Ig secretion and plasma cell (PC) maturation To this aim, LP-BM5-infected mice were treated with I-152, an *N*-acetyl-cysteine and cysteamine supplier. Intraperitoneal I-152 administration (30 μmol/mouse three times a week for 9 weeks) decreased plasma IgG and increased IgG/Syndecan 1 ratio in the lymph nodes where IgG were in part accumulated within the ER. PC containing cytoplasmic inclusions filled with IgG were present in all animals, with fewer mature PC in those treated with I-152. Infection induced up-regulation of signaling molecules involved in the UPR, i.e. CHAC1, BiP, sXBP-1 and PDI, that were generally unaffected by I-152 treatment except for PDI and sXBP-1, which have a key role in protein folding and PC maturation, respectively. Our data suggest that one of the mechanisms through which I-152 can limit hypergammaglobulinemia in LP-BM5-infected mice is by influencing IgG folding/assembly as well as secretion and affecting PC maturation.

Key words: hypergammaglobulinemia, UPR, endoplasmic reticulum, glutathione pro-drug, murine AIDS

1. INTRODUCTION

A syndrome characterized by lymphadenopathy, hypergammaglobulinemia, and immunodeficiency, known as murine AIDS (MAIDS), develops in C57BL/6 mice infected with LP-BM5 murine leukemia viruses [1-4]. Several abnormalities in immune function are characteristic of mice with MAIDS [5-7]. An early period characterized by high viral replication and immune responsiveness is followed by a lasting and profound immunosuppression that affects several aspects of cellular and humoral immunity [4]. LP-BM5 infection induces progressive lymph proliferation and most lymphoid cells are involved in the proliferative process [4]. Alterations in the humoral immune system such as rapid B cell proliferation, polyclonal activation of B cells, increase in Ig-secreting B cells and development of significant hypergammaglobulinemia have been described [4,8].

The terminal differentiation of B cells to plasma cells (PC) requires important changes in both the cellular structure and function [9]. During PC differentiation, the production of Ig heavy and light chain transcripts and proteins are significantly elevated. This coincides with a significant expansion of the rough endoplasmic reticulum (ER) where the nascent Ig chains are folded, assembled and, inspected by the ER quality control apparatus [10]. Moreover, in a viral infection, viruses exploit cellular machineries and resources to complete their life cycle. In virus-infected cells, the cellular translation machinery is hijacked by the infecting virus to produce large amounts of viral proteins, which inevitably perturb ER homeostasis and cause ER stress [11]. Disturbances of ER homeostasis cause overload of unfolded or misfolded proteins in the ER lumen resulting in ER stress with subsequent triggering of cytoprotective signaling pathway (UPR). ER stress can activate three parallel pathways: PKR-like endoplasmic reticulum kinase (PERK), activating transcription factor 6α (ATF6α), and inositol-requiring transmembrane kinase/endonuclease 1 (IRE1) [12].

The UPR up-regulates synthesis of ER chaperones and folding enzymes, i.e. BiP (Binding immunoglobulin protein), also referred to as Hspa5 (Heat shock 70-kDa protein 5) or GRP78 (glucose-regulated protein 78), protein disulfide isomerase (PDI), and transcription factors, i.e. X-box binding protein 1 (XBP-1) to ensure efficient antibody (Ab) assembly and to coordinate the enhanced membrane biosynthesis necessary for generation of the highly developed ER network that is characteristic of PC [9,13-15]. Hence, UPR signaling has increasingly been shown to have a crucial role in immunity [16]. Of the three ER stress responses, the best studied in PC is the IRE1 pathway. IRE1 is an ER-localized transmembrane protein with endoribonuclease activity that excises a 26-nt sequence from XBP-1 messenger RNA (mRNA) [17,18]. This event, termed XBP-1 splicing, shifts the reading frame to excise a premature stop codon, resulting in a full-length functional XBP-1 protein product (sXBP-1). sXBP-1 then translocates to the nucleus where it induces target genes expression involved in protein synthesis and secretion [19-21]. XBP-1 expression, is induced dramatically during PC differentiation in response to cytokines such as IL-4 and it is required for high Ig expression and the morphological changes that enable the PC to secrete large amounts of Ab [22-24]. Recent studies support the view that ER protein folding pathways are highly correlated with ROS production and that redox homeostasis is crucial for correct protein folding process and disulfide bond formation [25-27). Moreover, the correct concentrations of glutathione are necessary to maintain ER oxidoreductases in a reduced form or facilitate the

reduction of polypeptides destined for retro- translocation from the ER to the cytosol for degradation [28].

We have previously demonstrated that LP-BM5 infection induces significant drops in reduced glutathione (GSH) and/or cysteine concentration early during infection, i.e. 2-5 weeks post infection (p.i.), when the viral replicative rate is high and a Th2-type cytokine polarization develops [5]. Moreover, the treatment of LP-BM5-infected mice with a pro-GSH molecule [*N*-(*N*-acetyl-L- cysteinyl)-*S*-acetylcysteamine] named I-152, increases GSH levels in several organs and shifts the immune response towards the cellular immunity by influencing early Th1/Th2 cytokine secretion [5, 29). In this study, we investigated whether I-152 treatment could also affect the later phase of the disease characterized by the lymphoproliferative process and high IgG production. We found that the infection induced the major UPR components and increased the expression of UPR targets including the ER chaperons. I-152 treatment lowered plasma IgG concentration and partially accumulated IgG inside the ER of PC. In the lymph nodes of infected/treated mice, fewer mature PC . and a decrease in PDI and sXBP-1 expression were found. Taken together, these results suggest that I-152 treatment inhibits total IgG production by interfering with maturation and secreting capacity of PC as well as with the folding of Ig.

2. MATERIALS AND METHODSEthics statement

Adult mice were used according to the Italian law on animal experimentation (D.lgs 26/2014; research project permitted with authorization N. 279/2015-PR by Italian Ministry of Health). Every effort was made to minimize the number of animals used and their suffering.

2.2. Mice

Four-week-old female C57BL/6 (B6) mice were purchased from Charles River Laboratories Italy and housed in the animal facility of the Department of Biomolecular Sciences (University of Urbino), which is approved by the Health Ministry of Italy.

2.3. LP-BM5 virus inoculation and treatment with I-152

The LP-BM5 viral mixture was prepared by co-culturing G6 cells with uninfected SC-1 cells as previously described [2]. C57BL/6 mice were infected by two successive intraperitoneal (i.p.) injections at 24-h intervals of the LP-MB5 murine leukemia virus stock, in which each injection contained 0.25 units of reverse transcriptase. A group of LP-BM5-infected mice was left untreated (infected mice, I); another one was treated with i.p. injections of I-152 (30 μmol/mouse) three times a week, every other day, for a total of 9 weeks (infected/treated mice, I+I-152). I-152 was synthesized as previously described [30]. Mice were sacrificed at specific time points: early in the course of infection, i.e. 2 weeks post infection (p.i.), when a severe immunological reaction in response to infection develops; 5 weeks, when B cell proliferation and increased number of Ig- secreting cells result in the development of hypergammaglobulinemia and enlarged lymphoid organs; 9 weeks, when the absolute number of Ig-secreting cells and circulating Ig levels do not change or decline.

2.4. Plasma IgG, IgG1 and IgG2a determination

Total IgG, IgG1 and IgG2a levels were determined using an enzyme-linked immunosorbent assay (ELISA) technique as previously described [31]. Briefly, the microplates (Nunc-immuno Plate MaxiSorp Surface, Nunc) were coated with goat anti-mouse IgG (Sigma-Aldrich, Milan, Italy), IgG1 or IgG2a (Bio-Rad, Hercules, CA, USA). After blocking with 5% bovine serum albumin (BSA), serial dilutions of murine plasma were added to each well. Immunocomplexes were revealed by using goat anti-mouse IgG-horseradish peroxidase (HRP) conjugated (Bio-Rad, Richmond, CA, USA), and the 2,2′-azino-di-(3-ethylbenzthiazoline sulfonic acid) or ABTS (Roche Diagnostic, Penzberg, Germany) substrate. Absorbance was measured at 405 nm on a Model Benchmark Microplate reader (Bio-Rad, Hercules, CA, USA). Absolute plasma IgG concentrations were calculated using known concentrations of standard mouse IgG.

2.5. Gene expression analysis

Total RNA was extracted with miRNeasy mini kit (Qiagen) from lymph nodes (7-20 mg) disrupted in 700 μl Qiazol and homogenized using QIAshredder spin columns (Qiagen, Hilden, Germany). The cDNA was synthesized using the PrimeScript™ RT Master Mix (Perfect Real Time) (Takara, Kusatsu, Shiga, Japan) from 0.5 μg total RNA, according to the manufacturer's instructions.

The real time PCR reactions were performed in a RotorGene 6000 instrument (Corbett life science, Sydney,

Australia) in duplicate, using RT^2 SYBR® Green ROX FAST Mastermix (Qiagen, Hilden, Germany) and the primers listed in Table 1. The amplification conditions were: 95°C for 10 min, 40 cycles at 95°C for 10 s and 60°C for 50 s. Relative mRNA expression was determined with the $2^{-\Delta\Delta Ct}$ method (48), using β-2 microglobulin (B2M) as a reference gene and uninfected mice as calibrator.

Table 1. Target mRNA and real time PCR primers used in this study.

mRNA	Accession number	Primer F (5'-3')	Primer R (5'-3')	Ref
B2M	NM_009735	TGCTATCCAGAAAACCCCTCAA	GGATTTCAATGTGAGGCGGG	32
BiP	NM_001163434	TCCGGCGTGAGGTAGAAAAG	GGCTTCATGGTAGAGCGGAA	32
CHAC1	NM_026929	TATAGTGACAGCCGTGTGGG	GCTCCCCTCGAACTTGGTAT	32
sXBP-1	NM_001271730	CTGAGTCCGCAGCAGGT	TGTCCAGAATGCCCAAAAGG	32
P4hb (PDI)	NM_011032	GATCAAGCCCCACCTGATGA	ACCTCTTCAAAGTTCGCCCC	33

B2M, Mus musculus Beta-2-Microglobulin; BiP, Mus musculus heat shock protein 5;

CHAC1, Mus musculus ChaC, cation transport regulator 1;

sXBP-1, Mus musculus X-Box Binding Protein 1, transcript variant 2 (spliced);

P4hb (PDI), Mus musculus prolyl 4-hydroxylase, beta polypeptide (Protein disulfide-isomerase)

2.6. Organ homogenization and western immunoblotting analysis

The lymph nodes were excised flash frozen in dry ice and stored at -80°C until processing. Organs were homogenized by sonication at 100 Watts in 8 volumes (w/v) of a buffer containing 50 mM Tris- HCl, pH 7.8, 0.25 M sucrose, 2% (w/v) SDS (Sodium Dodecyl Sulphate), 10 mM N-ethylmaleimide, completed with a cocktail of protease (Roche, Basilea, Switzerland) and phosphatase inhibitors (1 mM NaF, 1 mM Na_3VO_4). The lysates were boiled and, after centrifugation, the protein content was determined in the supernatant by the Lowry assay, using bovine albumin as a standard. Proteins were resolved by SDS-PAGE and electroblotted onto a PVDF membrane (0.2 µm) (Bio-Rad, Hercules, CA, USA). The blots were probed with the following primary antibodies: anti-BiP (C05B12) and anti- PDI (C81H6) from Cell Signaling Technology (Danvers, Massachusetts, USA); anti-XBP-1 (M-186, sc- 7160) and anti Syndecan-1 (H-174, sc-5632) from Santa Cruz Biotechnology Inc., Dallas, Texas, USA). Anti-Actin (A 2066, Sigma-Aldrich, Milan, Italy) was used to check equal protein loading. The bands were detected by HRP-conjugate secondary antibody (Bio-Rad, Hercules, CA, USA) and the HRP activity was detected with the enhanced chemiluminescence detection kit WesternBright ECL (Advansta, Bering Dr, San Jose, CA USA). Lymph node IgG levels were detected by using goat anti- mouse IgG (H+L) HRP-conjugate (Bio-Rad, Hercules, CA, USA). Immunoreactive bands were visualized in a ChemiDoc MP Imaging System and quantified with the Image Lab software (Bio-Rad, Hercules, CA, USA).

2.7. Subcellular fractionation

IgG subcellular localization was studied by fractionation of lymph node homogenates by differential centrifugation. The lymph nodes were homogenized in a buffer consisting of 12 % (w/v) sucrose, 10 mM KCl, 2 mM $MgCl_2$, 100 mM Tris-Cl, pH 7.8. A continuous gradient between 16% and 55% (w/v) sucrose was made using the same buffer, and 1 mL of the homogenate was loaded on top of the gradient. After centrifugation at 141,000 x *g* for 4 h at 4°C in a Beckman SW28 rotor, fractions of 0.780 mL were collected. An equal aliquot of each fraction was analyzed by SDS-PAGE and protein blot with anti-mouse IgG-HRP and anti-BiP antibodies (as above).

2.8. Histological analysis

The lymph nodes were fixed in 10% neutral buffered formalin and paraffin-embedded with standard procedures. Four µm thick sections were stained with Haematoxylin and Eosin (H&E) for histological and morphological investigations. Image digitization and semiquantitative analysis of PC were performed using the microscope Eclipse Ci-L (Nikon Corporation, Japan) and NIS-Elements Br-2 as software (v 5.10; Nikon). For semiquantitative analysis, the sections were initially scanned at intermediate (20x) magnification to assess the distribution of PC. Then, at high magnification (40x), the fields containing more PC, were analyzed and the average of the counts of the cells performed in 5 microscopic fields was calculated.

Among the PC observed, a discrimination between mature (differentiated) and immature (undifferentiated) PC, was performed. Differentiated PC have a heavily clumped chromatin network, absence of nucleolus, a perinuclear pale zone and high cytoplasmic nuclear ratio. Mott cells (morular or graped cells) are included in this population. Immature PC showed instead one prominent nucleolus, finely dispersed/vesicular chromatin, a lower cytoplasmic nuclear ratio and a cytoplasm sometimes occupied by small optical empty vesicles. Flaming cells containing a large cytoplasm with several intracytoplasmic vacuoles and binucleated cells were also counted in immature cells.

2.9. Immunofluorescence staining

Sections of 6-µm thickness from paraffin-embedded lymph nodes were processed to detect the ER chaperon BiP and mouse IgG antibodies. Deparaffinized and rehydrated sections were rinsed in Tris 0.1 M, pH 7.6 at 37°C for 30 min and then incubated with pronase (*Streptomyces griseus*; Sigma- Aldrich, Milan, Italy). Then the sections were blocked with goat serum and horse serum before overnight incubation with the anti-BiP antibody. CY3-labelled goat anti-rabbit IgG (Amersham Bioscences, UK) and fluorescein (isothiocyanate) (FITC)-conjugated horse anti-mouse IgG antibody (DBA, Vector, Italy) were used to detect BiP and intracellular IgG, respectively. A Leica TCS-SL confocal microscope, equipped with Argon and He/Ne laser sources, was used to detect the florescence signal.

2.10. Statistical analysis

Statistical analysis was performed using one-way ANOVA followed by Tukey post-test when 3 experimental groups were compared or Mann Whitney test when 2 experimental groups were compared (GraphPad Software, Inc., La Jolla, CA, USA).

3. RESULTS

3.1. Plasma IgG and IgG isotypes are affected by I-152 treatment

LP-BM5-infected mice develop an unusual proliferation and polyclonal activation of B cells resulting in abnormal Ig production and secretion [3,8]. In agreement with previous findings [8], plasma IgG significantly increased in infected mice (I) at 2 weeks (Figure 1A), peaked at 5 weeks (Figure 1B) and then slightly declined at 9 weeks (Figure 1C). The same trend was observed in infected/treated mice (I+I-152); however, at 5 weeks, IgG levels were significantly lower compared with infected animals (Figure 1B).

IgG isotypes (IgG1 and IgG2a) displayed a predominance of IgG1 in infected mice, indicating a prevalent humoral immune response, in the early phase of infection (2 weeks) (Figure 1D), as previously reported [5]. Notably, IgG1 levels were significantly lower in infected/treated mice (I+I-152) compared to infected animals (I), in agreement with the propensity of I-152 to induce Th1 driven immune responses [5]. The progression of viral infection (5 weeks) was characterized in both experimental groups by a decrease in IgG1 levels and an increase in IgG2a concentration (Figure 1E). At 9 weeks, both IgG1 and IgG2a decreased, but interestingly, the Th1 associated IgG2a subtype was higher in infected/treated mice than in the infected ones (Figure 1F).

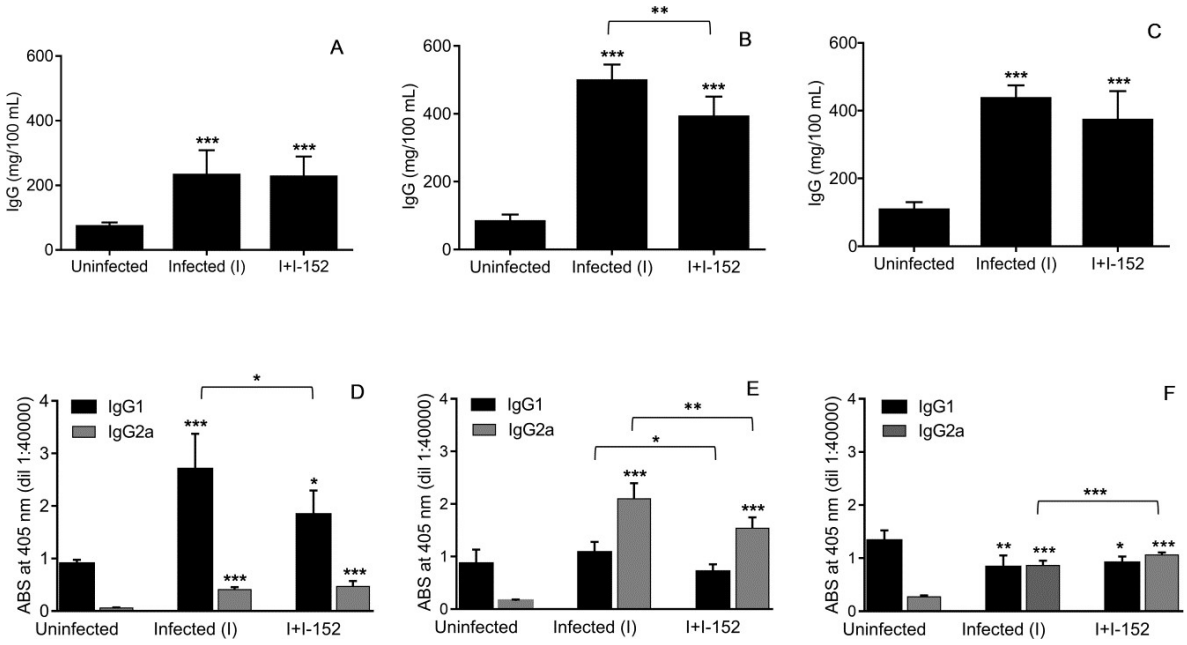

Figure 1. Plasma IgG (A-C), IgG1 and IgG2a (D-F) in uninfected, infected/untreated (I) and infected/treated (I+I-152) mice. Mice were infected by two successive i.p. injections at 24-h intervals each containing 0.25 units of reverse transcriptase. I-152-treated mice received I-152 intraperitoneally (30 μmoles/mouse), every other day, for a total of 9 weeks. At 2 (A, D), 5 (B, E), and 9 (C, F) weeks after virus inoculation, IgG and IgG isotypes were determined in plasma by a double- sandwich ELISA by using anti-mouse IgG, IgG1 or IgG2a as capture antibody and rabbit anti-mouse HRP-conjugated IgG as detection antibody. Detection was performed by addition of 2,2′-Azino-di-(3- ethylbenzothiazoline)-6-sulfonic acid) or ABTS as substrate for horseradish peroxidase (HRP) and absorbance was measured at 405 nm. The values are the mean ± S.D. of 5 animals per group. Statistically significant differences are represented as follows:
*$p < 0.05$; **$p < 0.01$, ***$p < 0.001$.

3.2. IgG levels in the lymph nodes are affected by I-152 treatment

To investigate the molecular mechanisms underlying the inhibitory effect exerted by I-152 on IgG

production/secretion, further analyses were performed on the lymph nodes that represent one of the major sites where B cells are activated to produce and release Ig [34].

As shown in Figure 2 (A-C), a statistically significant increase in the IgG content was detected at all the time points studied. In agreement with the results obtained in plasma, significantly lower IgG levels were found in the lymph nodes of infected/treated animals (I+I-152) than in infected mice (I) at 5 weeks p.i. (Figure 2B).

Expression of the PC marker Syndecan-1 [35,36] was significantly increased in infected (I) compared to uninfected mice at 2 and 5 weeks, consistently with the maturation of Ab-producing PC (Figure 2D, E). By contrast, in the infected/treated mice (I+I-152) Syndecan-1 levels were never significantly different from those detected in the uninfected group (Figure 2D, E), despite the increase in the IgG content observed (Figure 2A, B). At 5 weeks, Syndecan-1 staining was significantly lower in infected/treated animals than in infected mice, suggesting that an impairment in PC maturation/survival may occur after I-152 treatment (Figure 2E). This hypothesis may also explain the drop in the lymph node IgG content detected at the same time point (Figure 2B).

Interestingly, normalization of IgG levels on Syndecan-1 signal (Figure 2G-I) resulted in a significant higher value in I+I-152 mice compared to the infected ones at 2 weeks (Figure 2G), suggesting that the effect of I-152 on PC observed at 5 weeks is preceded by intracellular accumulation of IgG.

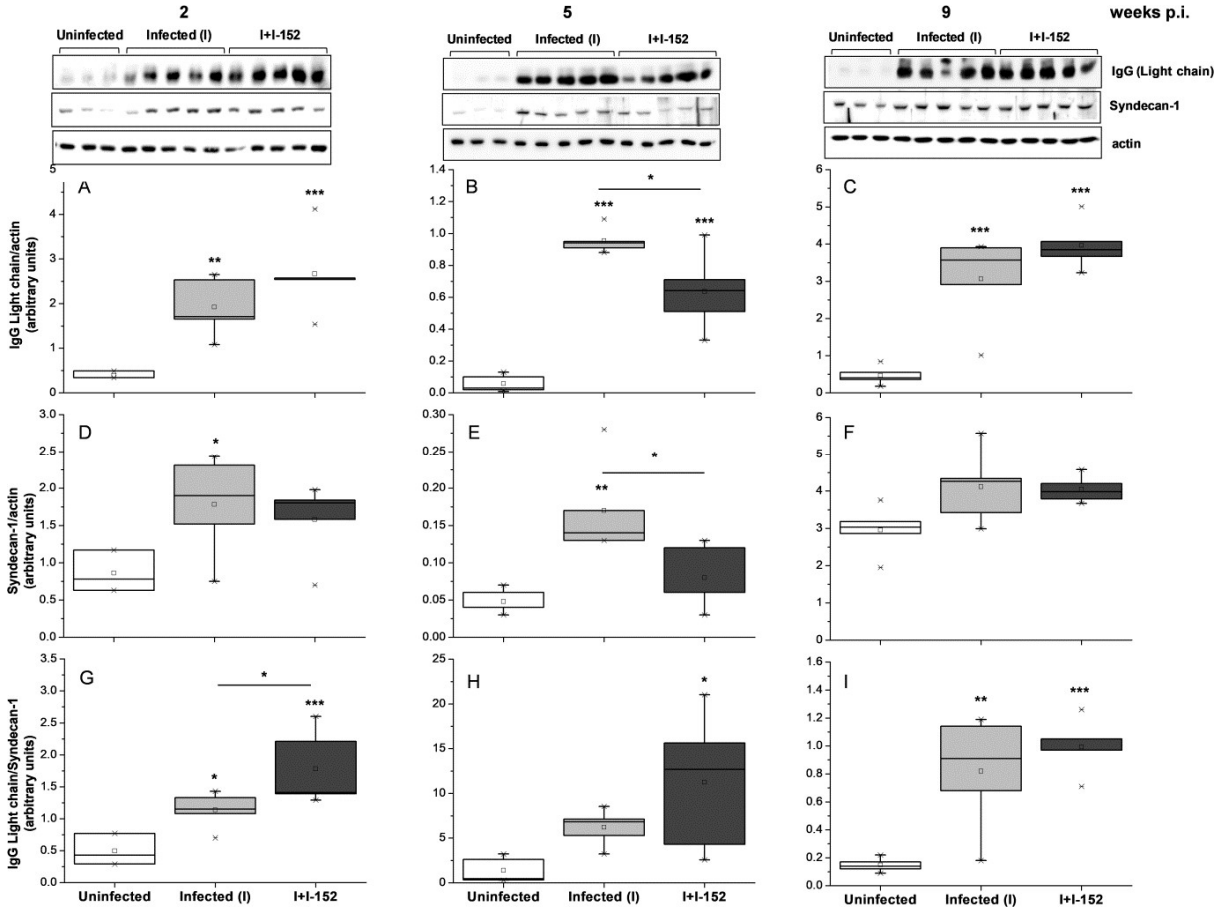

Figure 2. Western immunoblotting analysis of IgG (A-C) and Syndecan-1 (D-F) levels in the lymph nodes of uninfected, infected/untreated (I) and infected/treated (I+I-152) mice. Lymph nodes were excised at 2, 5 and 9 weeks p.i. After homogenization, lysates were separated on SDS-PAGE gels, transferred to PVDF membrane and probed for the indicated proteins by using specific antibodies. Actin was stained as loading control. Immunoreactive bands were quantified with the Image Lab software and IgG and Syndecan-1 levels, normalized on actin, are reported in the graphs. In the panels G-I, IgG/Syndecan-1 ratio calculated for each experimental group is reported. Bars represent the mean ± S.D. of at least 3 values obtained from uninfected mice and of 5 values obtained from infected/untreated and infected/treated mice. For simplicity, only the IgG light chain is shown. Statistically significant differences are represented as follows:
*$p < 0.05$; **$p < 0.01$, ***$p < 0.001$.

An imbalance of the redox state towards a more reducing environment is expected to affect folding of the Ig within the ER, because of an impairment in disulfide bond formation [25-27]. To test this hypothesis, the subcellular localization of IgG in the lymph nodes of LP-BM5-infected mice either untreated or treated with I-152, was evaluated by fractionation of whole homogenates by isopycnic sucrose gradient centrifugation. The results reported in Figure 3 show that a significant amount of IgG co-localizes with the ER marker BiP (fractions 10-12) in the infected/treated animals (I+I-152), but not in the infected group (I), supporting the idea that I-152 may interfere with IgG folding, leading to IgG accumulation within the ER, and impairing their extracellular secretion [37].

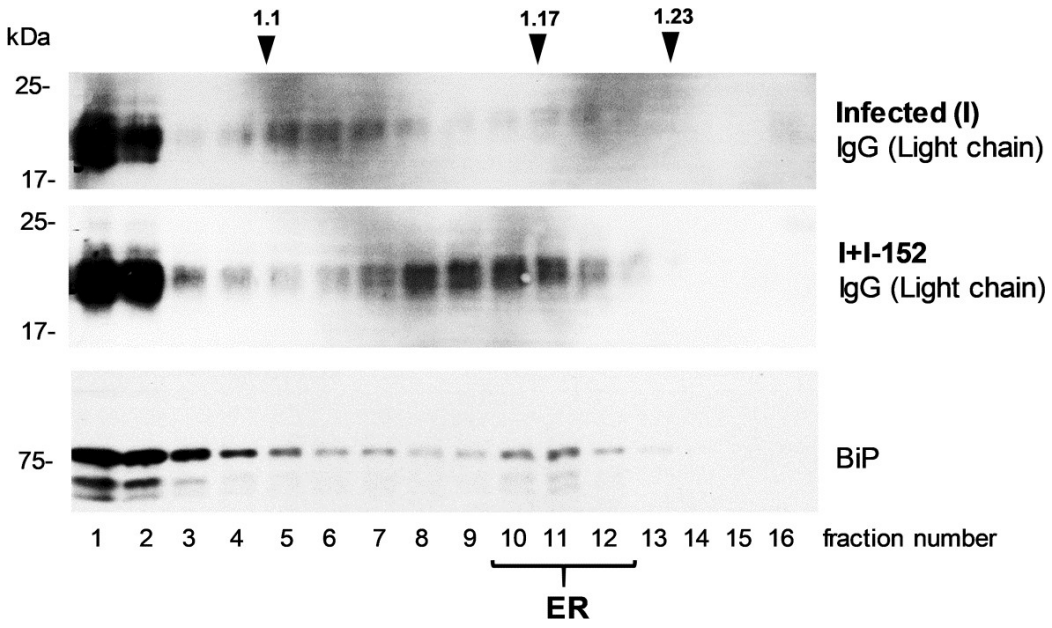

Figure 3. ER retention of IgG in lymph nodes of infected/untreated (I) and infected/treated (I+I-152) mice. Total proteins extracted from lymph nodes of LP-BM-infected mice either untreated (I) or treated with I-152 for 2 weeks (I+I-152) were fractionated by centrifugation on an isopycnic Suc gradient. Proteins from each fraction were analyzed by SDS-PAGE and immunoblotting using anti-IgG or anti-BiP antiserum. The top of the gradients is on the left; numbers on the top indicate density (g−1 mL); numbers on the bottom indicate the gradient fractions. ER fractions are underlined. The positions of molecular mass markers in kD are indicated by numbers on the left of the panels.

3.3. Activation of ER stress markers is partially affected by I-152 treatment

Maturation and folding of IgG rely on the activity of ER-resident chaperones and folding enzymes, particularly BiP and PDI. BiP has an important role in the folding and assembly of secretory proteins [38,39]; PDI forms and isomerizes disulfide bonds and its concentration in lymphocytes corresponds to their antibody secretion rate [40, 41]. The mRNA analysis showed that in infected mice, both I and I+I-152, BiP was induced at 2 weeks, then it further increased at 5 weeks, plateauing at 9 weeks (Figure 4A). A strong induction of BiP protein expression was also revealed by western blotting analysis; however, differences between the two groups were observed neither at 2 weeks (Figure 4B) nor at the following time points (not shown).

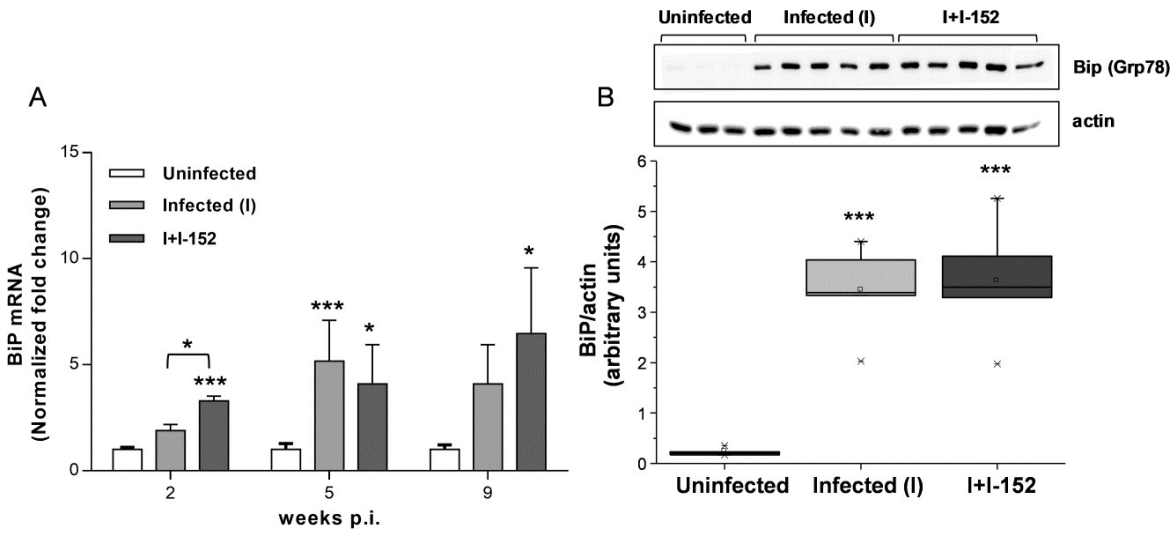

Figure 4. BiP expression in the lymph nodes of uninfected, infected/untreated (I) and infected/treated (I+I-152) mice. (A) Lymph nodes were excised at 2, 5 and 9 weeks p.i. After total RNA extraction and cDNA synthesis, relative mRNA expression was determined by real-time PCR with the $2^{-\Delta\Delta Ct}$ method using β-2 microglobulin (B2M) as a reference gene and uninfected mice as calibrator. The values are the mean ± S.D. of at least 3 animals per group. (B) protein extracts (5 µgs) obtained from mouse lymph nodes excised at 2 weeks p.i. were resolved onto a 10% SDS polyacrylamide gel and immunoblotted with an anti BiP antibody. Actin was stained as loading control. BiP levels, normalized on actin, are reported in the graph. Bars represent the mean ± S.D. of at least 3 values obtained from uninfected mice and of 5 values obtained from infected/untreated and infected/treated mice. Statistically significant differences are represented as follows:
*p < 0.05; **p < 0.01, ***p < 0.001.

In the case of PDI, mRNA levels were unchanged after infection, however, protein levels tended to increase in the 2 week-infected mice (I) as compared to the uninfected. Post-transcriptional induction of PDI was abrogated in I-152 treated mice (Figure 5B).

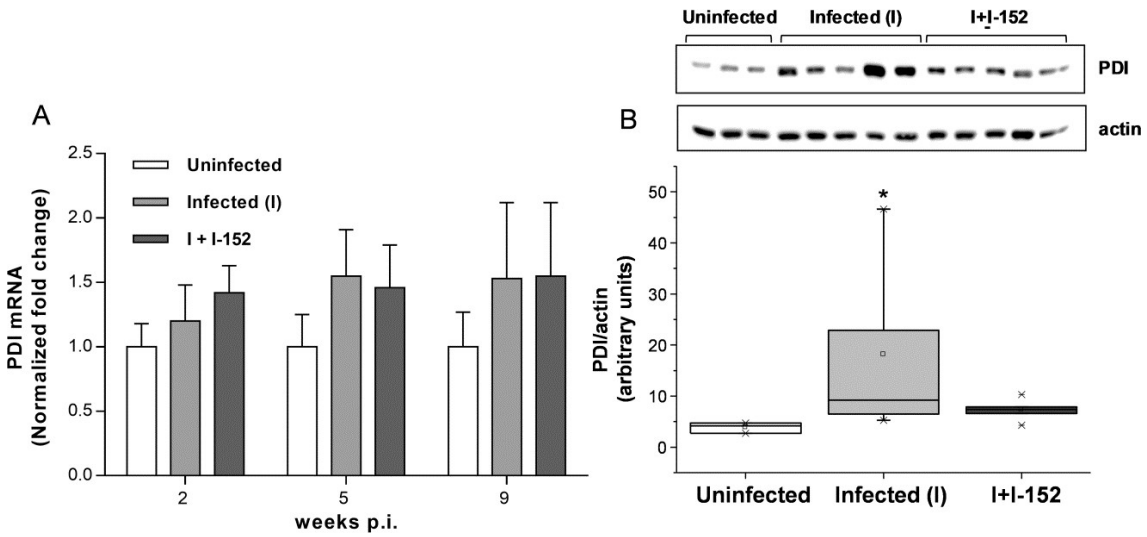

Figure 5. PDI expression in the lymph nodes of uninfected, infected/untreated (I) and infected/treated (I+I-152) mice. (a) Lymph nodes were excised at 2, 5 and 9 weeks p.i. After total RNA extraction and cDNA synthesis, relative mRNA expression was determined by real-time PCR with the $2^{-\Delta\Delta Ct}$ method using β-2 microglobulin (B2M) as a reference gene and uninfected mice as calibrator. The values are the mean ± S.D. of at least 3 animals per group. (b) protein extracts (5 µgs) obtained from mouse lymph nodes excised at 2 weeks p.i. were resolved onto a 10% SDS polyacrylamide gel and immunoblotted with an anti PDI antibody. Actin was stained as loading control. PDI levels, normalized on actin, are reported in the graph. Bars represent the mean ± S.D. of at least 3 values obtained from uninfected mice and of 5 values obtained from infected/untreated and infected/treated mice. *$p < 0.05$.

The UPR pathway plays also a central role in PC development and directs events leading to humoral immunity [19-22,24]. In particular, sXBP-1 regulates the transcription of genes involved in ER expansion, protein folding and synthesis in PC [17,20,21]. sXBP-1 mRNA and protein levels were strongly induced after infection (Figure 6). A significant reduction in sXBP-1 mRNA and protein contents were observed in infected/treated mice (I+I-152) compared to the infected ones (I) at 5 weeks (Figure 6A and 6B, respectively).

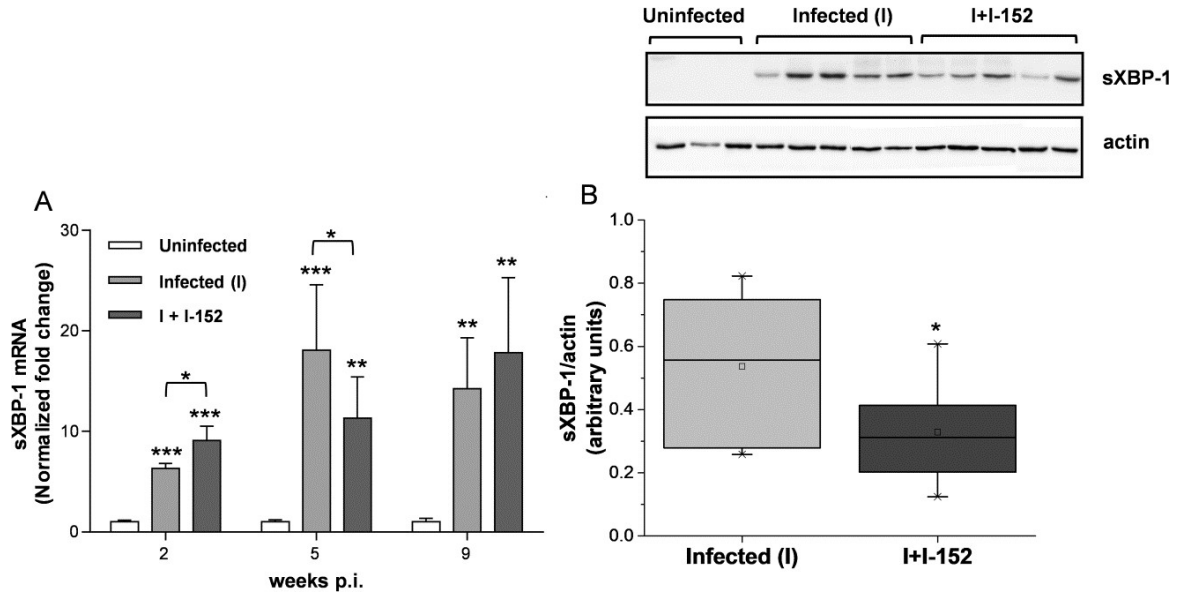

Figure 6. sXBP-1 expression in the lymph nodes of uninfected, infected/untreated (I) and infected/treated (I+I-152) mice. (A) Lymph nodes were excised at 2, 5 and 9 weeks p.i. After total RNA extraction and cDNA synthesis, relative mRNA expression was determined by real-time PCR with the $2^{-\Delta\Delta Ct}$ method using β-2 microglobulin (B2M) as a reference gene and uninfected mice as calibrator. The values are the mean ± S.D of at least 3 animals per group. (B) protein extracts (20 μgs) obtained from mouse lymph nodes excised at 5 weeks p.i. were resolved onto a 10% SDS polyacrylamide gel and immunoblotted with an antibody which recognizes the spliced XBP-1 isoform (sXBP-1). Actin was stained as loading control. sXBP-1 levels, normalized on actin, are reported in the graph. Bars represent the mean ± S.D. of 6 values obtained from infected/untreated and infected/treated mice. Statistically significant differences are represented as follows: *p < 0.05; **p < 0.01, ***p < 0.001.

Another ER-stress marker strongly up-regulated by infection was CHAC1 which is involved in degradation of cytosolic glutathione in mammalian cells through its γ-glutamylcyclotransferase activity [42]. As shown in Figure 7, differences in CHAC1 mRNA expression were not observed between I and I+I-152 mice; moreover, protein was undetectable at 2 weeks while it was immunostained at 5 and 9 weeks, but its content was not altered by I-152 treatment (not shown).

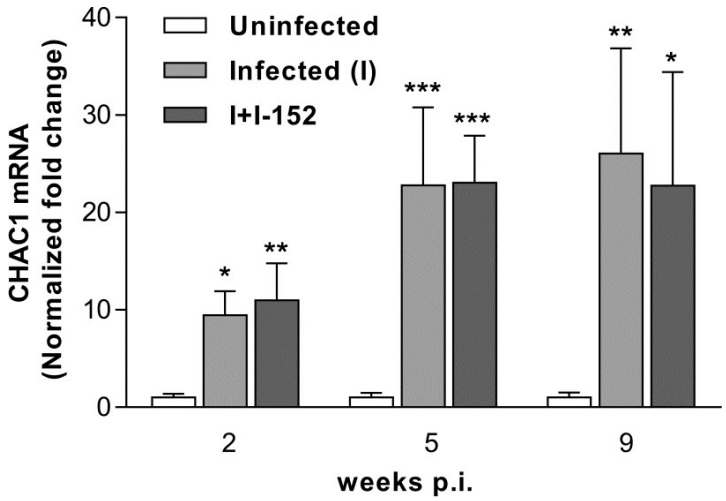

Figure 7. CHAC1 expression in the lymph nodes of uninfected, infected/untreated (I) and infected/treated (I+I-152) mice. Lymph nodes were excised at 2, 5 and 9 weeks p.i. After total RNA extraction and cDNA synthesis, relative mRNA expression was determined by real-time PCR with the $2^{-\Delta\Delta Ct}$ method using β-2 microglobulin (B2M) as a reference gene and uninfected mice as calibrator. The values are the mean ± S.D of at least 3 animals per group. Statistically significant differences are represented as follows:
*$p < 0.05$; **$p < 0.01$, ***$p < 0.001$.

3.4. PC morphological maturation is affected by I-152 treatment

Lymph node architecture is severely altered by LP-BM5 infection; for this reason, lymph node histopathology has been considered as a useful indicator of disease progression [43,44]. At 2 weeks, differences between infected and uninfected mice were not yet visible and secondary follicles with germinal centers were still present in infected animals (Figure 8A).

At 5 weeks after infection, the typical lymph node architecture was no longer present in infected mice as the presence of architectural effacement, characterized by cellular monomorphism, prevailed not allowing to distinguish the follicular structures (Figure 8B). Meanwhile, the number of PC was increased in response to LP-BM5 infection. By contrast, in I-152-treated mice the lymph node architecture, although modified, maintained some characteristics such as the presence of primary follicles (Figure 8C). An expanded lymphatic sinus network, which could reflect an increased lymph flow through the medullary lymphatic sinuses, was observed as well. The histological features of the lymph nodes after 9 weeks of infection were not significantly different from those observed at 5 weeks (not shown).

Particular attention was focused on PC morphology of infected mice (Figure 8D-F). It is known that excessive amount of proteins, which can neither be secreted nor degraded, can be accumulated into intracytoplasmic spherical inclusions, named Russell bodies [45-47]. At 5 weeks, in all the infected animals, either untreated or

treated, we observed several PC containing multiple varied size spherical inclusions, likely Russell bodies structures (Mott cells) (Figure 8D). To investigate the nature of the inclusions detected in PC of infected mice, we performed double immunofluorescence for IgG and BiP (Figure 8F). When the double labelling was examined simultaneously, there was a blending of the immuno-reactivity merge, suggesting co-localization of both proteins, likely in the ER (Figure 8F, yellow arrows). However, in all the infected samples, I-152-treated or not, we observed at all the times investigated, the presence of numerous spherical IgG positive inclusions that did not overlap with BiP positive structures (Figure 8F, blue arrows).

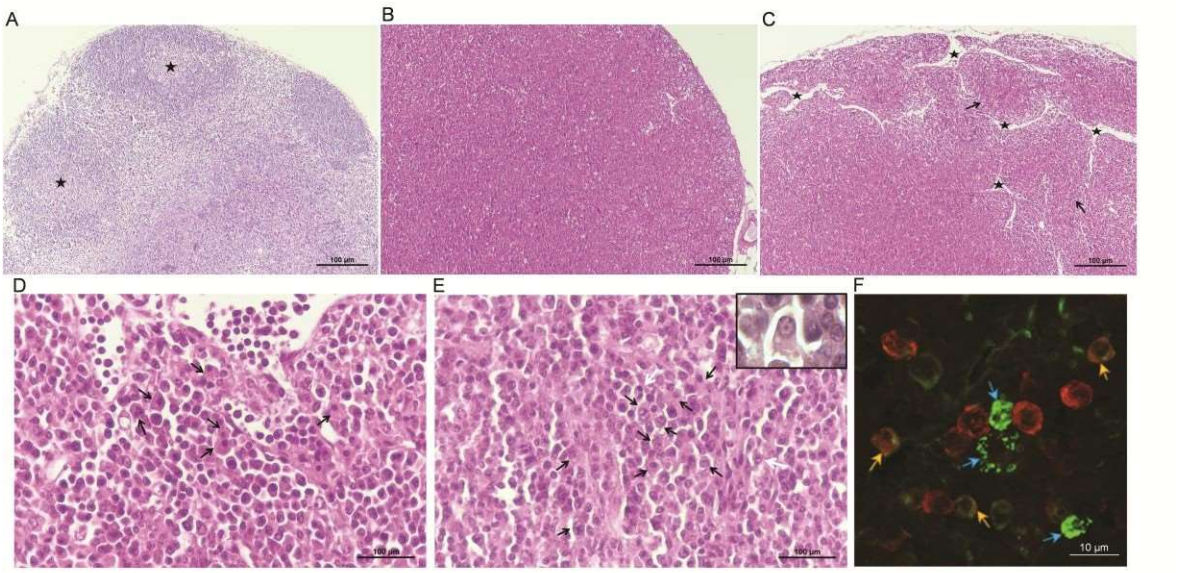

Figure 8. Hematoxylin and eosin (H&E) staining of sections of lymph nodes of uninfected, infected/untreated (I) and infected/treated (I+I-152) mice (A-E) and immunofluorescence staining of section of lymph nodes of infected mice (F).
At 2 weeks p.i., follicles with germinal centers (asterisks) are still visible (A).
At 5 weeks p.i., in mice belonging to the infected/untreated group the normal histological architecture was replaced by a monomorphic population of lymphocytes (B). Several mature PC, including Mott cells containing numerous Russel bodies (arrows) were present (D).
At 5 weeks p.i., in infected/treated mice, the presence of follicular structures (arrows) and expanded lymphatic sinus (asterisks) were observed (C). Undifferentiated PC containing vesicular chromatin often presenting intracytoplasmic vacuoles (black arrows) and binucleated cells (white arrows) predominated (E); flamed cell (insert).
At 5 weeks p.i., in infected mice, either untreated or treated, IgG (green) colocalize with BiP (red) (yellow arrows) or are accumulated in Russell bodies-like structures (blue arrows) (F).

Immature PC, having eccentrically placed vesicular nuclei, (clock faced nuclei) (Figure 8E) and several flamed cells (insert of Figure 8E) were observed particularly in I-152-treated mice. After 5 weeks of infection, an inverted relationship between immature and mature cells was detected in the lymph nodes of infected and infected/treated mice, as revealed by semiquantitative analysis (Figure 9B). No differences were found at the other time points investigated (Figure 9A and 9C).

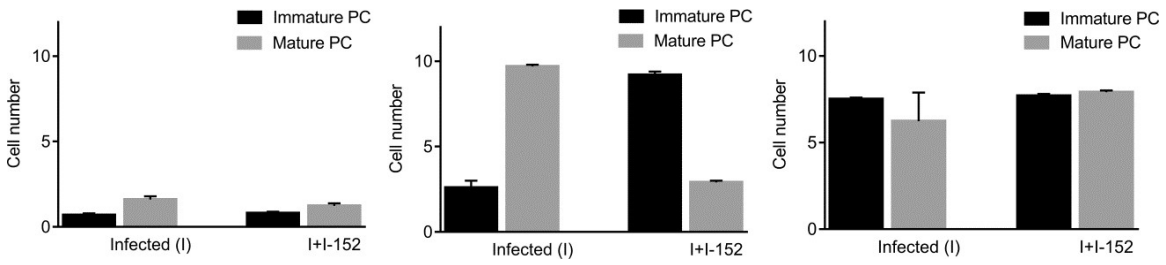

Figure 9. Immature and mature PC in the lymph nodes of infected/untreated (I) and infected/treated (I+I-152) mice. Semiquantitative cell counts were performed in H&E stained sections of lymph nodes at 2 (A), 5 (B) and 9 (C) weeks p.i. The cell number represents the average of the counts of the PC performed at 40x magnification in 5 microscopic fields/mouse.

4. DISCUSSION

One of the primary events in the development of MAIDS is the infection and polyclonal activation of B cells, resulting in a rapid increase in plasma Ig levels [3].

We have previously demonstrated that I-152 treatment of LP-BM5-infected mice reduces the levels of Th2 cytokines, i.e. IL-4 and IL-5 [5]. These cytokines had been reported to have an important role in promoting humoral immunity and inducing IgG1 antibodies [48,49]. Based on these evidences we hypothesized that I-152 could hinder the signs of the disease by dual mechanisms of action: on the one hand, it can directly hamper viral replication [5,30]; on the other hand, in the early phases of infection it regulates the induction of IL-12 and Th1/Th2 cytokine production by modulating intra- macrophage glutathione-redox status [5]. Consistent with this hypothesis, herein we show that I-152 treatment reduces IgG1 titer at 2 weeks p.i., supporting the conclusion that I-152 shifts the ratio Th1/Th2 towards Th1. It would be interesting to investigate whether the redox state can also have a role in the development and/or function of T follicular helper (Tfh) cells, which have emerged as an important cell type required for the formation of germinal centers and related B cells responses [50]. However, these data appear to indicate that the lower plasma IgG levels measured in infected I-152- treated animals may be the consequence of a further mechanism by which I-152 affects the later phases of the disease (i.e. 5 weeks p.i.) characterized by rapid B cell proliferation and high frequency of Ig-secreting cells [8]. Data presented show that I-152 modulates the antibody-mediated immune response by impairing the secretory capacity as well as the maturation of PC. These cells are particularly dependent on the ER quality control system to ensure that only correctly assembled Ig molecules are transported to the cell surface. The results reported in this paper show that in the lymph nodes of infected mice treated with I-152, a great quantity of IgG is indeed retained within the PC at 2 weeks p.i and in part accumulated in the ER. It is well known that the ER resident chaperons BiP and PDI act synergistically to fold Ig. In agreement with these observations, BiP expression was strongly induced after infection with no significant differences between the untreated and treated groups. Conversely, PDI protein levels were higher in the lymph nodes of infected mice but not in I-152-treated mice at 2 weeks p.i., despite the fact that PDI mRNA levels were neither increased following infection nor affected by I-152. These data suggest that PDI protein levels augmented through post-transcriptional mechanisms in infected mice to support a higher demand of IgG folding, and that this event was affected by I-152 treatment, leading to IgG accumulation. It has been suggested that PDI turnover may be related to the redox state of the cell [51]. Moreover, I-152 treatment could influence the redox-sensitive cysteines that have been widely demonstrated to be important for its activity [52, 53]. The more oxidative environment created by GSH depletion during LP-BM5 infection [5] would favour oxidation of PDI and disulfide bond

formation which could be impaired by the more reduced environment created by I-152. In support to this hypothesis, it has been previously demonstrated that an increase in the intracellular GSH content interferes with the PDI-dependent maturation of influenza virus hemagglutinin [54], and that *in vivo* up-regulation of PDI induced by influenza infection can be counterbalanced by GSH increase [55]. Interestingly, accumulation of IgG in the PC observed in the early phases of infection (i.e. 2 weeks p.i.) was followed by a drastic drop in

plasma and intracellular IgG levels found at later times (i.e. 5 weeks p.i.) where the ability of I-152 to affect PC maturation was clearly evident. In fact, while lymph node architecture was partially preserved by 152 treatment, a lower quantity of mature PC was present as suggested by Syndecan-1 quantification and confirmed by histological analysis. Differentiation of B cells into PC requires some morphological changes, which guarantee increased capacity of Ab synthesis and secretion, such as expansion of cytoplasm and ER as well as decrease in nuclear area. The splicing of XBP-1 is induced during PC differentiation in response to Th2 cytokines, such as IL-4, and this event up-regulates Ig gene transcription leading the PC to synthesize and secrete antibodies [22,24,56,57]. Fewer mature PC in treated mice are compatible with the decreased expression of sXBP-1 found in the lymph nodes of these animals. The defective expression of sXBP-1 can undoubtedly affect the differentiation of a PC, but it has also been demonstrated that blockade of the IRE1α-XBP-1 pathway contributes to the death of myeloma cells under ER stress conditions [58]. Thus, secretory cells that require an active UPR to ensure proper processing of proteins in the ER may be particularly susceptible to apoptosis by agents that evoke ER stress but impair the UPR. Hence, inhibition of IRE1α-XBP-1 signalling and increased amount of misfolded/unfolded IgG caused by I-152 treatment could ultimately induce death of PC that are particularly sensitive to this effect due to their high levels of Ab production [59].

Moreover, in all the infected animals, either untreated or treated, despite the activation of UPR branches, likely to cope with Ig over expression, a cellular indigestion caused by an excessive quantity of unfolded IgG, not proceeding along the secretory pathway, occurs. This conclusion is supported by the presence in PC of numerous Russell bodies-like vesicles [47]. As previously proposed by Valetti et al [47], these bodies filled with Ig seem to be an "emergency" response of the cell to accumulation of unfolded Ig. Although most commonly found in patients with multiple myeloma, Russell bodies don't necessarily correspond to malignant changes of PC, but they can be associated with sustained immunologic stimulation and/or inflammation in association with abnormal synthesis, trafficking, or excretion of the Ig [60]. Several ER-storage diseases are characterized by the formation of inclusion bodies where mutated or unfolded proteins are sequestered outside the secretory pathway. These bodies are membrane-limited and seem different from autophagosomes or lysosomes [61].

The presence of loads of unfolded or misfolded proteins is common during viral infection [62] and, as expected, LP-BM5 infection resulted in the induction of UPR activation. Among the up-regulated mRNAs, ChaC glutathione-specific γ-glutamylcyclotransferase 1 (*CHAC1*) showed dramatically increased expression (about 20 times over basal levels at 5 weeks p.i.). Various stimuli that trigger ER stress, including infection, have been reported to upregulate CHAC1 mRNA expression and consequent depletion of cellular GSH levels and accumulation of ROS [63]. Several mechanisms by which different viruses induce a decrease in GSH content have been described [64]. Thus, we suggest that increased expression of CHAC1 could be one important factor leading to GSH depletion in LP-BM5 infection, presumably to make the environment suitable for correct protein folding and virus replication. Notably, I-152 treatment did not affect CHAC1 expression, suggesting that in this experimental model the molecule can raise intracellular GSH levels by providing precursors to synthesize GSH and/or by influencing the pathways involved in GSH synthesis rather than affect GSH

degradation.

The data show that a further mechanism by which I-152 could inhibit IgG production during LP-BM5 infection is by inducing perturbation in ER redox state leading to impaired IgG folding/secretion as well as to reduced maturation and, probably survival, of PC (Figure 10).

Conclusions. Intracellular redox state has a key role in folding and secretion of Ig as well as in maturation of PC where UPR is highly activated. Compounds that shift the intracellular environment towards a more reduced state affect PDI and sXBP1 expression. These molecules may be potential therapeutic agents for the treatment of multiple myeloma and other tumours that originate from secretory cells.

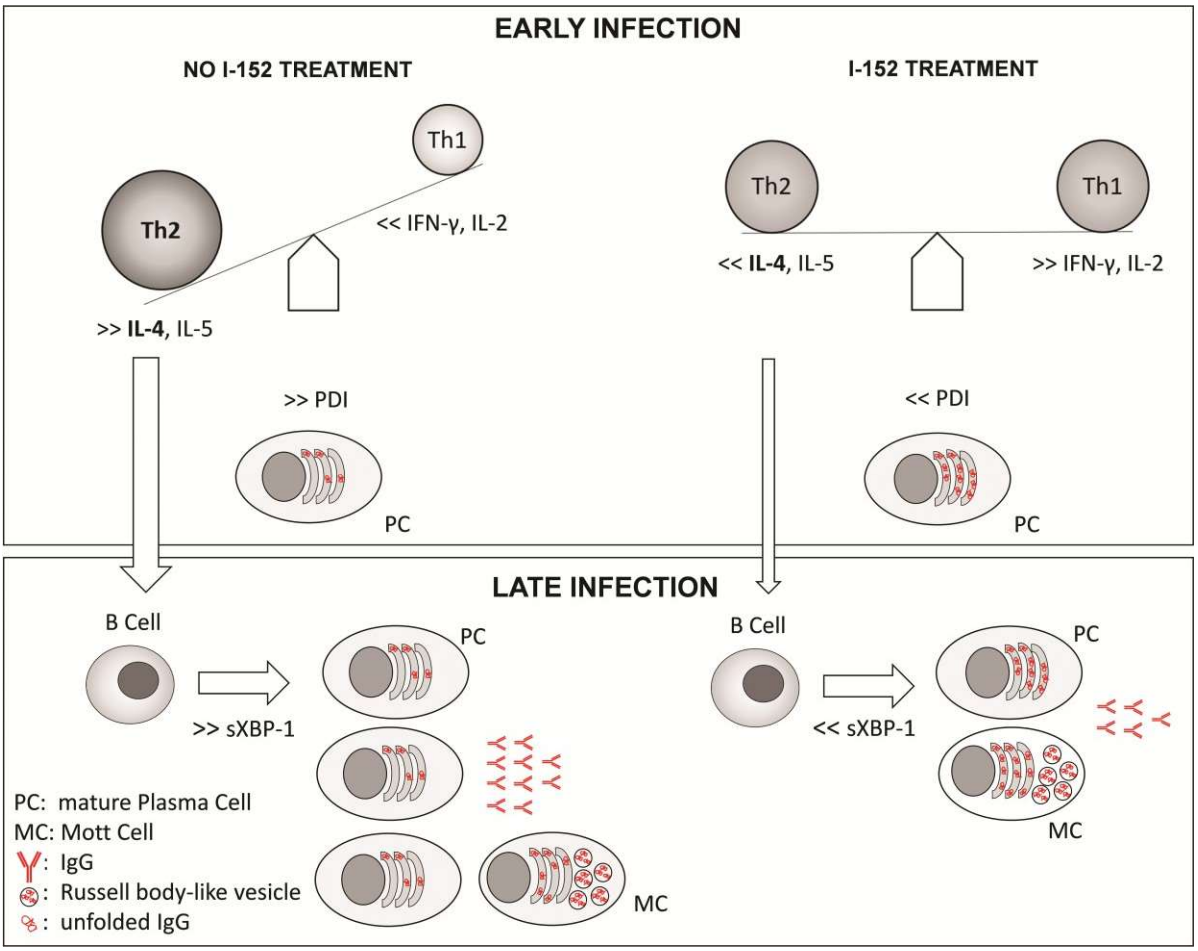

Figure 10. I-152 immunomodulatory effects in LP-BM5 infection. During the early LP-BM5 infection, I-152 treatment influences Th1/Th2 cytokine production in favour of Th1 (4) and accumulates unfolded IgG inside the ER (above). During the late LP-BM5 infection, I-152 treatment impairs differentiation and secretory capacity of PC (below).

Acknowledgements: This work was funded by Ministero dell'Istruzione, dell'Università e della Ricerca (MIUR). (PRIN [Research Projects of National Interest] 2010-2011-prot. 2010PHT9NF_004). Furthermore, we are grateful to University of Urbino Carlo Bo for partial financial support to this research.

REFERENCES

[1] J.W. Hartley, T.N. Fredrickson, R.A. Yetter, M. Makino, H.C. Morse 3rd, Retrovirus-induced murine acquired immunodeficiency syndrome: natural history of infection and differing susceptibility of inbred mouse strains, J. Virol. 63 (1989) 1223–1231.

[2] S.P. Klinken, T.N. Fredrickson, J.W. Hartley, R.A. Yetter, H.C. Morse 3rd, Evolution of B cell lineage lymphomas in mice with a retrovirus induced immunodeficiency syndrome, MAIDS, J. Immunol. 140 (1988) 1123-1131.

[3] D.E. Mosier, R.A. Yetter, H.C. Morse 3rd, Retroviral induction of acute lymphoproliferative disease and profound immunosuppression in adult C57BL/6 mice, J. Exp. Med. 161 (1985) 766–784. https://doi.org/10.1084/jem.161.4.766.

[4] D.E. Mosier, Animal models for retrovirus-induced immunodeficiency disease, Immunol. Invest. 15 (1986) 233-261. https://doi.org/10.3109/08820138609026687.

[5] S. Brundu, L. Palma, G.G. Picceri, D. Ligi, C. Orlandi, L. Galluzzi, L. Chiarantini, A. Casabianca, G.F. Schiavano, M. Santi, F. Mannello, K. Green, M. Smietana, M. Magnani, A. Fraternale, Glutathione depletion is linked with Th2 polarization in mice with a retrovirus-induced immunodeficiency syndrome, murine AIDS: role of proglutathione molecules as immunotherapeutics, J. Virol. 90 (2016) 7118-7130. https://doi.org/10.1128/JVI.00603-16.

[6] R.T. Gazzinelli, M. Makino, S.K. Chattopadhyay, C.M. Snapper, A. Sher, A.W. Hügin, H.C. Morse 3rd, CD4- subset regulation in viral infection. Preferential activation of Th2 cells during progression of retrovirus induced immunodeficiency in mice, J. Immunol. 148 (1992) 182– 188.

[7] A. Sher, R.T. Gazzinelli, I.P. Oswald, M. Clerici, M. Kullberg, E.J. Pearce, J.A. Berzofsky, T.R. Mosmann, S.L. James, H.C. Morse 3rd, Role of T-cell derived cytokines in the downregulation of immune responses in parasitic and retroviral infection, Immunol. Rev. 127 (1992) 183- 204. https://doi.org/10.1111/j.1600-065x.1992.tb01414.x.

[8] D.M. Klinman, H.C. Morse 3rd, Characteristics of B cell proliferation and activation in murine AIDS, J. Immunol. 142 (1989) 1144-1149.

[9] J.N. Gass, N.M. Gifford, J.W. Brewer, Activation of an unfolded protein response during differentiation of antibody-secreting B cells, J. Biol. Chem. 277 (2002) 49047-49054. https://doi.org/10.1074/jbc.M205011200.

[10] Y. Ma, Y. Shimizu, M.J. Mann, Y. Jin, L.M. Hendershot, PC differentiation initiates a limited ER stress response by specifically suppressing the PERK-dependent branch of the unfolded protein response, Cell Stress Chaperones 15 (2010) 281-293. https://doi.org/10.1007/s12192-009-0142-9.

[11] L. Zhang, A. Wang, Virus-induced ER stress and the unfolded protein response, Front. Plant. Sci. 3 (2012) 293. https://doi.org/10.3389/fpls.2012.0029.

[12]L. Galluzzi, A. Diotallevi, M. Magnani, Endoplasmic reticulum stress and unfolded protein response in infection by intracellular parasites, Future Sci. OA 3 (2017) FSO198. https://doi.org/10.4155/fsoa-2017-0020.

[13]M.J. Feige, L.M. Hendershot, J. Buchner, How antibodies fold, Trends Biochem. Sci. 35 (2010) 189-198. https://doi.org/10.1016/j.tibs.2009.11.005.

[14]J.N. Gass, K.E. Gunn, R. Sriburi, J.W. Brewer, Stressed-out B cells? Plasma-cell differentiation and the unfolded protein response, Trends Immunol. 25 (2004) 17-24. https://doi.org/10.1016/j.it.2003.11.004.

[15]A.M. Reimold, N.N. Iwakoshi, J. Manis, P. Vallabhajosyula, E. Szomolanyi-Tsuda, E.M. Gravallese, D. Friend, M.J. Grusby, F. Alt, L.H. Glimcher, PC differentiation requires the transcription factor XBP-1, Nature 412 (2001) 300-307. https://doi.org/10.1038/35085509.

[16]J. Grootjans , A. Kaser , R.J. Kaufman , R.S. Blumberg, The unfolded protein response in immunity and inflammation, Nat. Rev. Immunol. 16 (2016) 469-484. https://doi.org/10.1038/nri.2016.62.

[17]K. Lee , W. Tirasophon , X. Shen , M. Michalak , R. Prywes , T. Okada , H. Yoshida , K. Mori , R.J. Kaufman, IRE1-mediated unconventional mRNA splicing and S2P-mediated ATF6 cleavage merge to regulate XBP1 in signaling the unfolded protein response, Genes Dev. 16 (2002) 452-466. https://doi.org/10.1101/gad.964702.

[18]H. Yoshida, T. Matsui, A. Yamamoto, T. Okada, K. Mori, XBP1 mRNA is induced by ATF6 and spliced by IRE1 in response to ER stress to produce a highly active transcription factor, Cell 107 (2001) 881-891. https://doi.org/10.1016/s0092-8674(01)00611-0.

[19]A.H. Lee, G.C. Chu, N.N. Iwakoshi, L.H. Glimcher, XBP-1 is required for biogenesis of cellular secretory machinery of exocrine glands, EMBO J. 24 (2005) 4368-4380. https://doi.org/10.1038/sj.emboj.7600903.

[20]A.L. Shaffer, M. Shapiro-Shelef, N.N. Iwakoshi, A.H. Lee, S.B. Qian, H. Zhao, X. Yu, L. Yang, B.K. Tan, A. Rosenwald, E.M. Hurt, E. Petroulakis, N. Sonenberg, J.W. Yewdell, K. Calame, L.H. Glimcher, L.M. Staudt, XBP1, downstream of Blimp-1, expands the secretory apparatus and other organelles, and increases protein synthesis in PC differentiation, Immunity 21 (2004) 81-93. https://doi.org/10.1016/j.immuni.2004.06.010.

[21]H. Zhu, B. Bhatt, S. Sivaprakasam, Y. Cai, S. Liu, S.K. Kodeboyina, N. Patel, N.M. Savage, A. Sharma, R.J. Kaufman, H. Li, N. Singh, Ufbp1 promotes PC development and ER expansion by modulating distinct branches of UPR, Nat. Commun. 10 (2019) 1084. https://doi.org/10.1038/s41467-019-08908-5.

[22]N.N. Iwakoshi, A.H. Lee, P. Vallabhajosyula, K.L. Otipoby, K. Rajewsky, L.H. Glimcher, PC differentiation and the unfolded protein response intersect at the transcription factor XBP-1, Nat. Immunol. 4 (2003) 321-329. https://doi.org/10.1038/ni907.

[23]J.S. So, Roles of endoplasmic reticulum stress in immune responses, Mol. Cells 41 (2018) 705-716. https://doi.org/10.14348/molcells.2018.0241.

[24]N. Taubenheim, D.M. Tarlinton, S. Crawford, L.M. Corcoran, P.D. Hodgkin, S.L. Nutt, High rate of antibody secretion is not integral to plasma cell differentiation as revealed by XBP-1 deficiency, J.

Immunol. 189 (2012) 3328-3338. https://doi.org/10.4049/jimmunol.1201042.

[25] W.C. Chong, M.D. Shastri, R. Eri, Endoplasmic reticulum stress and oxidative stress: a vicious nexus implicated in bowel disease pathophysiology, Int. J. Mol. Sci. 18 (2017) 771. https://doi.org/10.3390/ijms18040771.

[26]V. Plaisance, S. Brajkovic, M. Tenenbaum, D. Favre, H. Ezanno, A. Bonnefond, C. Bonner, V. Gmyr, J. Kerr-Conte, B.R. Gauthier, C. Widmann, G. Waeber, F. Pattou, P. Froguel, A. Abderrahmani, Endoplasmic reticulum stress links oxidative stress to impaired pancreatic beta-cell function caused by human oxidized LDL, PLoS One 11 (2016) e0163046. https://doi.org/10.1371/journal.pone.0163046.

[27]J. Wang , K.A. Pareja , C.A. Kaiser , C.S. Sevier, Redox signaling via the molecular chaperone BiP protects cells against endoplasmic reticulum-derived oxidative stress, Elife J3 (2014) e03496. https://doi.org/10.7554/eLife.03496.

[28]S. Chakravarthi, N.J. Bulleid, Glutathione is required to regulate the formation of native disulfide bonds within proteins entering the secretory pathway, J. Biol. Chem. 279 (2004) 39872-39879. https://doi.org/10.1074/jbc.M406912200.

[29]R. Crinelli, C. Zara, M. Smietana, M. Retini, M. Magnani, A. Fraternale, Boosting GSH using the co-drug approach: I-152, a conjugate of N-acetyl-cysteine and β-mercaptoethylamine, Nutrients 11 (2019) 1291. https://doi.org/10.3390/nu11061291.

[30]J. Oiry , P. Mialocq , J.Y. Puy , P. Fretier , N. Dereuddre-Bosquet , D. Dormont , J.L. Imbach , P. Clayette, Synthesis and biological evaluation in human monocyte-derived macrophages of N- (N-acetyl-L-cysteinyl)-S-acetylcysteamine analogues with potent antioxidant and anti-HIV activities, J. Med. Chem. 47 (2004) 1789-1795. https://doi.org/10.1021/jm030374d.

[31] A. Fraternale, M.F. Paoletti, S. Dominici, A. Caputo, A. Castaldello, E. Millo, E. Brocca-Cofano, M. Smietana, P. Clayette, J. Oiry, U. Benatti, M. Magnani, The increase in intra-macrophage thiols induced by new pro-GSH molecole directs the Th1 skewing in ovalbumin immunized mice, Vaccine 28 (2010) 7676-7682. https://doi.org/10.1016/j.vaccine.2010.09.033.

[32]L. Galluzzi, A. Diotallevi, M. De Santi, M. Ceccarelli, F. Vitale, G. Brandi, M. Magnani, Leishmania infantum induces mild unfolded protein response in infected macrophages, PLoS One 11 (2016) e0168339. https://doi.org/10.1371/journal.pone.0168339.

[33]M. De Santi, G. Baldelli, A. Diotallevi, L. Galluzzi, G.F. Schiavano, G. Brandi, Metformin prevents cell tumorigenesis through autophagy-related cell death, Sci. Rep. 9 (2019) 66. https://doi.org/10.1038/s41598-018-37247-6.

[34]K.A. Pape, D.M. Catron, A.A. Itano, M.K. Jenkins, The humoral immune response is initiated in lymph nodes by B cells that acquire soluble antigen directly in the follicles, Immunity 26 (2007) 491-502. https://doi.org/10.1016/j.immuni.2007.02.011.

[35]R.D. Sanderson, P. Lalor, M. Bernfield, B lymphocytes express and lose syndecan at specific stages of differentiation, Cell Regul. 1 (1989) 27-35. https://doi.org/10.1091/mbc.1.1.27.

[36]J. Tellier, S.L. Nutt, Standing out from the crowd: How to identify PC, Eur. J. Immunol. 47 (2017) 1276-

1279. https://doi.org/10.1002/eji.201747168.

[37]F. De Marchis, C. Balducci, A. Pompa, H.M. Riise Stensland, M. Guaragno, R. Pagiotti, A.R. Menghini, E. Persichetti, T. Beccari, M. Bellucci, Human α-mannosidase produced in transgenic tobacco plants is processed in human α-mannosidosis cell lines, Plant Biotechnol. J. 9 (2011) 1061-1073. https://doi.org/10.1111/j.1467-7652.2011.00630.x.

[38]M.J. Gething, J. Sambrook, Protein folding in the cell, Nature. 355 (1992) 33-45. https://doi.org/10.1038/355033a0.

[39]L.M. Hendershot, Immunoglobulin heavy chain and binding protein complexes are dissociated in vivo by light chain addition, J. Cell Biol. 111 (1990) 829-837. https://doi.org/10.1083/jcb.111.3.829.

[40]R.B. Freedman, T.R. Hirst, M.F. Tuite, Protein disulfide isomerase: building bridges in protein folding, Trends Biochem. Sci. 19 (1994) 331-336. https://doi.org/10.1016/0968-0004(94)90072-8.

[41]R.A. Roth, M.E. Koshland, Role of disulfide interchange enzyme in immunoglobulin synthesis, Biochemistry 20 (1981)6594-6599. https://doi.org/10.1021/bi00526a012.

[42]A. Kumar, S. Tikoo, S. Maity, S. Sengupta, S. Sengupta, A. Kaur, A.K. Bachhawat, Mammalian proapoptotic factor ChaC1 and its homologues function as γ-glutamyl cyclotransferases acting specifically on glutathione, EMBO Rep. 13 (2012) 1095-1101. https://doi.org/10.1038/embor.2012.156.

[43]L.C. Clouser, C.M. Holtz, M. Mullett, D.L. Crankshaw, J.E. Briggs, M.G. O'Sullivan, S.E. Patterson, L.M. Mansky, Activity of a novel combined antiretroviral therapy of gemcitabine and decitabine in a mouse model for HIV-1, Antimicrob Agents Chemother. 56 (2012) 1942– 1948. https://doi.org/10.1128/AAC.06161-11.

[44]R.A. Yetter, R.M. Buller, J.S. Lee, K.L. Elkins, D.E. Mosier, T.N. Fredrickson, H.C. Morse 3rd, CD4+ T cells are required for development of a murine retrovirus-induced immunodeficiency syndrome(MAIDS), J. Exp. Med. 168 (1988) 623-635. https://doi.org/10.1084/jem.168.2.623.

[45]R.R. Kopito, R. Sitia, Aggresomes and Russell bodies, Symptoms of cellular indigestion?, EMBO Rep. 1 (2000) 225-231. https://doi.org/10.1093/embo-reports/kvd052.

[46]J. Stoops, S. Byrd, H. Hasegawa, Russell body inducing threshold depends on the variable domain sequences of individual human IgG clones and the cellular protein homeostasis, Biochim.Biophys.Acta. 1823 (2012) 1643-1657. https://doi.org/10.1016/j.bbamcr.2012.06.015.

[47]C. Valetti, C.E. Grossi, C. Milstein, R. Sitia, Russell bodies: a general response of secretory cells to synthesis of a mutant immunoglobulin which can neither exit from, nor be degraded in, the endoplasmic reticulum, J. Cell. Biol. 115 (1991) 983-994. https://doi.org/10.1083/jcb.115.4.983.

[48]B.J. Kim, B.R. Kim, Y.H. Kook, B.J. Kim, Potential of recombinant Mycobacterium paragordonae expressing HIV Gag as a prime vaccine for HIV infection, Sci. Rep. 9 (2019) 15515. https://doi.org/10.1038/s41598-019-51875-6.

[49]A.R. Mathers, C.F. Cuff, Role of Interleukin-4 (IL-4) and IL-10 in Serum Immunoglobulin G Antibody Responses following Mucosal or Systemic Reovirus Infection, J. Virol. 78 (2004) 3352-3360. https://doi.org/10.1128/jvi.78.7.3352-3360.2004.

[50]S. Crotty, T Follicular helper cell biology: a decade of discovery and diseases, Immunity 50 (2019) 1132-1148. https://doi.org/10.1016/j.immuni.2019.04.011.

[51]T. Grune, T. Reinheckel, R. Li, J.A. North, K.J. Davies, Proteasome-dependent turnover of protein disulfide isomerase in oxidatively stressed cells, Arch. Biochem. Biophys. 397 (2002) 407-413. https://doi.org/10.1006/abbi.2001.2719.

[52]A. Kozarova, I. Sliskovic, B. Mutus, S.E. Simon, P.C. Andrews, P.O. Vacratsis, Identification of redox sensitive thiols of protein disulfide isomerase using isotope coded affinity technology and mass spectrometry, J. Am. Soc. Mass Spectrom. 18 (2007) 260-269. https://doi.org/10.1016/j.jasms.2006.09.023.

[53]M. Okumura, K. Noi, S. Kanemura, M. Kinoshita, T. Saio, Y. Inoue, T. Hikima, S. Akiyama, T. Ogura, K. Inaba, Dynamic assembly of protein disulfide isomerase in catalysis of oxidative folding, Nat. Chem. Biol. 15 (2019) 499-509. https://doi.org/10.1038/s41589-019-0268-8.

[54]R. Sgarbanti, L. Nencioni, D. Amatore, P. Coluccio, A. Fraternale, P. Sale, C.L. Mammola, G. Carpino, E. Gaudio, M. Magnani, M.R. Ciriolo, E. Garaci, A.T. Palamara, Redox regulation of the influenza hemagglutinin maturation process: a new cell-mediated strategy for anti- influenza therapy, Antioxid. Redox Signal. 15 (2011) 593-606. https://doi.org/10.1089/ars.2010.3512.

[55]D. Amatore, I. Celestino, S. Brundu, L. Galluzzi, P. Coluccio, P. Checconi, M. Magnani, A.T. Palamara, A. Fraternale, L. Nencioni, Glutathione increase by the n-butanoyl glutathione derivative (GSH-C4) inhibits viral replication and induces a predominant Th1 immune profile in old mice infected with influenza virus, FASEB BioAdvances 1 (2019) 296-305. https://doi.org/10.1096/fba.2018-00066.

[56]D. Cortes Selva, A.L. Ready, K.C. Fairfax, Interleukin-4 (IL-4) maintains lymphocyte-stromal cellaxis in peripheral lymph nodes, J. Immunol. 198 (2017) 63.19. https://doi.org/10.1002/eji.201847789.

[57]I.S. Junttila, Tuning the cytokine responses: an update on interleukin (IL)-4 and IL-13 receptor complexes, Front. Immunol. 9 (2018) 888. https://doi.org/10.3389/fimmu.2018.00888.

[58]A.H. Lee, N.N. Iwakoshi, K.C. Anderson, L.H. Glimcher, Proteasome inhibitors disrupt the unfolded protein response in myeloma cells, Proc Natl Acad Sci USA. 100 (2003) 9946-9951. https://doi.org/10.1073/pnas.1334037100.

[59]B.G. Barwick, V.A. Gupta, P.M. Vertino, L.H. Boise, Cell of origin and genetic alterations in the pathogenesis of multiple myeloma, Front. Immunol. 10 (2019) 1121. https://doi.org/10.3389/fimmu.2019.01121.

[60]B. Ribourtout, M. Zandecki, PC morphology in multiple myeloma and related disorders, Morphologie 99 (2015) 38-62. https://doi.org/10.1016/j.morpho.2015.02.001.

[61]S. Granell, G. Baldini, Inclusion bodies and autophagosomes: are ER-derived protective organelles different than classical autophagosomes?, Autophagy 4 (2008) 375-377. https://doi.org/10.4161/auto.5605.

[62]K. Asha, N. Sharma-Walia, Virus and tumor microenvironment induced ER stress and unfolded protein response: from complexity to therapeutics, Oncotarget 9 (2018) 31920- 31936.

https://doi.org/10.18632/oncotarget.25886.

[63]R.R. Crawford, E.T. Prescott, C.F. Sylvester, A.N. Higdon, J. Shan, M.S. Kilberg, I.N. Mungrue, Human CHAC1 protein degrades glutathione, and mRNA induction is regulated by the transcription factors ATF4 and ATF3 and a BiPartite ATF/CRE regulatory element, J. Biol. Chem. 290 (2015) 15878-15891. https://doi.org/10.1074/jbc.M114.635144.

[64]A. Fraternale, M.F. Paoletti, A. Casabianca, L. Nencioni, E. Garaci, A.T. Palamara, M. Magnani, GSH and analogs in antiviral therapy, Mol. Aspects Med. 30 (2009) 99-110. https://doi.org/10.1016/j.mam.2008.09.001.

CHAPTER 3

In this work, we wanted to examine whether redox alteration induced by I-152 and the N-butanoyl GSH derivative (C4-GSH) could influence the replication and survival of *Mycobacterium avium* and modulate cytokine production by the macrophage host.

Original article published in International Journal of Antimicrobial Agents
Volume 56, Issue 4, October 2020, 106148
Preprint version

Redox homeostasis as a target for new antimycobacterial agents

Alessandra Fraternale[a], Carolina Zara[a], Francesca Pierigè[a], Luigia Rossi[a], Daniela Ligi[a], Giulia Amagliani[a], Ferdinando Mannello[a], Michaël Smietana[b], Mauro Magnani[a], Giorgio Brandi[a], Giuditta Fiorella Schiavano[c]

[a] Department of Biomolecular Sciences, University of Urbino Carlo Bo, Urbino, Italy

[b] Institut des Biomolécules Max Mousseron, Université de Montpellier, CNRS, ENSCM, Montpellier, France

[c] Department of Humanities, University of Urbino Carlo Bo, Urbino, Italy

Corresponding author: Dr. Alessandra Fraternale, PhD

Department of Biomolecular Sciences,

University of Urbino Carlo Bo, 61029 Urbino, Italy

Phone:+39-0722-305243

e-mail: alessandra.fraternale@uniurb.it

Abbreviations:

GSH: reduced glutathione

NAC: N-acetyl-cysteine

M. avium: *Mycobacterium avium*

ERG: ergothioneine

MSH: mycothiol

Mtb: *Mycobacterium tuberculosis*

IL: interleukin

IFN: interferon

ROI: reactive oxygen intermediates

RNI: reactive nitrogen intermediates

PBMC: peripheral blood mononuclear cells

g.u.: genomic units

MOI: multiplicity of infection

Abstract

Despite early treatment with anti-mycobacteria combination therapy, drug resistance continues to emerge. Maintenance of redox homeostasis is essential for *Mycobacterium Avium* (*M. avium*) survival and growth. The aim of the present study was to investigate the antimycobacterial activity of two pro-glutathione (GSH) drugs, which are able to induce redox stress in *M. avium* and to modulate cytokine production from macrophages. Hence, we investigated two molecules shown to possess antiviral and immunomodulatory properties: C4-GSH, an N-butanoyl GSH derivative, and I-152, a pro-drug of N-acetyl-cysteine (NAC) and beta-mercaptoethylamine (MEA). Both molecules showed activity against replicating *M. avium*, both in the cell-free model and inside macrophages. Moreover, they were even more effective in reducing the viability of the bacteria that had been kept in water for seven days, proving to be active against both replicating and non-replicating bacteria. By regulating the macrophage redox state, I-152 modulated cytokine production. In particular, higher levels of IFN-γ, IL-1b, IL-18, and IL-12, which are known to be crucial for the control of intracellular pathogens, were found after I-152 treatment. Our results show that C4-GSH and I-152, by inducing perturbation of redox equilibrium, exert bacteriostatic and bactericidal activity against *M. avium*. Moreover, I-152 can boost the host reponse by inducing the production of cytokines which serve as key regulators of the Th1 response.

Keywords: *M. avium*, redox homeostasis, glutathione, pro-glutathione molecules, anti-mycobacterial compounds

1. Introduction

Mycobacterial infections are major causes of worldwide morbidity and mortality. *Mycobacterium avium* (*M. avium*), a member of the Mycobacterium avium complex (MAC), is an opportunistic pathogen, normally present in the environment, that has now emerged the main bacterial infection in patients with AIDS [1], [2]. A common characteristic shared by many mycobacterial species is that upon host invasion, these bacteria arrange an army of factors, which circumvent macrophage defences to elude macrophage killing and to replicate within these phagocytes [3]. Moreover, *M. avium* can manipulate its host's complex immune signalling pathways by influencing the cytokine environment and inhibiting essential immune functions [4], [5]. Treatment with conventional antimycobacterial drugs does not ensure the elimination of intracellular bacteria [6]. Most current bactericidal antimicrobials inhibit DNA synthesis, RNA synthesis, cell wall synthesis, or protein synthesis [7]. The identification of new antibacterial compounds with novel mechanisms of action has become an urgent need in light of the growing threat of drug-resistant infections [8]. The bactericidal potential of a drug can be influenced significantly by its mode of action within cellular metabolic and signalling networks. One susceptible pathway in the bacterial cell is the thiol-based redox metabolism, which plays a key role in many cellular processes, including protection of the bacterial cell against endogenous and exogenous reactive oxygen species, proper protein folding, and DNA synthesis [9]. While glutathione (GSH) is rarely detected in pathogenic prokaryotes, ergothioneine (ERG) and mycothiol (MSH) are the most important low molecular weight thiols in mycobacteria [9], [10]. They preserve cellular homeostasis by maintaining a reducing environment, and function as detoxification agents against antibiotics, alkylating agents, electrophiles, and other reactive intermediates [10]. Several studies have shown that MSH is also important to the virulence and survival of Mycobacterium tuberculosis (Mtb), as the loss of MSH biosynthesis and MSH-dependent detoxification inhibit the growth of mycobacteria [11]. Moreover, MSH is an important component that combats acidic stress during Mycobacterium infection [11], [12]. Due to their beneficial role, ERG and MSH can be considered valid targets for the development of antibacterial drugs. Indeed, several studies have demonstrated that affecting the redox balance in Gram-positive bacteria results in bacterial cell death, and depletion of thiol pools is a promising target to promote Mtb killing and potentiation of antimicrobials [13].

On the other hand, it is known that redox modulation of macrophage pro-inflammatory innate immune signalling pathways may play a critical role in the immune response [14]. Previously, we have shown that it is possible to shift the intra-macrophage environment towards a more reduced state by using pro-glutathione (GSH) molecules, namely the N-butanoyl derivative of GSH (C4-GSH) or I-152, a precursor of N-acetyl-cysteine (NAC) and cysteamine (MEA). We established that these molecules increase the intracellular GSH content [15], while other studies have shown that Mycobacterium growth is sensitive to GSH and NAC [16], [17]. Hence, we hypothesized that C4-GSH and I-152 could unbalance oxidation-reduction reactions orchestrated by *M. avium* to maintain metabolic homeostasis. Moreover, they could modulate the production of anti/pro-inflammatory cytokines in the macrophage host to make the immune response more effective. In

fact, C4-GSH and I-152 have been shown to influence macrophage cytokine production in both *in vitro* and *in vivo* models, favouring Th1 responses, although by different mechanisms and by influencing the signalling pathways involved in cytokine production in different ways [15], [18], [19], [20]. In this paper, we report preliminary results regarding the bacteriostatic and bactericidal activity of C4-GSH and I-152 against *M. avium*. Moreover, we show that these molecules can regulate the production of macrophage cytokines involved in the immune and inflammatory processes.

2. Materials and methods

2.1. The preparation of pro-GSH molecules

I-152 was synthesized as previously described [21] and C4-GSH was kindly provided by GLUOS S.r.l. Both molecules were dissolved in culture medium at the highest concentration and then serially diluted.

2.2. Bacterial strain, media and culture preparation

M. avium strain 662, obtained from the blood of AIDS patients (L. Sacco Hospital, Milan, Italy) who had never been treated for mycobacterial infection, was used. The strain was identified by polymerase chain reaction (PCR) as described by Schiavano et al [22].

The bacteria were grown in Middlebrook 7H10 agar (Difco Laboratories, Detroit, MI, USA) with oleic acid albumin dextrose catalase (OADC) and in Middlebrook 7H9 broth with ADC enrichment at 35°C for eight to ten days. Before the experiments, all the bacterial suspensions were sonicated for 6 s, washed and quantified by spectrophotometry to an optical density of 0.12 at 650 nm. Ten µl of each dilution suspension was plated in triplicate on Middlebrook 7H10 agar and incubated at 35°C for eight to ten days for the enumeration of colony-forming units (CFUs)/ml.

2.3. Evaluation of I-152 and C4-GSH efficacy on *M. avium* growth and viability

The effect of I-152 or C4-GSH on *M. avium* growth and viability was determined in mycobacterial suspensions in supplemented Middlebrook 7H9 broth or in sterile distilled water respectively. Following a seven-day incubation at 35°C, each sample was two-fold serially diluted and 10 µl of the diluted sample was plated in triplicate on Middlebrook 7H10 agar for the enumeration of CFUs/ml. A control without compounds was included in each series.

2.4. Separation of monocytes from human blood and infection with *M. avium*

Monocyte-derived macrophages were prepared from leukocyte buffy coats obtained from healthy volunteers and purified as previously described [6], [22].

The macrophage cultures were exposed for four hours to bacteria at a multiplicity of infection (MOI) of 60:1 (bacilli:macrophage). After removal of extracellular bacilli, one sample of infected macrophages was lysed to assess the intracellular CFUs (infection at time 0). The final macrophage lysate suspension was serially diluted and plated onto 7H10 agar for the enumeration of CFUs. For the assay of antimycobacterial activity, the compounds were added at the concentration of 10 mM to the macrophage culture in RPMI supplemented with 10% FCS without penicillin/streptomycin. After four days, the supernatants were removed, replaced with fresh medium containing the molecules and processed for the CFU counts. On the seventh day of the culture, supernatants and adherent macrophages were processed to evaluate the viable extracellular and intracellular mycobacteria. Total viable counts were expressed by adding the supernatant and intracellular CFU counts on day seven to the supernatant CFU counts on day four. Control samples were run in parallel and treated in the

same manner as the experimental macrophage cultures; no detachment of cells from the wells of the culture plate was observed. Total macrophage protein content was quantified on the supernatant and adherent cells.

2.5. Determination of GSH and cysteine in *M. avium*-infected macrophages

Macrophages, exposed to *M. avium* as described in the previous section (2.4), were washed and processed for thiol determination as previously described [15]. GSH and cysteine levels were determined by high performance liquid chromatography (HPLC) [15]. The procedure was performed at different times from *M. avium* exposure and then repeated seven days after *M. avium* removal.

2.6. *M. avium* quantification by real-time PCR

M. avium-infected macrophages, treated with 10 mM of I-152 and lysed as described for bacterial plate counts, were used for total DNA extraction as described by Pathak et al. [23]. Five µl were amplified by qPCR with the *M. avium* trasposon element (IS1245) Advanced kit (genesig, Primerdesign, Camberley, UK) according to the manufacturer's instruction. The amplification reaction included an *M. avium* specific primer/probe mix targeting the insertion sequence IS1245 and an endogenous control primer/probe mix (human β-actin) used to normalize the number of *M. avium* genomic units (g.u.) against the macrophage number. The declared detection sensitivity was less than 100 copies of target template.

2.7. Magnetic multiplex immunoassay of cytokines

Cytokine concentrations in supernatants from macrophages (collected after four and seven days of infection) were determined through a multiplex suspension immunomagnetic assay, as previously detailed [19]. Levels of analytes were determined using a Bio-Plex 200 array reader (Bio-Rad Labs, Hercules, CA, USA). Data were collected and analyzed using a Bio-Plex 200 instrument equipped with BioManager analysis software (Bio-Plex Manager Software v. 6.1). Levels of cytokines (IFN-γ, IL-1b, IL-8, IL-18, IL-12p40, IL-10, IL-6 and TNF-α) were determined in the supernatants of three separate experiments plated in duplicate. Final values represent the sum of the fourth and seventh day values. Comparable levels were obtained in two experiments, while in the third experiment, although the trend was similar to the other two, the values were lower, and IL-10 and IL-12 were not detectable. Hence, the results obtained from this experiment were not considered in the final results.

2.8. Statistical analysis

Statistical analysis was performed with GraphPad Instat. Data were analyzed with the two-tail unpaired Student's t test. A P value <0.05 was considered significant.

3. Results

3.1. Pro-GSH molecules possess bacteriostatic and bactericidal activity vs *M. avium*

3.1.1 Effect of I-152 and C4-GSH on *M. avium* growth

N-acetyl-cysteine is the molecule of choice to increase intracellular GSH levels. It has shown potent anti-mycobacterial activity and significant improvement in mycobactericidal responses when combined with antibiotic treatment [17], [24]. Moreover, several pro-GSH molecules with improved bioavailability and targeting capacity have been synthesized [25].

The antimycobacterial activity of I-152 and C4-GSH was evaluated by incubating *M. avium* in Middlebrook 7H9 broth in the presence of different concentrations of I-152 (5, 10 and 20 mM) or C4-GSH (5 and 10 mM). The 20 mM concentration of C4-GSH was not tested because C4-GSH concentrations higher than 10 mM did not dissolve in the medium. Mycobacterium replication was compared to that of mycobacteria grown in the absence of the molecules. The results showed that both I-152 (Figure 1a) and C4-GSH (Figure 1b) significantly inhibited the growth of the bacterium at all the tested doses. I-152 yielded similar results when used in 10 and 20 mM concentrations; therefore, subsequent experiments were performed with 10 mM or 5 mM I-152. On the other hand, C4-GSH interfered with *M. avium* replication in a concentration dependent manner. It was found that 10 mM of GSH exerted a significantly lower activity than C4-GSH administered at the same concentration (Figure 1b, white column). These experiments showed that I-152 and C4-GSH inhibited *M. avium* proliferation, indicating bacteriostatic activity.

3.1.2 Effect of I-152 and C4-GSH on *M. avium* viability

Most antibiotics that are used against Mycobacterium target biosynthetic processes essential for cell growth. Inhibition of nucleic acid, protein, or cell wall synthesis leads to cessation of growth [6], [7]. Indeed, we proposed a model in which an imbalance in the redox homeostasis may be at least partially responsible for cell death. Hence, we investigated whether I-152 and C4-GSH have bactericidal activity. To this end, bacterial suspensions were maintained in sterile distilled water at 35°C for seven days in the presence or absence of I-152 or C4-GSH, as described in section 2.3. Dose-dependent effects were observed. Indeed, the highest concentration of I-152 (10 mM) reduced the number of viable bacteria by about 4.5 logs, while a 5 mM concentration of I-152 resulted in a 2 log reduction (Figure 2a). Similar results were obtained with C4-GSH treatment (Figure 2b). Thus, exposure to I-152 or C4-GSH markedly reduced the number of bacterial cells, indicating bactericidal activity.

3.2. Pro-GSH molecules inhibit intra-macrophage replication of *M. avium* and modulate cytokine production

3.2.1. The effect of I-152 and C4-GSH on *M. avium* growth in human macrophages

To assess the ability of I-152 and C4-GSH to affect the intracellular growth of *M. avium* and the macrophage cytokine response, macrophages were exposed to *M. avium* for four hours and then treated with I-152 or C4-GSH, as described in section 2.4. GSH has been shown to have direct antimycobacterial effects [16], [17]. Moreover, the addition of NAC to antibiotics improves their mycobactericidal responses against Mtb infection [24]. Upon infection, macrophages undergo morphological and functional changes, including variations in redox equilibrium [26], [27], [28]. Thus, we first measured GSH levels after infection with *M. avium*. We found that, although differences were observed in basal GSH levels in macrophages exposed to *M. avium*, the infection caused an intracellular GSH increase that was significant compared to the uninfected cells after four hours of infection, and it was still appreciable after seven days (Figure 3a). On the contrary, we found no differences in the GSH content at early times of infection (within 1 hour) or in cysteine levels at all the tested times (not shown). To evaluate the antimycobacterial activity of the pro-GSH molecules, I-152 and C4-GSH were added to *M. avium*-infected macrophages at a concentration of 10 mM. In this case, we observed a marked reduction in bacterial loads, demonstrating the ability of the drugs to limit mycobacterial growth within macrophages (Figure 3b).

To quantify *M. avium* inside macrophages real-time PCR was performed following the procedure described in section 2.6. In this preliminary study, we chose to investigate this parameter only in the cells having received the most effective treatment in terms of growth inhibition, i.e. 10 mM of I-152. The $\Delta\Delta C_T$ method was used to estimate fold differences in intracellular *M. avium* g.u. between treated and untreated macrophages by relative quantification. The results, reported in Table 1, show that *M. avium* g.u. were more than three times higher in I-152-treated macrophages than in untreated cells.

3.2.2. Modulation of cytokine production in human macrophages by I-152 and C4-GSH

Macrophage cytokines play a major role in determining the outcome of mycobacterial infections [4], [5], [24], [28], [29], [30]. In the present study, we assessed a panel of eight cytokines secreted from macrophages upon *M. avium* infection examining how they were modulated by treatment with pro-GSH molecules. Infection of macrophage cells with *M. avium* strain 662 resulted in a high production of IL-6, IL-8 and TNF-α, a medium level production of IL-12 and IL-10 and a low production of IFN-γ, IL-1b and IL-18 (Figure 4). When the macrophages were treated with I-152, although the bacterial growth rate was significantly inhibited, IFN-γ, IL-1b, IL-18, IL-8, IL-10 and IL-12 levels showed a three- to six-fold increase compared to infected/untreated cells (I). By contrast, IL-6 concentration was not affected by the treatment and TNF-α concentration was decreased (Figure 4, light grey columns). Cytokine production was less influenced by C4-GSH, as reported in Figure 4 (dark grey columns).

Table 1. Real-time PCR relative quantification of intracellular *M. avium* DNA.

Samples	***M. avium* g.u. fold differences (± SD)**
Infected untreated macrophages	1
Infected and I-152-treated macrophages	3.4±0.5

The g.u., genomic units; SD, standard deviation. Results are expressed as fold differences between macrophages treated with 10 mM of I-152 and untreated macrophages (average of two separate experiments, four replicates).

4. Discussion

C4-GSH and I-152 have been used as cellular redox modifiers for controlling *M. avium* infection on the one hand and to modulate macrophage cytokine production on the other hand.

It was not our aim to compare the antibacterial activity of the two molecules, but it is interesting to note that, although both C4-GSH and I-152 are GSH-boosting drugs, their activity against *M. avium* was found to be different. Indeed, I-152 was shown to be more effective than C4-GSH in all the experimental conditions under study. We think that, as has already been reported for other pro-GSH molecules [16], [17], [31], the antimycobacterial activity of I-152 and C4-GSH can be ascribed to GSH. Extracellular GSH is converted to dipeptide (Cys-Gly) due to the action of transpeptidase, and the dipeptide is then transported into the bacterial cells [32]. However, while this mechanism can explain the inhibitory effects of the molecules within macrophages, it does not explain the antimycobacterial activity found in cell-free systems. In fact, it is known that mycobacteria do not synthesize GSH. Hence, we can hypothesize that the accumulation of reducing equivalents is sensed through mycobacteria redox sensors causing DNA and protein synthesis inhibition as well as modifications in metabolic pathways [33], [34]. The proposed mechanism also suggests that eukaryotic thiol pools may be targets for C4-GSH and I-152. Indeed, this assumption has been demonstrated in macrophage cells treated with high I-152 concentrations, in which temporary GSH depletion was shown, but not in cells treated with C4-GSH [15], [20]. I-152 and C4-GSH are pro-GSH molecules that act through different mechanisms. C4-GSH, as it is, can enter the cell or act through a mechanism similar to the one described above for GSH, i.e., it can be a substrate for the enzyme gamma-glutamyl transpeptidase. The cysteine derived from C4-GSH metabolism can be used to synthesize GSH in a eukaryotic cell or may interfere with MSH within the Mycobacterium. On the other hand, I-152 induces a transient GSH depletion since it may be considered xenobiotic and conjugated with GSH. However, no significant macrophage cytotoxicity has been observed for I-152, probably because the thiol species provided by I-152, in the form of NAC and MEA, are promptly used to restore the GSH pool [19], [20]. We can hypothesize that I-152 may have a similar effect inside the mycobacterium, where the MSH concentration and/or activity may be affected by I-152 itself and by the aberrant increase in reducing equivalents provided by the molecule. On the other hand, the initial GSH depletion within the macrophage could contribute to creating an adverse environment for mycobacterium replication, while subsequently, high levels of GSH could modulate the cytokine production. It is known that reactive oxygen intermediates (ROI) and reactive nitrogen intermediates (RNI) are generated by phagocytic cells to inhibit growth of intracellular pathogens [28]. When ROI and RNI are generated, there is a simultaneous synthesis of GSH, which protects against the toxic effects of the reactive species. In fact, we found a significant GSH increase upon *M. avium* infection, regardless of different basal macrophage GSH levels, which depended on the blood sample from which macrophages derived. Despite these differences in basal GSH levels, we preferred to use primary cells since they provide a more representative result than immortalized macrophage cell-lines. Monocyte-derived macrophages matured in absence of any stimuli give rise to a mixed culture of both the M1 and M2 phenotype, and such cultures have been reported to be suitable

for infection studies with *M. avium.* In fact, it is not known whether *M. avium* infects a particular phenotype [26], [35].

In this study, we demonstrate that the antimicrobial efficacy of C4-GSH and I-152 is not limited to growing bacteria, but extends to quiescent bacterial cells, suggesting a functional linkage between redox changes and survival. High concentrations of C4-GSH and I-152 may create a reductive stress which the bacterium cannot control, leading to cell death [32], [33]. In short, our experiments show that pro-GSH molecules could exert bactericidal activity by weakening redox homeostasis in *M. avium*. Of course, further studies are necessary to delineate the precise mechanisms of action and in particular, to investigate the significance of the preliminary result obtained by the molecular analysis of infected macrophages treated with I-152. In fact, this assay revealed higher amounts of intra-macrophage *M. avium* DNA, possibly deriving from both live and dead cells. On the other hand, the amounts of total viable *M. avium* cells were found to be significantly lower. We can thus hypothesize that most intracellular bacteria were dead. Indeed, as previously reported [23], while the plating method is a measure of live bacteria, the qPCR measures the total number of bacterial genomes, regardless of whether they derive from dead or live cells. Future studies will aim to establish the subcellular localization of mycobacteria in infected macrophages treated with I-152 and the fate of those cells.

By altering the glutathione-redox balance in macrophages, it is possible to modulate cytokine production [31], [34], [35], [36]. Hence, we investigated inflammatory and anti-inflammatory cytokine production. Both GSH and NAC have been shown to diminish tuberculosis pathology and inflammation by immune-modulation [24], [34]. In our experimental conditions, infected macrophages produced high concentrations of IL-6, IL-8 and TNF-α, medium levels of IL-12 and IL-10 and low levels of IFN-γ, IL-1b and IL-18. It is known that high levels of intra-macrophage GSH favor the Th1 response, mainly by modulating IL-12 production [36]. All the cytokines that were examined were found to be present at higher levels in I-152-treated macrophages, with the exception of IL-6 and TNF-α, a finding which is partially in agreement with the reported data on NAC therapy for tuberculosis infection [30]. Increased levels of IL-12, whose biological functions are pivotal in both innate and adaptive immunity [37], confirm previous findings regarding the capacity of I-152 to induce the production of macrophage cytokines able to support the Th1 response [18], [19]. Regarding the IL-18 effect, although there is conflicting evidence in the literature, most studies support its role in synergizing with IL-12 to induce IFN-γ production in dendritic cells, macrophages, and B cells [38]. It is generally accepted that IL-1 has a role in increasing survival and decreasing pulmonary bacterial loads in Mtb infection, probably through different mechanisms described for IL-12 or IFN-γ [36]. Hence, we can generally conclude that I-152, by increasing the levels of the cited cytokines, could be useful in controlling mycobacteria infection. It is more difficult to interpret the effect exerted on TNF-α, IL-10 and IL-6 because these cytokines are induced by mycobacteria but have different effects according to the nature of the challenge and the experimental conditions [38]. It is therefore difficult to foresee the final effect of I-152 because it will likely differ according to the experimental conditions and should be analyzed in concert with the other cytokines. In the present study, C4-GSH treatment did not markedly influence cytokine production although we have previously found that production of all the main inflammatory cytokines is blocked by C4-GSH through inhibition of NFkB mediated

signaling [39]. We hypothesize that these differences may be due to the different experimental models, in particular, in relation to the intracellular redox state and the stimulus triggering the cytokine response. Moreover, we have previously demonstrated that I-152 and C4-GSH can regulate cytokine production by modulating different signaling pathways. Hence, there is no doubt that the tested pro-GSH molecules can modulate cytokine production, but the exact effect on the single cytokine cannot be foreseen. In conclusion, C4-GSH and I-152 limit *M. avium* infection through direct antimicrobial activity and regulation of the cytokine response. Our most interesting finding was the inhibitory activity of the molecules on the survival of *M. avium*. In fact, most bacteria can survive inside macrophages by eluding the killing mechanisms of the host, and conventional antimicrobial agents are effective against actively growing bacteria.

Conclusions: these data suggest that the redox state of mycobacteria could be a novel target for killing dormant bacteria and pro-GSH drugs may target the bacteria in a persistent/latent infection. Moreover, thanks to its immune modulation, the addition of I-152 to the existing anti-Mycobacterium drugs could be a valid strategy for clearance of *M. avium*.

DECLARATIONS

Funding: This work was supported by the University of Urbino Carlo Bo (DISB_ROSSI_PROGETTI_VALORIZZAZIONE_ 2017 Delibera n. 87/2017)
Competing interests: None
Ethical Approval: Not required

References

[1] Nightingale SD, Byrd LT, Southern PM, Jockusch JD, Cal SX, Wynne BA. Incidence of *Mycobacterium avium-intracellulare* complex bacteremia in human immunodeficiency virus-positive patients. J Infect Dis 1992;165:1082-85. https://doi.org/10.1093/infdis/165.6.1082.

[2] Karakousis PC, Moore RD, Chaisson RE. Mycobacterium avium complex in patients with HIV infection in the era of highly active antiretroviral therapy. Lancet Infect Dis 2004;4:557-65. https://doi.org/10.1016/S1473-3099(04)01130-2.

[3] Queval CJ, Brosch R, Simeone R. The Macrophage: A Disputed Fortress in the Battle against Mycobacterium tuberculosis. Front Microbiol 2017;8:2284. https://doi.org/10.3389/fmicb.2017.02284.

[4] Vankayalapati R, Wizel B, Samten B, Griffith DE, Shams H, Galland MR, et al. Cytokine Profiles in Immunocompetent Persons Infected with Mycobacterium avium Complex. J Infect Dis 2001;183:478-84. https://doi.org/10.1086/318087.

[5] Wagner D, Sangari FJ, Kim S, Petrofsky M, Bermudez LE. Mycobacterium avium infection of macrophages results in progressive suppression of interleukin-12 production in vitro and in vivo. J Leukoc Biol 2002;71:80-8. https://doi.org/10.1189/jlb.71.1.80.

[6] Schiavano GF, Celeste AG, Salvaggio L, Sisti M, Brandi G. Efficacy of macrolides used in combination with ethambutol, with or without other drugs, against Mycobacterium avium within human macrophages. Int J Antimicrob Agents. 2001;18:525-30. https://doi.org/10.1016/S0924-8579(01)00461-7.

[7] Kohanski MA, Dwyer DJ, Collins JJ. How antibiotics kill bacteria: from targets to networks. Nat Rev Microbiol 2010;8:423-35. https://doi.org/10.1038/nrmicro2333.

[8] Boucher HW, Talbot GH, Bradley JS, Edwards JE, Gilbert D, Rice LB, et al. Bad bugs, no drugs: no ESKAPE! An update from the Infectious Diseases Society of America. Clin Infect Dis 2009;48:1-12. https://doi.org/10.1086/595011.

[9] Ritz D, Beckwith J. Roles of thiol-redox pathways in bacteria. Annu Rev Microbiol 2001;55:21-48. https://doi.org/10.1146/annurev.micro.55.1.21.

[10] Sao Emani C, Gallant JL, Wiid IJ, Baker B. The role of low molecular weight thiols in Mycobacterium tuberculosis. Tuberculosis (Edinb) 2019;116:44-55. https://doi.org/10.1186/s12929-018-0458-9.

[11] Pacl HT, Reddy VP, Saini V, Chinta KC, Steyn AJC. Host-pathogen redox dynamics modulate Mycobacterium tuberculosis pathogenesis. Pathog Dis 2018;76:fty036. https://doi.org/10.1093/femspd/fty036.

[12] Harbut MB, Vilchèze C, Luo X, Hensler ME, Guo H, Yang B, et al. Auranofin exerts broad-spectrum bactericidal activities by targeting thiol-redox homeostasis. Proc Natl Acad Sci USA 2015;112:4453-8. https://doi.org/10.1073/pnas.1504022112.

[13] Coulson GB, Johnson BK, Zheng H, Colvin CJ, Fillinger RJ, Haiderer ER, et al. Targeting Mycobacterium tuberculosis sensitivity to thiol stress at acidic pH kills the bacterium and potentiates antibiotics. Cell Chem Biol 2017;24:993-1004.e4. https://doi.org/10.1016/j.chembiol.2017.06.018.

[14] Gostner JM, Becker K, Fuchs D, Sucher R. Redox regulation of the immune response. Redox Rep 2013;18:88-94. https://doi.org/10.1179/1351000213Y.0000000044.

[15] Fraternale A, Crinelli R, Casabianca A, Paoletti MF, Orlandi C, Carloni E, et al. Molecules altering the intracellular thiol content modulate NF-kB and STAT-1/IRF-1 signalling pathways and IL-12 p40 and IL-27 p28 production in murine macrophages. PLoS One 2013;8:e57866. https://doi.org/10.1371/journal.pone.0057866.

[16] Venketaraman V, Rodgers T, Linares R, Reilly N, Swaminathan S, Hom D, et al. Glutathione and growth inhibition of Mycobacterium tuberculosis in healthy and HIV infected subjects. AIDS Res Ther 2006;3:5. https://doi.org/10.1186/1742-6405-3-5.

[17] Amaral EP, Conceição EL, Costa DL, Rocha MS, Marinho JM, Cordeiro-Santos M, et al. N-acetyl-cysteine exhibits potent anti-mycobacterial activity in addition to its known anti-oxidative functions. BMC Microbiol 2016;16:251. https://doi.org/10.1186/s12866-016-0872-7.

[18] Fraternale A, Paoletti MF, Dominici S, Caputo A, Castaldello A, Millo E, et al. The increase in intra-macrophage thiols induced by new pro-GSH molecules directs the Th1 skewing in ovalbumin immunized mice. Vaccine 2010;28:7676-82. https://doi.org/10.1016/j.vaccine.2010.09.033.

[19] Brundu S, Palma L, Picceri GG, Ligi D, Orlandi C, Galluzzi L, et al. Glutathione Depletion Is Linked with Th2 Polarization in Mice with a Retrovirus-Induced Immunodeficiency Syndrome, Murine AIDS: Role of Proglutathione Molecules as Immunotherapeutics. J Virol 2016;90:7118-30. https://doi.org/10.1128/JVI.00603-16.

[20] Crinelli R, Zara C, Smietana M, Retini M, Magnani M, Fraternale A. Boosting GSH Using the Co-Drug Approach: I-152, a Conjugate of N-acetyl-cysteine and β-mercaptoethylamine. Nutrients 2019;11.pii:E1291. https://doi.org/10.3390/nu11061291.

[21] Oiry J, Mialocq P, Puy JY, Fretier P, Dereuddre-Bosquet N, Dormont D, et al. Synthesis and biological evaluation in human monocyte-derived macrophages of N-(N-acetyl-L-cysteinyl)-S-acetylcysteamine analogues with potent antioxidant and anti-HIV activities. J Med Chem 2004;47:1789-95. https://doi.org/10.1021/jm030374d.

[22] Schiavano GF, De Santi M, Sisti M, Amagliani G, Brandi G. Disinfection of *Mycobacterium avium* in drinking tap water using ultraviolet germicidal irradiation. Environ Technol 2018;39:3221-7. https://doi.org/10.1080/09593330.2017.1375028.

[23] Pathak S, Awuh JA, Anders Leversen N, Flo TH, Åsjø B. Counting Mycobacteria in Infected Human Cells and Mouse Tissue: A Comparison between qPCR and CFU. PLoS One 2012;7:e34931. https://doi.org/10.1371/journal.pone.0034931.

[24] Teskey G, Cao R, Islamoglu H, Medina A, Prasad C, Prasad R, et al. The Synergistic Effects of the Glutathione Precursor, NAC and First-Line Antibiotics in the Granulomatous Response Against Mycobacterium tuberculosis. Front Immunol 2018;9:2069. https://doi.org/10.3389/fimmu.2018.02069.

[25] Cacciatore I, Cornacchia C, Pinnen F, Mollica A, Di Stefano A. Prodrug approach for increasing cellular glutathione levels. Molecules 2010;15:1242-64. https://doi.org/10.3390/molecules15031242.

[26] Eligini S, Crisci M, Bono E, Songia P, Tremoli E, Colombo GI, et al. Human monocyte-derived macrophages spontaneously differentiated in vitro show distinct phenotypes. J Cell Physiol 2013;228:1464-72. https://doi.org/10.1002/jcp.24301.

[27] Greenwell-Wild T, Vázquez N, Sim D, Schito M, Chatterjee D, Orenstein JM, et al. Mycobacterium avium infection and modulation of human macrophage gene expression. J Immunol 2002;169:6286-97. https://doi.org/10.4049/jimmunol.169.11.6286.

[28] Venketaraman V, Dayaram YK, Talaue MT, Connell ND. Glutathione and nitrosoglutathione in macrophage defense against Mycobacterium tuberculosis. Infect Immun 2005;73:1886-9. https://doi.org/10.1128/II.73.3.1886-1889.2005.

[29] Shi L, Jiang Q, Bushkin Y, Subbian S, Tyagi S. Biphasic dynamics of macrophage immunometabolism during Mycobacterium tuberculosis infection. mBio 2019;10:e02550-18. https://doi.org/10.1128/mBio.02550-18.

[30] Cooper AM, Mayer-Barber KD, Sher A. Role of innate cytokines in mycobacterial infection. Mucosal Immunol 2011;4:252–60. https://doi.org/10.1038/mi.2011.13.

[31] Guerra C, Morris D, Sipin A, Kung S, Franklin M, Gray D, et al. Glutathione and adaptive immune responses against Mycobacterium tuberculosis infection in healthy and HIV infected individuals. PLoS One 2011;6:e28378. https://doi.org/10.1371/journal.pone.0028378.

[32] Dayaram YK, Talaue MT, Connell ND, Venketaraman V. Characterization of a glutathione metabolic mutant of Mycobacterium tuberculosis and its resistance to glutathione and nitrosoglutathione. J Bacteriol 2006;188:1364-72. https://doi.org/10.1128/JB.188.4.1364-1372.2006.

[33] Mavi PS, Singh S, Kumar A. Reductive Stress: New Insights in Physiology and Drug Tolerance of Mycobacterium. Antioxid Redox Signal 2019; https://doi.org/10.1089/ars.2019.7867.

[34] Young C, Walzl G, Du Plessis N. Therapeutic host-directed strategies to improve outcome in tuberculosis. Mucosal Immunol 2020;13:190-204. doi: 10.1038/s41385-019-0226-5.

[35] Rocco JM, Irani VR. Mycobacterium avium and modulation of the host macrophage immune mechanisms. Int J Tuberc Lung Dis 2011;15:447-52. https://doi.org/10.5588/ijtld.09.0695.

[36] Domingo-Gonzalez R, Prince O, Cooper A, Khader S. Cytokines and Chemokines in Mycobacterium tuberculosis infection. Microbiol Spectr 2016;4. https://doi.org/10.1128/microbiolspec.TBTB2-0018-2016.

[37] Alam K, Ghousunnissa S, Nair S, Valluri VL, Mukhopadhyay S. Glutathione-redox balance regulates c-rel-driven IL-12 production in macrophages: possible implications in antituberculosis immunotherapy. J Immunol 2010;184:2918-29. https://doi.org/10.4049/jimmunol.0900439.

[38] Méndez-Samperio P. Role of interleukin-12 family cytokines in the cellular response to mycobacterial disease. Int J Infect Dis 2010;14:e366-71. https://doi.org/10.1016/j.ijid.2009.06.022.

[39] Limongi D, Baldelli S, Checconi P, Marcocci ME, De Chiara G, Fraternale A, et al. GSH-C4 Acts as Anti-inflammatory Drug in Different Models of Canonical and Cell Autonomous Inflammation Through NFκB Inhibition. Front Immunol 2019;10:155. https://doi.org/10.3389/fimmu.2019.00155.

Legends to the figures

Figure 1. Inhibition of *M. avium* growth by I-152 (a) or C4-GSH (b).

Bacteria suspensions, grown in Middlebrook 7H9 broth, were exposed to different concentrations of the molecules for seven days at 35°C. Inhibition growth was evaluated by plating, at the beginning and at the end of the experiment, 10 µl of suspensions on Middlbrook 7H10 agar for the enumeration of CFUs/ml. Mean values ± standard deviations for three experiments are shown. Significant *M. avium* growth inhibition vs not treated is indicated as follows: *p<0.05; **p<0.01; ***p<0.001.

Figure 2. Inhibition of *M. avium* viability by I-152 (a) or C4-GSH (b).

Viability was determined in mycobacterial suspensions in sterile distilled water containing or not containing the molecules (5 and 10 mM) at 35° C. Cell viability was evaluated by plating in triplicate 10 µl of each suspension on Middlebrook 7H10 agar for the enumeration of CFUs/ml. The results are the mean of two independent experiments.

Figure 3. Glutathione (GSH) levels in uninfected and *M. avium*-infected macrophages (a). Intracellular growth of *M. avium* in human macrophages in the presence of 10 mM of I-152 or 10 mM of C4-GSH (b).

The macrophage cultures were exposed for four hours to bacteria at a MOI of 60:1 (bacilli:macrophage). At this time and seven days after bacterium suspension removal, GSH was determined in the macrophage cells by HPLC. For the assay of antimycobacterial activity, I-152 and C4-GSH were dissolved in the culture medium at a concentration of 10 mM and added to the macrophages. After four days, the medium was replaced with fresh medium containing the pro-GSH molecules. CFUs, determined as described in section 2.4 , were evaluated per total macrophage proteins. The results of antimycobacterial activity are given as percentage of growth inhibition vs infected and untreated macrophages. Mean values ± standard deviations for three experiments are shown. Significant *M. avium* growth inhibition is indicated as follows: *p<0.05; **p<0.01.

Figure 4. Modulation of cytokine production in *M. avium*-infected macrophages untreated or treated with I-152 or C4-GSH.

The cytokines were determined in the supernatants collected after four and seven days of infection by a multiplex biometric ELISA-based immunoassay. The interleukin concentrations were calculated using a standard curve and software provided by the manufacturer (Bio-Plex manager software, v.6.1). Final values represent the sum of the fourth day values and the seventh day values. The results represent the mean of two separate experiments and are given as cytokine pg/CFU.

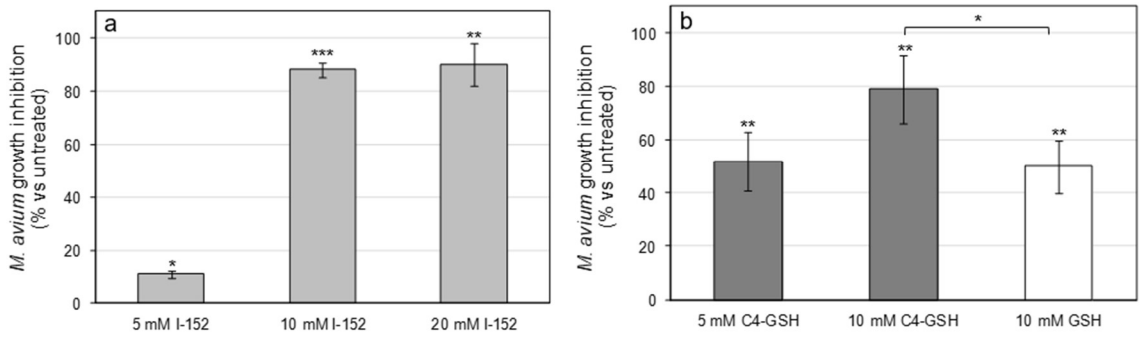
a
M. avium growth inhibition (% vs untreated)
100
80
60
40
20
0
*
***
**
5 mM I-152
10 mM I-152
20 mM I-152
b
M. avium growth inhibition (% vs untreated)
100
80
60
40
20
0
**
**
**
*
5 mM C4-GSH
10 mM C4-GSH
10 mM GSH

Figure 1

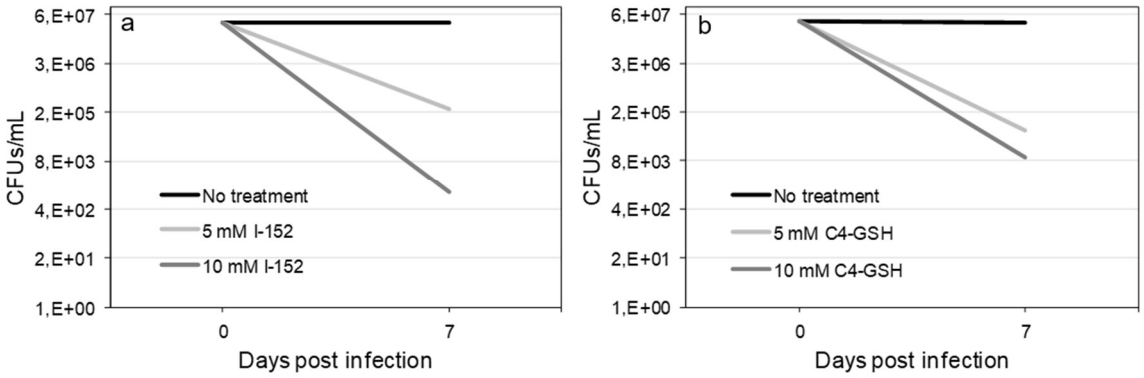
a
6,E+07
3,E+06
2,E+05
8,E+03
4,E+02
2,E+01
1,E+00
CFUs/mL
No treatment
5 mM I-152
10 mM I-152
0
7
Days post infection
b
6,E+07
3,E+06
2,E+05
8,E+03
4,E+02
2,E+01
1,E+00
CFUs/mL
No treatment
5 mM C4-GSH
10 mM C4-GSH
0
7
Days post infection

Figure 2

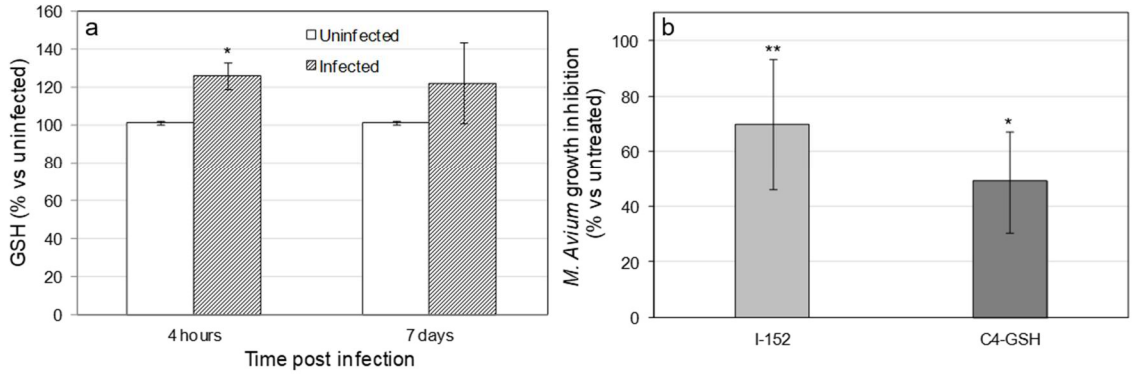
a
Uninfected
Infected
GSH (% vs uninfected)
160
140
120
100
80
60
40
20
0
*
4 hours
7 days
Time post infection
b
M. Avium growth inhibition (% vs untreated)
100
80
60
40
20
0
**
*
I-152
C4-GSH

Figure 3

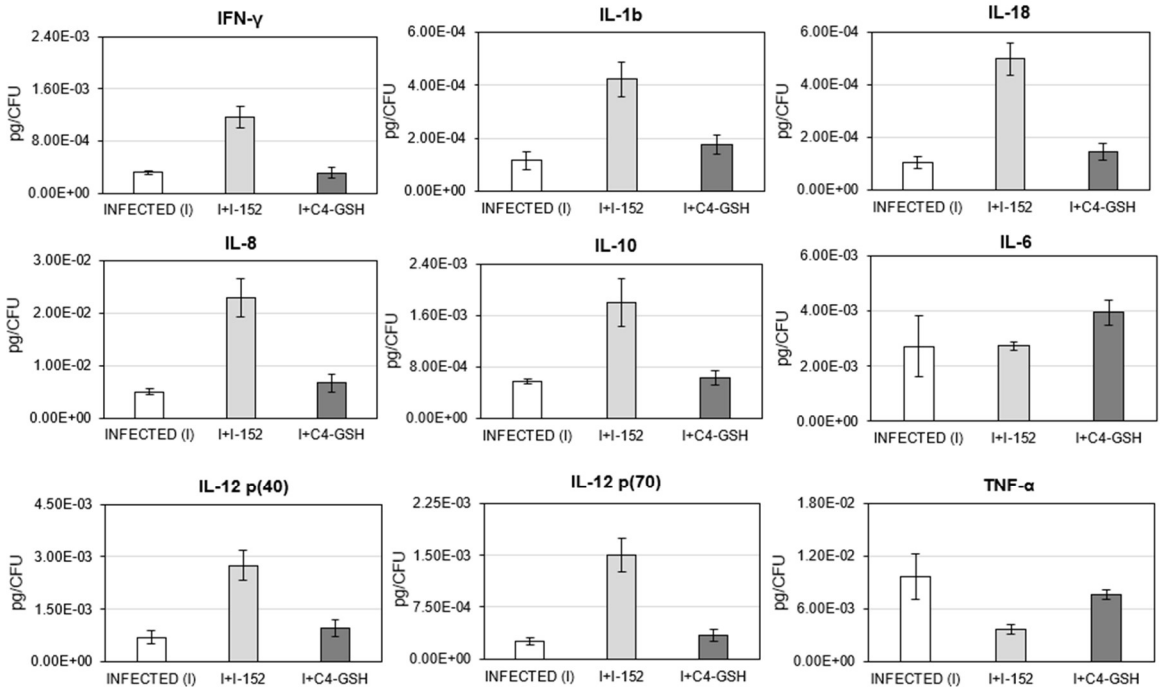
IFN-γ
IL-1b
IL-18
IL-8
IL-10
IL-6
IL-12 p(40)
IL-12 p(70)
TNF-α
pg/CFU
INFECTED (I)
I+I-152
I+C4-GSH

Figure 4

CHAPTER 4

In this chapter, the modulatory effects of I-152 on the production of anti/pro-inflammatory cytokines were studied both in macrophages obtained from transgenic $CFTR^{-/-}$ mice, and in murine macrophage RAW 264.7 cell line. This work was performed in collaboration with Professor Emanuela Bruscia from Yale University. All the data were obtained by the author of this thesis first during the abroad experience at Yale University, and then at the University of Urbino.

(Unpublished data)

4.1 Introduction

Cystic fibrosis (CF) is a common life-limiting autosomal recessive genetic disorder, with the highest prevalence in Europe, North America, and Australia CF is caused by mutations in a 230 kb gene on chromosome 7 encoding a chloride-conducting transmembrane channel named cystic fibrosis transmembrane conductance regulator (CFTR) [135]. Functional failure of CFTR results in mucus retention and chronic infection and subsequently in local airway inflammation that is harmful to the lungs. CFTR dysfunction mainly affects epithelial cells, although there is evidence of a role in immune cells [135][136]. CF is a multisystemic disease, however, morbidity and mortality result from chronic lung disease [137].

CFTR mutations

At the molecular level, the CFTR gene undergoes transcription and is then translated into the functioning CFTR ion channel that translocates to the cell membrane. This gene can be altered by more than 2000 mutations [135], which are mostly missense alterations, but also frameshift, splicing, nonsense, large and in-frame deletion/insertion, and promoter; it is thought that non-pathological variants could account for 15% [138]. Each mutation can interfere with important aspects for the final functionality of the CFTR protein (i.e. synthesis, ion conductance, stability at the cell membrane), bringing to a different outcome of the disease that can be characterized either by severe or mild lung phenotype; these different effects are a useful tool that allowed the grouping of the CFTR mutations into six classes [138], (Table 4.1).

Table 4.1. CFTR mutation classes.

Phenotype	*Class*	*CFTR defect*	*Type of mutation*	*Examples*
Severe	I	No protein synthesized	Nonsense, frameshift	G542X, W1282X
	II	Immature protein synthesized	Missense, amino acid deletion	F508del, N1303K
	III	Gating defect	Missense, Amino acid change	G551D, S549N
	IV	Decreased protein conductance	Missense, Amino acid change	R347P, D1152H
Mild	V	Decreased synthesis of normal protein	Splicing defect, Missense	3849+10kb C→T, 2789+5 G→A, A455E
	VI	Decreased cell surface stability	Missense, Amino acid change	1811+1.6kb A→G

This classification, based on the similar consequences of the mutations on the CFTR protein, is useful since it allows to identify of mutation-specific therapy strategies, but it also has limits. Unfortunately, many mutations nowadays are still not classified, and others that possess traits belonging to more than one class of

mutation, like F508del. The latter, a three base pair deletion that codes for phenylalanine at position 508 of the CFTR protein [139], is normally considered a class II mutation (immature protein synthesized), but it also possesses characteristics typical of class III (gating defect) and class VI (decreased cell surface stability) [135][138].

According to the Cystic Fibrosis Foundation (CFF, https://www.cff.org/), the highest percentage of people with CF who have at least one mutation in class II is about 88%, which is followed by class I (22%) while the other classes are relatively rare. The most common mutation among all CF patients is the F508del [139][140], while other mutations, like G551D, show heterogeneous geographic distribution [139][140]. It is interesting to note that some mutations are sometimes mentioned using their geographical origin (e.g. Italian mutation, Mediterranean mutation, Celtic mutation) [138]. In conclusion, the frequency of each mutation depends on the belonging class and the geographic position.

The role of the CFTR channel in the pathophysiology of CF in the lung is either due to its absence or lack of functionality, which leads to mucus obstruction, infection, and inflammation. The effect on the mucus is a result of the reduced secretion of chloride and bicarbonate, which causes dehydration of airway surfaces. Moreover, the CFTR malfunction has been linked to increased activity of the epithelial sodium channel (ENaC) and, consequently, increased absorption of Na^+ in the airways that causes airway surface liquid (ASL) depletion, mucus adhesion, and impaired mucus transport [141][142]. The mucus is secreted by goblet cells and it needs about 115 mM bicarbonate to be secreted and expand properly, a concentration that is not reached if a CFTR malfunction is present like in the CF disease [143]. The reduced bicarbonate secretion also causes a decreased ASL pH resulting in defective antibacterial mechanism in the lung [144]. The final result of mucus obstruction, impaired mucociliary clearance, and reduced bacterial killing is the lack of the innate pulmonary defense system, that favors the colonization of the lung environment by opportunistic bacteria like *Pseudomonas aeruginosa* (*P. aeruginosa*; PA) and the consequent severe and chronic inflammatory response [145]. All these aspects taken together will cause progressive pulmonary damage, and eventually lead to a decline in lung function and death.

Inflammation

Cystic fibrosis is characterized by chronic lung inflammation, because of infections that the immune system is not able to resolve properly, thus leading to accumulation and overactivation of neutrophils, their consequent constant recruitment, and their inability to undergo apoptosis but instead necrosis [146]. All of these aspects bring to overproduction of oxidants and proteases, and the releasing of intracellular contents by neutrophils that can finally harm the airway tissues [147] and can be used as predictor factors of bronchiectasis, like in the case of the protease neutrophil elastase (NE) that damages the airway wall architecture [148]. NE is one of the components of neutrophil extracellular traps (NETs); NETs formation (NETosis) is an important mechanism of defense that neutrophils put in place to fight pathogens [149], which has been associated to the increased inflammatory response in CF [150]. Another interesting aspect is that neutrophils express CFTR in their

phagolysosome, which when absent or defective causes the impaired microbial killing ability of these cells [151].

Other immune cells implicated in the inflammatory response in the lungs are macrophages, both resident [alveolar, and interstitial], and recruited in response to a stimulus [monocite derived macrophages coming from the circulation] [152][153]. Macrophage activation can be influenced by the presence in the environment of either pathogen-associated molecules (PAMPs),e.g. lipopolysaccharide (LPS), or damage-associated molecular patterns (DAMPs), e.g. cytoplasmic and nuclear components, that are recognized by pattern-recognition receptors (PRRs), e.g. toll-like receptors (TLRs) [154][155]. The recognition of a specific ligand by a PRR will initiate a signal transduction mechanism of many pathways (e.g. NF-kB, MAPK) which will bring to the production of inflammatory mediators, e.g. pro-inflammatory cytokines, reactive oxygen species (ROS), nitric oxide (NO), and the consequent inflammatory response [154]; one important cytokine involved in inflammation is IL-1, which is in fact considered as the regulator of inflammation [156][157]. The aim is to exacerbate pathogen infections, resolve inflammation, repair the tissue, and remove dead cells and tissue debris. To do that, macrophages, that belong to a heterogeneous population, once activated can show either pro-inflammatory (M1) or anti-inflammatory phenotype (M2) [158]. Classically activated M1 macrophages derive from undifferentiated macrophages (M0) after exposure to LPS or IFN-γ, they secrete high concentration of pro-inflammatory mediators like IL-6, IL-12, TNF-α, and low levels of IL-10, and are involved in phagocytosis of pathogens, and in promoting and sustain inflammation; on the contrary, the polarization of M0 in alternatively activated M2 macrophages, is stimulated by the exposure to IL-4, IL-10 and is characterized by the secretion of IL-4 and IL-13, and by anti-inflammatory, immunoregulatory and tissue-repair properties [153]. The acute inflammatory response starts with the recruitment of neutrophils in the first 3 days; a few days later, M1 macrophages arrive in the site of infection, while M2 macrophages appear over the next 10 or more days to resolve the inflammation and to clear any presence of apoptotic cells by efferocytosis [159]. Macrophages are characterized by plasticity, which is the ability to switch between M1 and M2 phenotype based on the environmental stimulation, an important characteristic for the appropriate modulation of the inflammatory response [160]. It is interesting to note that in healthy state, macrophages in the lungs are not activated, but they act as sentinels that do not react in a pro-inflammatory way to antigens, otherwise they would harm the lung structure [160]. CF macrophages are characterized by a hyperinflammatory response when exposed to bacteria such as *P. aeruginosa*, and PAMPs like LPS [161][162]. It is interesting to note that TLR4 expression is increased in CF, which could lead to sustained signal transduction and activation of the NF-kB pathway; this is probably due to abnormal trafficking of the transmembrane receptor, which is not internalized and consequently degraded [163]. The overactivation of the NF-kB pathway brings to the M1 phenotype, which shows a little capacity of efferocytosis and autophagy [164]. This leads to an ineffective bactericidal function, and an inefficient inflammation resolution [165].

Redox state in CF

Lungs are highly exposed to both endogenous and exogenous oxidants (e.g. ROS produced by activated phagocytes, and oxidants both inhaled and produced by pathogens respectively) [166], so a reducing environment composed of enzymatic e non-enzymatic antioxidants, as it is found in healthy lungs, is important to prevent an exaggerated inflammatory response. Cystic fibrosis lungs, however, are characterized by an oxidative environment, which leads to an alteration in ion transport (including chloride secretion) [167], increased synthesis and secretion of mucins [168], and to overactivation of intracellular signaling cascades resulting in excessive inflammation, mediator release, and tissue injury-events [166]. An important aspect is that the antioxidants, which are normally found in healthy airway surface fluid (ASF) are also present in CF ASF, although at lower concentrations; one of them is glutathione (GSH) [98]. The CFTR channel is mostly known for the transport of chloride and bicarbonate, but *in vitro* studies showed that it transports other molecules like GSH [98], resulting in a systemic decrease and not necessarily due to inflammation [169]. This reduction may be connected with the severe oxidative stress characterizing the chronic inflammation on the CF lung [170], suggesting that the CFTR channel presence/functionality may have an important role in the inflammatory response. Furthermore, the transfection of functional CFTR in a pulmonary epithelial cell line characterized by a defective CFTR, showed the restoration of GSH secretion [171], supporting the hypothesis that the CFTR protein is involved in antioxidant homeostasis in the lung. Other reasons why GSH is lower in CF ASF compared to non-CF could be chronic infection and inflammation; when an infection occurs, the recruited neutrophils produce myeloperoxidases (MPO) to convert hydrogen peroxide to an array of ROS in order to kill bacteria. In CF this mechanism is over-enhanced, leading to a reaction of ROS with GSH and the consequent depletion of the latter [172]. GSH decrease found in young individuals with CF could mean that they may be more vulnerable to oxidative stress [173]. These findings suggest that supplementation of GSH could be useful to counteract the increased inflammatory response typical in CF patients.

GSH supplementation and GSH precursors in CF

Glutathione supplementation can be achieved via both oral and inhaled GSH administration. Trials conducted in healthy volunteers showed that oral supplementation did not increase GSH concentration in plasma [174], probably because it is rapidly metabolized by the GGT, and because its half-life is less than 3 minutes [109]. Some success in increasing GSH in lymphocytes [175] was assessed by increasing cysteine stores using lipoic acid [176] or whey protein [177]. The supplementation of the tripeptide by inhalation was tested in CF patients and showed increased levels of GSH in BALF (bronchoalveolar lavage fluid), significant improvements in lung function, but no significant differences in the numbers of neutrophils, lymphocytes, or macrophages [178]. Results from a small uncontrolled observational study showed that after the GSH regimen (both oral and inhaled) the CF patients had higher levels of the tripeptide both in blood and ASL, and fewer infection exacerbations [179], suggesting that a GSH concentration increase could benefit the health of CF patients. On the contrary, another study showed that in CF patients the GSH supplementation increased the tripeptide concentration in lymphocytes, but no improvements in sputum neutrophils or lung function [180],

probably due to well-established disease, inadequate dose, or the short period of the study. The inhaled GSH approach could have side effects and various complications, like inducing bronchospasm in individuals with mild asthma [181], GSH rapid clearance [182], and oxidation [183] in the lung. Another important aspect is that treatment with the tripeptide could potentially compromise the host defenses in the airway [169]. All these aspects suggest that future studies aimed to investigate the effectiveness of inhaled GSH should consider the half-life of the tripeptide, as well as the overall safety, optimal dose, duration of treatment, and efficacy [166] GSH has, however, unfavorable pharmacokinetic properties [109], which means that administration of high doses is necessary to reach a therapeutic value [108]. For this reason, another useful approach to increase intracellular glutathione in CF is by using GSH pro-drugs, like NAC, and MEA.

NAC is the most common agent used as a mucolytic agent in CF, able to break disulfide bonds between mucin macromolecules *in vitro* and *in vivo* [115], thus depolymerizing mucus and facilitating its removal from the respiratory tract. Also, NAC may act as an oxygen radical scavenger [184]. NAC can be administered both by inhalation and orally. Inhaled administration is usually prescribed to CF patients to improve the expectoration of sputum by reducing its tenacity but it has some side-effects, like its unpleasant sulfurous smell; moreover, it can cause bronchospasm, it is a time-consuming procedure, and it is rapidly oxidized in the highly oxidizing CF airway [185]. Oral administration is considered more efficient [186] because it is absorbed by the intestinal epithelium, and it can be rapidly metabolized to liberate cysteine, which can be used by cells to synthesize GSH in the cytoplasm, in order to increase the antioxidant capacity in the lung [187]. A study conducted on cultured CF airway epithelial cells showed that NAC could have some effects upon CFTR function, like improving the duration and frequency rate of chloride efflux by probably changing the redox potential that affects CFTR channel gating [188][189]. NAC may also restore the activity of Nrf2, which is decreased in CF, and decrease the production of inflammatory cytokines such as IL-8 and IL-6 [187]. Conrad and colleagues designed a long-term treatment of orally administered NAC, which results showed that this molecule is safe and can be used to prevent lung deterioration [187].

MEA, approved by the FDA in 1994, is used for the treatment of the rare disease known as cystinosis [187]. It has been used for more than 20 years, thus there are a lot of data that indicate MEA as a safe drug. However, its activity has not been fully established in CF; moreover, its pharmacokinetics and tolerability might be different in CF patients and can not be extrapolated from the cystinosis data. For this reason, Devereaux and colleagues tested oral administration of MEA and found that MEA levels were higher in the bronchial secretion than in the plasma [190]. MEA has received an Orphan Drug Designation in CF as a mucolytic because of its ability to break disulfide bonds [191], an interesting characteristic that could be useful in the treatment of CF. It was also demonstrated that MEA has antimicrobial properties and is able to disrupt the bacterial biofilm, suggesting that it could be used in addition to the classical antibiotic treatments used in CF [192]. Interestingly, it was found to improve the clearance activity against *P. aeruginosa* of macrophages with the F508del CFTR mutation [193].

4.2 Aim of the study

Because of the fundamental role of redox state and GSH depletion in CF, we investigated if I-152 was able to modulate the inflammatory response in CF macrophages by altering the redox homeostasis of these cells. The CF inflammatory response is characterized by the fact that it increases until it becomes self-perpetuating, leading to a deterioration of the CF lung function. Therefore, the aim was to find a way to help the macrophages to decrease the pro-inflammatory state, without suppressing the inflammatory response. Moreover, I-152, as said above, is a molecule able to release NAC and MEA. The interesting characteristics of both molecules as mucolytic, antimicrobic, biofilm breaker, could make I-152 a valuable drug for CF able to alter the redox state and, at the same time, to show the features of both NAC and MEA.

The experiments were performed on the CF model consisting of monocytes obtained from transgenic $CFTR^{-/-}$ ($B6.129P2\text{-}Cftr^{tm1Unc}$) mice and differentiated *in vitro* into macrophages.

Thereafter, the anti-inflammatory capacity of I-152 was confirmed in RAW 164.7 cells, which is a murine macrophage cell line.

4.3 Materials and methods

4.3.1 Reagents

I-152 was synthesized by a research group at the Institut des Biomolecules Max Mousseron, Universitè Montpellier (France), with which the Department of Biomolecular Sciences collaborates [127].

Pseudomonas aeruginosa LPS (PA-LPS) (Sigma-Aldrich) was prepared in PBS at 100X stock solution and used at a concentration of 10 µg/ml.

4.3.2 CF bone marrow-derived macrophages: isolation, culture, and treatments

These experiments were performed in collaboration with Professor Emanuela Bruscia from Yale University, with whom the Section of Biochemistry and Biotechnology has been collaborating for some years. Cells were obtained from transgenic CFTR$^{-/-}$ (B6.129P2-Cftr^{tm1Unc}) (CF cells) and wildtype (WT cells) mice. The animals were sacrificed, and bone-marrows (BM) were collected. Briefly, bones were ground with a mortar and pestle and then filtered in a 50 ml vial with PBS to eliminate any residual muscle tissue. The bone marrows were centrifuged at 1400 rpm for 6 minutes. The pellet was resuspended in Dulbecco's Modified Eagle Medium High Glucose (DMEM) supplemented with 10% heat-inactivated FBS, 2 mM L-glutamine, 100 U/ml penicillin, 100 µg/ml streptomycin (Gibco, Thermo Fisher Scientific, USA), 20 ng/ml recombinant macrophage colony-stimulating factor (M-CSF) (ConnStem Inc., USA), and were put in culture in a 75 cm^2 flask overnight. The next day, the nonadherent cells were transferred to a 175 cm^2 flask and let to differentiate for about 7 days [162]. Finally, cells were detached, counted, and plated at a concentration of 1x10^6 cells/well in 6-well plates (Ø35 mm dishes) (Corning Incorporated, USA). Treatments were performed the next day.

To determine GSH and cysteine levels, and IkB-α and p-p65 expression after LPS stimulation, CF and WT cells were incubated with 10 µg/ml of *P. aeruginosa* LPS for 15, 30 minutes, and 1 hour; two wells were prepared per condition for each time point. The cells, after 2 washes with PBS, were lysed and treated for thiols quantification (paragraph 4.3.4), and Western immunoblotting analysis (paragraph 4.3.13).

In the experiments aimed at determining cytokine expression and thiols quantification, after 1h treatment with LPS (10 µg/ml), I-152 at different concentrations (0.25, 1, and 5 mM) was added to the cells for 6h. Two wells were prepared per condition, the cells of one well were collected for the study of RNA expression at 6 hours (paragraph 4.3.10), while in another well, after washing, fresh medium was added until the next morning. At this time, the culture medium was collected and stored at -80°C until analysis (paragraph 4.3.8), and cells were lysed for intracellular thiol quantification (paragraph 4.3.6).

4.3.3 RAW 264.7 cells: culture and treatments

RAW 264.7 cells, a murine macrophage cell line, were cultured in DMEM, supplemented with 10% heat-inactivated fetal bovine serum (FBS), 2 mM L-glutamine, 100 µg/ml streptomycin, and 100 U/ml penicillin (Sigma Aldrich, Milan, Italy). Cells were plated in 6-well plates (Ø35 mm dishes) (Greiner Bio-One, Germany) at an initial concentration of 4-10x10^4 cells/ml in a volume of 2 ml of culture media, and let to incubate at

37°C and 5% CO_2. After three days, when the cells had a confluence of 70-80%, two washes with physiological saline solution (NaCl 0.9%, K_2HPO_4, pH 7.4; PBS) were performed, and then we proceeded with the treatments.

To determine GSH and cysteine levels after LPS stimulation, RAW 264.7 cells were incubated with 10 µg/ml of *E. coli* LPS for 15, 30 minutes, and 1, 2, 4, 6 hours. At each time point, the cells, after 2 washes with PBS, were lysed and treated as described (paragraph 4.3.6).

To determine intracellular thiol species after treatment with I-152, RAW 264.7 cells were incubated with the molecule at the concentration of 1 mM, and after 30 min they were washed with PBS, lysed, and processed for thiol analysis as described (paragraph 4.3.6).

In the experiments aimed at determining the cytokine expression after challenging with LPS (10 µg/ml for 1h), I-152 at different concentrations (0.062 - 1 mM) was added to the cells for 6h. Two wells were prepared per condition, as the cells of one well were collected for the study of RNA expression at 6 hours, while in another well, after washing with PBS, fresh medium was added until the next morning. At this time, the culture medium was collected and stored at -80°C until analysis (paragraph 4.3.12).

4.3.4 Preparation of samples for the determination of GSH, cysteine, and other thiol species

After the treatments, cells were washed twice with PBS. Thereafter, 100 µl of lysing solution (0.1% (v/v) Triton X-100, 0.1 M Na_2HPO_4, 5 mM EDTA, pH 7.5), 15 µl of 0.1 N HCl, and 140 µl of precipitating solution (100 ml containing 1.67 g of glacial metaphosphoric acid, 0.2 g of disodium EDTA, and 30 g of NaCl) were added to each dish. The lysates were recovered by using a rubber scraper, transferred into 1.5 ml microtubes (Sarstedt, Germany), and kept on ice for 10 minutes. After centrifugation at 12000 rpm for 10 minutes at 4°C, the pellet was separated from the supernatant. The former was used for spectrophotometric determination of the proteins (paragraph 4.3.5), while the latter was used for the determination of thiol species by HPLC (paragraph 4.3.6).

4.3.5 Spectrophotometric determination of proteins

The pellet obtained as described in paragraph 4.3.4 was dissolved in 0.1 N NaOH, and protein concentration was determined by the Bradford assay. A 1 ml plastic cuvette (10x4x45 mm Sarstedt, Germany) containing 800 µl of double-distilled H_2O + 200 µl of Protein Assay Dye Reagent (Bio-Rad, USA) was used as blank. In the other two cuvettes were added 5 or 10 µl of protein extract + 795 or 790 µl of double-distilled H_2O respectively + 200 µl of Protein Assay Dye Reagent Concentrate. Absorbance measurements were performed with a spectrophotometer at 595 nm. Quantitative measurements (µg of total proteins) were obtained by using a calibration curve, obtained with different concentrations of albumin dissolved in 0.1 N NaOH.

4.3.6 Determination of GSH and other thiol species by high-performance liquid chromatography (HPLC)

The supernatant obtained as described in paragraph 3.3.4 was filtered through a 0.22 µm pore size membrane. Therefore, to 60 µl of the sample was added 15 µl of 0.3 M Na_2HPO_4, and 7.5 µl of DTNB (50 ml containing 20 mg of 5,5'-dithio-bis-(2-nitrobenzoic acid), and 1% sodium citrate tribasic dihydrate). The obtained mixture was immediately stirred for 1 min at room temperature (RT), left in the dark for 5 min at RT, and lastly used for determination of GSH and other thiol species by HPLC; this method was developed to specifically determine intracellular and intra-tissue thiol species [194]. A Teknokroma Tracer Excel guard-column with a 10x3.2 mm ODS filter (Teknokroma Analitica SA, Spain) and a BDS Hypersi ITM C18 150x4.6 mm column (TermoFisher Scientific, United States) was used for the analysis. The mobile phase consisted of buffer A containing 10 mM KH_2PO_4 solution, pH 6, and buffer B consisting of 40% (v/v) of buffer A and 60% (v/v) of acetonitrile. The elution conditions were: 100% buffer A for 10 min, 15 min up to 100% buffer B, and hold 5 min. The gradient was brought back to 100% buffer A in 3 min. The flow rate was 1 ml/min, and the detection was performed at 330 nm. Quantitative measurements were obtained by injection of standards of known concentration (paragraph 4.3.7) and values were normalized on protein concentration (paragraph 4.3.5), by using the following mathematical formula:

$$\frac{peak\ area\ of\ the\ thiol\ species}{STD\ area} \times \frac{255}{50} \times DF \times \frac{1000}{\mu g\ of\ protein} = \frac{picomoles\ of\ the\ thiol\ species}{\mu g\ of\ protein}$$

STD area = 1 nmole area of the thiol species considered;

255 = initial volume (µL) of the sample (100 µL lysant +15 µL HCl + 140 µL precipitating solution);

50 = volume (µL) injected into HPLC;

DF = dilution factor (in this case it corresponds to 1.375).

4.3.7 Preparation of standard solutions for HPLC

The spectrophotometric determination of standard solutions (STD) of thiol species was determined at 412 nm. A 1 ml plastic cuvette (10x4x45 mm Sarstedt, Germany) containing 200 µL of double-distilled H_2O + 600 µL of Na_2HPO_4 was used as blank (B); while another 1 ml cuvette contained 200 µL of 0.05 mM STD + 600 µL of Na_2HPO_4. Absorbance was determined both before and after the addition of 80 µL of a solution containing DTNB (prepared as described in paragraph 3.3.6). The following formula is then applied to determine the actual concentration of the prepared STD:

$$\frac{\Delta|STD| - \Delta|B|}{13600} \times 4.4$$

13600 = Absorbance (Abs) of 1µmole of TNB^-;

4.4 = sample dilution.

The STD were then injected into HPLC at a concentration of 20 µM, prepared by adding 10 µl of DTNB solution to 100 µL of 22 µM STD. The samples were stirred for 1 minute at RT and kept for 5 minutes in the dark at RT.

4.3.8 Cytokine quantification by ELISA

The cytokines (IL-6, TNF-α, IL-10) released into the culture medium by the cells were determined by an ELISA (enzyme-linked immunosorbent assay) procedure following the instructions described in the kit (ELISA MAX Deluxe Set Mouse BioLegend, San Diego). In each well of the ELISA plate, 100 µl of Capture Antibody diluted in Coating Buffer A 1X was added and the plate was then left to incubate at 4°C overnight. The following day 4 washes were made with TPBS (10 mM NaH_2PO_4, 154 mM NaCl, pH 7 (PBS) + 0.1% Tween-20) and each well was blocked with 200 µl of Assay Diluent A 1X for 1 hour under stirring at RT. All subsequent incubations were carried out in this way. After 4 washes with TPBS, 100 µl per sample well, and the standards serially diluted (500-15.6 pg/ml) were plated in 1X Assay Diluent A and the plate was left to incubate for 2h. At the end of the incubation, 4 other washes were carried out with TPBS and 100 µl of Detection antibody 1X diluted in Assay Diluent A 1X were plated. After 1 hour of incubation, after 4 washes with TPBS, 100 µl of Avidin-HRP were plated and the plate was left to incubate for 30 minutes. After a final wash, 100 µl of TMB Substrate Solution (50% Substrate Solution A and 50% Substrate Solution B) was plated and the plate was left to incubate for 20 minutes in the dark at RT. Finally, 100 µl of Stop Solution (2N H_2SO_4) was added and the absorbances were read at 450 nm and 570 nm using a Model Benchmark microplate reader (Bio-Rad, USA). Concentrations were calculated using a standard curve obtained from known cytokine concentrations included in the assay kit.

4.3.9 CF: Extraction and quantification of total RNA

The RNeasy mini kit (Qiagen) was used for the extraction of total RNA and the manufacturer's instructions were followed. The cells were lysed with 700 µl of Trizol and the lysates were collected in 1.5 ml microtubes. 140 µl of chloroform were added to each tube and the solution was manually mixed a few times. After 2-3 min of incubation at RT, the lysates were centrifuged at 12000 rcf for 15 sec at 4°C. Next, the resulted clear liquids on top were collected and put in a second set of 1.5 ml microtubes, and about 360 µl of EtOH 100% was added and moved into columns to start the RNA extraction. The mix was centrifuged at 8000 rpm for 15 sec and the flow-through was discarded. After a wash with the washing buffer RWT, the DNAse mix was added to each column and left to incubate for 30 min at RT. Next, the columns were washed again with RWT. 500 µl of RPE buffer were added and columns were then centrifuged 3 times; the last time columns were centrifuged for 1 min at maximum speed to dry the membranes. Finally, RNA was eluted in 1.5 ml microtubes with 30-50 The columns were first centrifuged for 1 min at maximum speed to dry the membranes, then placed in 1.5 ml microtubes in which the RNA was eluted with 30-50 µl of RNase-free water. The total RNA extracted was

measured spectrophotometrically by NanoDrop and the purity of the sample was measured by the ratio between the absorbances A260/A280.

4.3.10 CF: Synthesis of cDNA and Real-Time PCR for the analysis of genes that code for inflammatory cytokines

The SuperScript™ II Reverse Transcriptase kit (Thermo Fisher Scientific, USA) was used to obtain cDNA from 0.5 µg of total RNA, following the manufacturer's specifications. A first reaction containing Oligo(dT), RNA and dTNP Mix was prepared. The solution was heated to 65°C for 5 min and quickly chilled on ice. Next, First-Strand Buffer, DTT, and RNaseOUT™ were added and left to incubate at 42°C for 2 min. Finally, 200 units of SuperScript™ II RT were added. The resulting 20 µl solution was incubated at 42°C for 50 min, and the reaction was inactivated by heating at 70°C for 15 min. The analysis of the target genes involved in inflammation (IL-6, TNF-α, IL-10) was performed by real-time PCR, with a quantitative-comparative approach; 18s was used as housekeeping. The analysis was performed with a Bio-Rad iCycler (Bio-Rad, USA) using TaqMan technology. The data analysis was based on the ΔΔCt method with the normalization of raw data on the housekeeping gene, and the results were calibrated on the cDNA of the untreated cells. The used primers were purchased from Applied Biosystems (Life Technology).

4.3.11 RAW 264.7: Extraction and quantification of total RNA

The RNeasy Plus Mini Kit (Qiagen) was used for the extraction of total RNA and the manufacturer's instructions were followed. The cells were lysed with 350 µl of RLT buffer and the material was collected in sterile 1.5 ml microtubes (Sarstedt, Germany). The genomic DNA of the lysate was eliminated thanks to the use of gDNA Eliminator columns provided by the kit, which were centrifuged for 30 seconds at 8000 xg. 350 µl of 70% ethanol were added to the flow-through and the final 700 µl were transferred to columns to proceed with the RNA extraction. The columns were centrifuged for 15 seconds at 8000 xg and the flow-through was eliminated. A first wash was carried out for 15 seconds at 8000 xg with 700 µl of buffer RW1 to eliminate biomolecules such as carbohydrates, proteins, and fatty acids. The flow-through was eliminated and two washes were carried out with 500 µl each of buffer RPE, useful for eliminating any traces of salts present in the column. The columns were first centrifuged for 1 min at maximum speed to dry the membranes, then placed in 1.5 ml microtubes in which the RNA was eluted with 30-50 µl of RNase-free water. The total RNA extracted was measured spectrophotometrically by NanoDrop and the purity of the sample was measured by the ratio between the absorbances A260/A280.

4.3.12 RAW 264.7: Synthesis of cDNA and Real-Time PCR for the analysis of genes that code for inflammatory cytokines

Complementary DNA (cDNA) was synthesized by reverse transcribing 0.5 µg of total RNA, a reaction catalyzed by reverse transcriptase, using the PrimeScript RT Master Mix (Perfect Real Time) kit (Takara Bio Inc.) and following the manufacturer's directions. The reverse transcription process was performed in a final

volume of 10 µl and the latter was subjected to a cycle of 15 minutes at 37°C and 15 sec at 85°C to inactivate the reverse transcriptase. The samples were kept at -80°C until they were used. The analysis of the target genes involved in inflammation (IL-6, TNF-α, IL-10) was performed by real-time PCR, with a quantitative-comparative approach; 18s was used as housekeeping. The reactions were carried out on a final volume of 25 µl, using the Hot-Rescue Real-Time PCR Kit Sybr Green (Diatheva s.r.l.), 2 µl of cDNA, and primers at a concentration of 200 nM. The amplification was conducted using the 7500 Real-Time PCR System Applied Biosystems (Thermo Fisher Scientific, USA) instrument. The data analysis was based on the ΔΔCt method with the normalization of raw data on the housekeeping gene, and the results were calibrated on the cDNA of the untreated cells. The PCR protocols consisted of a 10-minute cycle at 95°C followed by 40 specific cycles for each target gene, the indications of which are shown in Table 4.2. The primers used for gene amplification are shown in Table 4.3.

Table 4.2 Real-Time PCR protocols used to amplify the target gene involved in the inflammation (IL-10, IL-6, and TNF-α) in RAW 264.7 cells. For the IL-10 gene target, it was performed a 3-steps cycle (denaturation, annealing, and extension), while for the gene targets IL-6 and TNF-alpha it was performed a 2-steps cycle.

Target gene	Denaturation	Annealing	Extension
IL-10	95°C, 15 sec	65°C 20 sec	72°C, 35 sec
IL-6	95°C, 15 sec	60°C, 45 sec	
TNF-α	95°C, 15 sec	60°C, 45 sec	

Table 4.3 Primers used for gene expression analysis of target genes involved in inflammation (IL-10, IL-6, and TNF-α) and of the housekeeping gene (18s) in RAW 264.7 cells.

Target gene	Forward primer	Reverse primer
IL-10	CCAGTTTTACCTGGTAGAAGTGATG	TGTCTAGGTCCTGGAGTCCAGCAGACTC
IL-6	ACTTCACAAGTCGGAGGCTT	TGCCATTGCACAACTCTTTTC
TNF-α	CCCACGTCGTAGCAAACCA	ACAAGGTACAACCCATCGGC
18s	GTAACCCGTTGAACCCCATT	CCATCCAATCGGTAGTAGCG

4.3.13 Western immunoblotting analysis of the NF-kB pathway

After the treatment described in paragraph 4.3.2, two washes with PBS were performed and cells were lysed for Western immunoblotting analysis on ice. To do that 100 µl of lysis buffer [50 mM Tris / HCl pH 8.0, 2% (w/v) SDS (Sodium dodecyl sulfate), 40 mM N-ethylmaleimide (NEM), 0.25 mM of sucrose supplemented with protease inhibitors] were put on each well, and whole-cell lysates were collected into 1.5 ml microtubes using a rubber scraper, and immediately put on ice. Next, the contents of the microtubes were boiled for 5 minutes, sonicated at 70W for 40 sec, and centrifuged 12000 rpm at RT. The protein content was determined in the supernatant according to the Lowry assay. Proteins were resolved by SDS polyacrylamide gel electrophoresis (SDS-PAGE) and electroblotted onto polyvinyldene difluoride (PVDF) membrane. Next, the membrane was blocked in 5% (w/v) nonfat dry milk powder (Cell Signaling Technologies) dissolved in TTBS

(150 mM Tris-HCl pH 7.4; 150 mM NaCl; 0.1% (v/v) Tween-20) for 1h at RT. The membrane was then incubated overnight at 4°C with the following primary antibodies: IkBα (Cell Signaling Technologies, #9242), p-p65 (Cell Signaling Technologies, #3033), and β-ACTIN (Cell Signaling Technologies, #4967). The next morning, the primary antibodies were removed and incubation with horseradish peroxidase (HRP)-conjugated secondary antibody (Bio-Rad, Hercules, CA, USA) was performed for 1h at RT. Finally, the immunoreactive bands were visualized by the enhanced chemiluminescence detection kit WesternBright ECL (Advansta, Bering Dr, San Jose, CA USA); detection and quantification were performed by using the Image Lab software (Bio-Rad, Hercules, CA, USA).

4.3.14 Statistical analysis

The statistical analysis was performed using the t-test, and a Prism software version 6.0 was used (GraphPad, San Diego, CA, United States). p values ≤ 0.05 were considered significant.

4.4 Results

4.4.1 Results obtained in the CF model

Most results obtained in this model derive from one experiment; this is because of the inability to attempt replicate experiments due to the limited quantity of cells that can be isolated from the BM of each mouse.

4.4.1.1 Western immunoblotting analysis

The NF-kB pathway, involved in the production of cytokines implicated in the inflammatory response, is known to be activated by the linkage between LPS, a component of the bacterial cell wall, and the TLR4 present on the cell membrane of cells like macrophages [195]. To investigate the ability to activate this cascade, CF cells were challenged with PA-LPS at a concentration of 10 µg/ml for different times, and Ikb-α and p-p65 levels were examined. Ikb-α is the protein that keeps NF-kB in an inactivated state in the cytoplasm; after LPS stimulation the NF-kB cascade is activated and leads to IkB-α degradation [196] p-p65 is the phosphorylated subunit of NF-kB, which was found to be LPS-induced [197].

The results of the western immunoblotting analysis seem to suggest that LPS treatments decrease IkB-α levels with respect to NO LPS and that the protein remains low at all the time points considered, even if a slight time-dependent increase can be observed (Figure 4.1a). The levels of p-p65 appear to increase after LPS treatment at all time points, especially after 15 min (Figure 4.1b).

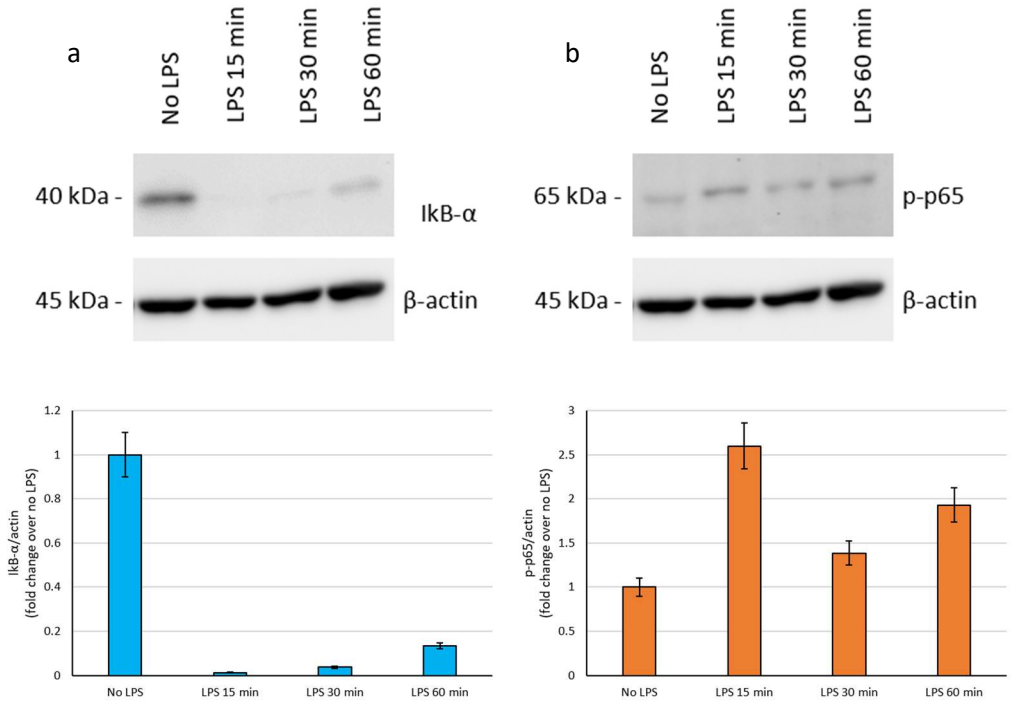

Figure 3.1 Western immunoblotting analysis of Ikb-α (a) and p-p65 (b) expressions in CF cells after PA-LPS stimulation at a concentration of 10 µg/ml. At the time point shown in the figure (15, 30, and 60 min), cells were lysed and the proteins were resolved by electrophoretic separation in SDS-PAGE, blotted onto a PVDF membrane, and probed with antibodies against IkB-α and p-p65. Immunoreactive bands were quantified with the Image Lab software and normalized on actin. The reported results come from a single experiment. Each value is the average of two technical replicates.

4.4.1.2 Determination of GSH levels after stimulation with LPS from *P. aeruginosa*

Data present in the literature show an alteration of the redox state during the inflammatory process [198]. It is known that stimulation with LPS brings to the activation of genes implicated in the inflammatory response [199]. Furthermore, in some experimental models stimulation with LPS causes an increase in ROS, and a decrease in GSH content with consequent oxidative stress [198]. For these reasons, GSH and cysteine levels were determined at different time points after stimulation with PA-LPS at a concentration of 10 µg/ml. The results reported in Figure 4.2 seem to suggest a slight depletion of the GSH levels after 30 min of LPS exposure, while at 1h the tripeptide content appear to be higher than the unstimulated control; it was not possible to determine cysteine levels because of the exiguous number of cells.

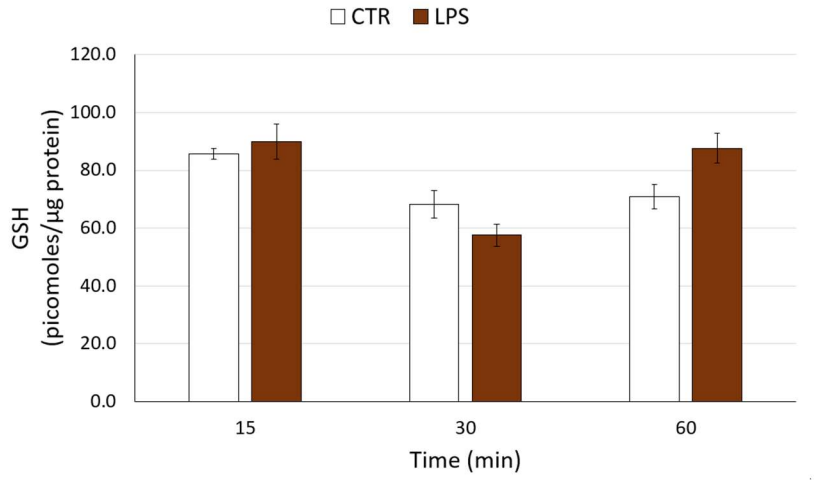

Figure 4.2 Intracellular GSH content in CF cells after LPS stimulation of *P. aeruginosa* at a concentration of 10 µg/ml. At the time point shown in the figure (15, 30, and 60 min), the cells were lysed with a solution containing Triton-X, and the proteins precipitated with metaphosphoric acid as described in Materials and Methods. GSH levels were determined by an HPLC method by derivatizing thiol species with DTNB [194]. The reported results come from a single experiment. Each value is the average of two technical replicates.

4.4.1.3 Determination of GSH and cysteine content after LPS and I-152 treatment

Since PA-LPS seems to influence the intracellular GSH levels, we wanted to determine whether it was possible to affect the overall thiol content by using I-152. To do that, CF cells were challenged with PA-LPS and then fresh medium with or without I-152 was added, as described in Figure 4.3; after 24h the intracellular levels of GSH and cysteine were determined. The effects of the different treatments on the GSH content seem suggest a higher concentration of the tripeptide in all the samples challenged with LPS. In particular, the highest concentration was detected in the cells stimulated with LPS and treated with 5 mM I-152 (Figure 4.3a). Interestingly, cysteine levels seem to be very low in the LPS-challenged sample while, as foreseeable, they appear to be higher in the cells after the treatment with LPS and I-152, particularly in those treated with 5 mM I-152 (Figure 4.3b).

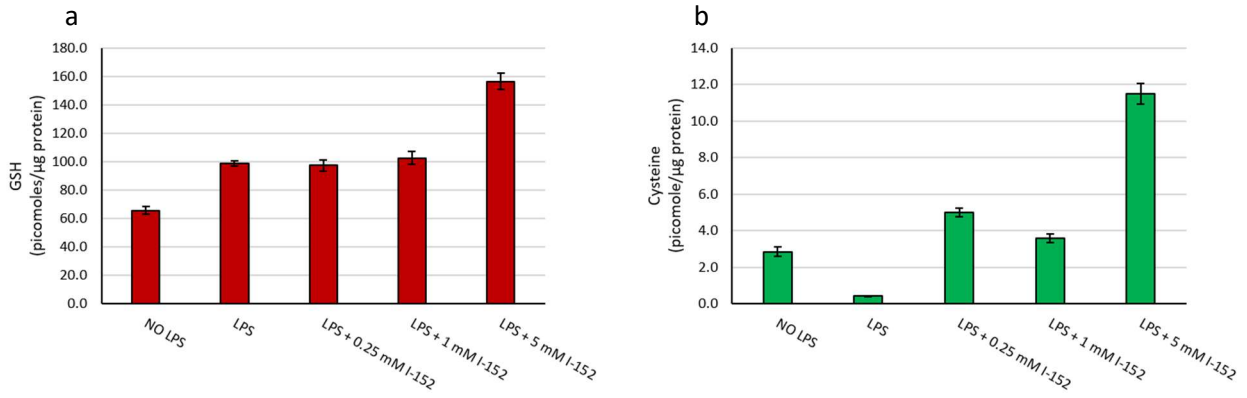

Figure 4.3 GSH (a) and cysteine (b) content in CF cells stimulated with PA-LPS (10 µg/ml) for 1h, then treated for 6h with I-152 at the indicated concentrations, and finally, after washes with PBS, fresh medium was added until the next morning. Cells were lysed with a solution containing Triton-X and the proteins precipitated with metaphosphoric acid as described in Materials and Methods. GSH levels were determined by an HPLC method by derivatizing thiol species with DTNB [194]. The reported results come from a single experiment. Each value is the average of two technical replicates.

4.4.1.4 Modulation of LPS-induced cytokine production by I-152

It is known that the redox state, and in particular GSH levels, play an important role in regulating the cellular responses involved in the immune response including the production of cytokines by macrophages [200]; moreover, inflammation is a relevant and problematic aspect in the pathogenesis of CF. For this reason, we investigated whether the shift of the redox balance towards a reduced state by I-152 could affect the cytokine response induced by PA-LPS in CF macrophages. To this aim, the cells were stimulated with LPS for 1h, and then I-152 was added at different concentrations. It was studied how the LPS treatment stimulated the production of both anti-inflammatory (IL-10) and pro-inflammatory (IL-6 and TNF-alpha) cytokines, and how the treatment with I-152 influenced this response. To do that, both the expression of mRNA and the secretion of cytokines in the culture medium were studied.

The mRNA analysis of IL-10 (Figure 4.4a) shows that the expression is significantly decreased only by 5 mM I-152, while the lower concentrations (0.25 and 1 mM) do not affect it. The protein expression of IL-10 (Figure 4.4b) seems to be moderately affected by 0.25 mM I-152 while the effect may be more consistent when I-152 was used at concentrations of 1 and 5 mM.

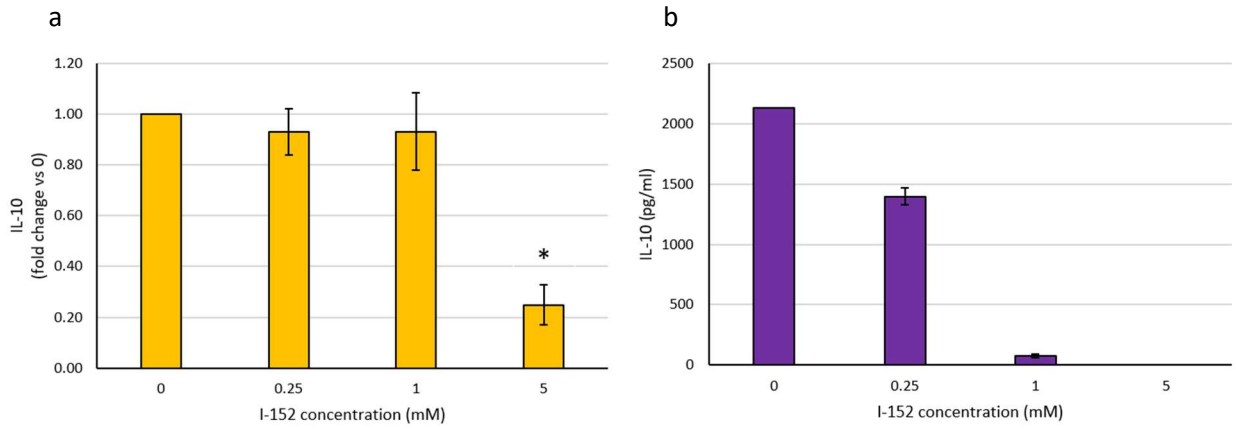

Figure 4.4 IL-10 levels in CF cells stimulated with PA-LPS (10 μg/ml) for 1h and then treated for 6h with I-152 at the indicated concentrations. After cells were lysed, total RNA was extracted and retrotranscribed into cDNA. Relative mRNA expression was determined by real-time PCR technique and calculated with the ΔΔCt method using the 18s gene as housekeeping, as described in Materials and Methods. The values are the mean ± S.D. of three independent experiments (a). IL-10 secretion was determined in the culture medium by the ELISA method and the concentration was calculated using a standard curve, as described in Materials and Methods. The values are the mean ± S.D. of two technical replicates (b). Condition 0 represents cells stimulated with LPS for 1h, to which, after removal of the stimulus, a medium not containing I-152 was added. *p<0.05.

The mRNA analysis of IL-6 (Figure 4.5a) shows a slight decrease of this parameter at concentrations of 0.25 and 1 mM I-152 while the reduction becomes statistically significant with the treatment of 5 mM I-152. The protein expression appears to be similar to the mRNA trend, showing a decrease in the concentration of the secreted protein (Figure 4.5b), which is particularly evident at the highest concentration of I-152 (5 mM).

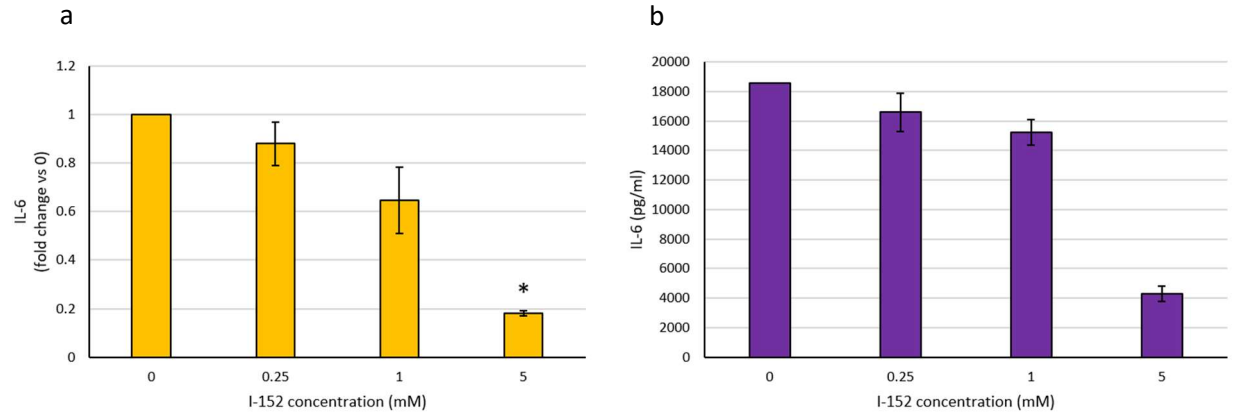

Figure 4.5 IL-6 levels in CF cells stimulated with PA-LPS (10 μg/ml) for 1h and then treated for 6h with I-152 at the indicated concentrations. After cells were lysed, total RNA was extracted and retrotranscribed into cDNA. Relative mRNA expression was determined by real-time PCR technique and calculated with the ΔΔCt method using the 18s gene as housekeeping, as described in Materials and Methods. The values are the mean ± S.D. of three independent experiments (a). IL-6 secretion was determined in the culture medium by the ELISA method and the concentration was calculated using a standard curve, as described in Materials and Methods. The values are the mean ± S.D. of two technical replicates (b). Condition 0 represents cells stimulated with LPS for 1h, to which, after removal of the stimulus, a medium not containing I-152 was added. *p<0.05

The study of TNF-α expression shows no differences in mRNA expression after I-152 treatment compared to LPS-stimulated and untreated cells (Figure 4.6a). On the contrary, the protein production seems to decrease in a dose-dependent way (Figure 4.6b). It should be emphasized that the results regarding the secretion of

proteins for all the cytokines analyzed are preliminary and their trend may be considered indicative, as they come from a single experiment.

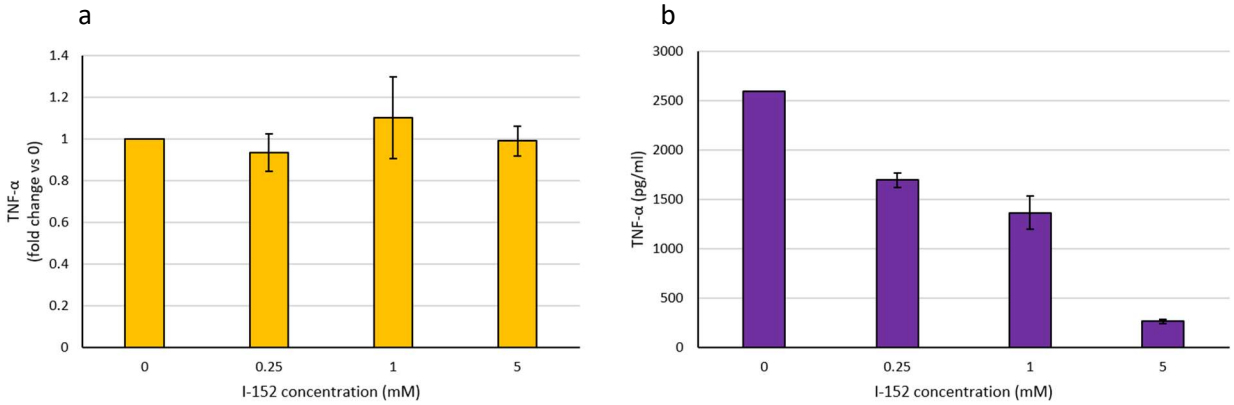

Figure 4.6 TNF-α levels in CF cells stimulated with PA-LPS (10 µg/ml) for 1h and then treated for 6h with I-152 at the indicated concentrations. After cells were lysed, total RNA was extracted and retrotranscribed into cDNA. Relative mRNA expression was determined by real-time PCR technique and calculated with the ΔΔCt method using the 18s gene as housekeeping, as described in Materials and Methods. The values are the mean ± S.D. of three independent experiments (a). TNF-α secretion was determined in the culture medium by the ELISA method and the concentration was calculated using a standard curve, as described in Materials and Methods. The values are the mean ± S.D. of two technical replicates (b). Condition 0 represents cells stimulated with LPS for 1h, to which, after removal of the stimulus, a medium not containing I-152 was added.

4.4.2 Results obtained in RAW 264.7

4.4.2.1 Determination of GSH levels after stimulation with LPS from *E. coli*

A further investigation was performed on a second model of inflammation consisting of RAW 264.7 cells challenged with LPS from *E. coli* at the concentrations of 5 and 10 µg/ml. The results reported in Figure 4.7a seem to confirm the slight decrease of GSH content after 30 min of LPS stimulation at a concentration of 10 µg/ml. In this model, it was possible to investigate the changes in GSH levels for more time points, until 6h of stimulation. At later time points (2h, 4h, and 6h) data seem to suggest a progressive increase of the intracellular content of the tripeptide compared to the relative unstimulated controls. The stimulation with LPS at a concentration of 5 µg/ml does not appear to cause any decrease in GSH content; on the contrary, the tripeptide levels are higher than the relative unstimulated controls at all the time points considered, except for the 15 min stimulation. In Figure 4.7b the trend of cysteine levels only in cells stimulated with 10 µg/ml are reported; it may be observed a slight decrease of the amino acid at 1h and 2h, while at later time points (4h and 6h) the concentrations seem to be higher than the relative controls.

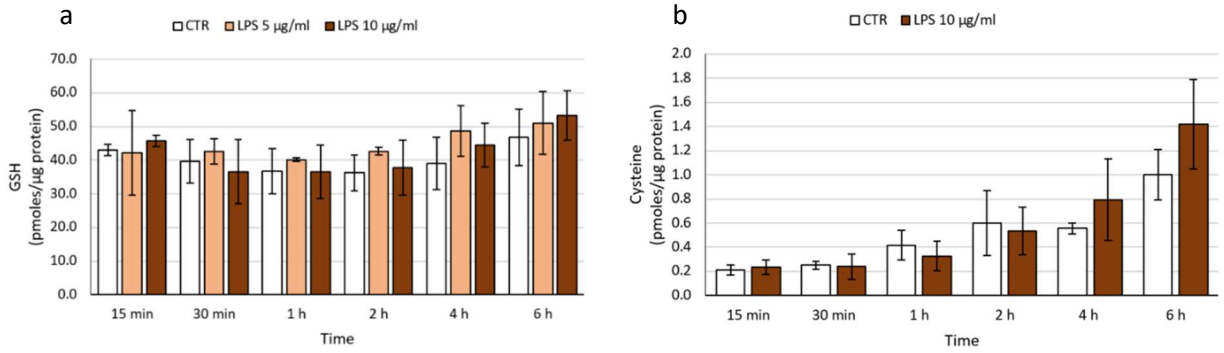

Figure 4.7 Intracellular content of GSH (a) and cysteine (b) in RAW 264.7 cells after stimulation with LPS from *E. coli* at the concentrations of 5 and 10 µg/ml. At the time points shown in the figures (15, 30 min and 1, 2, 4, and 6h), the cells were lysed with a solution containing Triton-X, and the proteins precipitated with metaphosphoric acid as described in Materials and Methods. GSH and cysteine levels were determined by an HPLC method by derivatizing thiol species with DTNB [194]. The results represent the mean ± S.D. of 2 values from independent tests. Each value is the average of two technical replicates.

4.4.2.2 Determination of GSH and other thiol species content after 30 min I-152 treatment

In order to evaluate the ability of I-152 to increase intracellular GSH level just at the time when a drop in GSH was observed after LPS stimulation, RAW 264.7 cells were treated with 1 mM I-152 for 30 min. The treatment with I-152 seems to induce an increase of GSH above physiological levels (Figure 4.8a). Moreover, other thiol species can be found, such as the amino acid cysteine, NAC, and MEA coming from the metabolism of I-152, and I-152 itself. It may be observed that MEA is the thiol species at the lowest concentration, while NAC is the one present at the highest concentrations (Figure 4.8b).

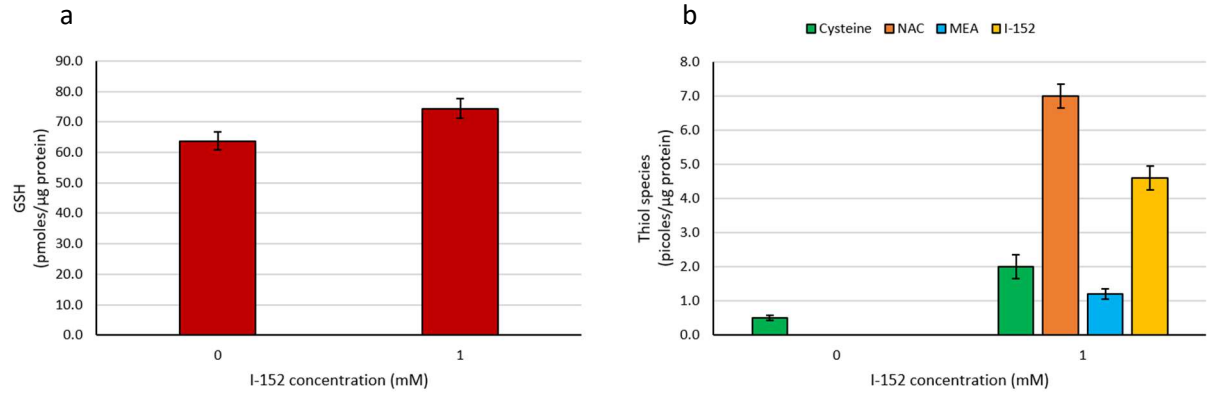

Figure 4.8 Intracellular content of GSH (a) and other thiol species (CIST, NAC, MEA, I-152) (b) in RAW 264.7 cells after treatment with I-152 1 mM for 30 min. The cells were lysed with a solution containing Triton-X and the proteins precipitated with metaphosphoric acid as described in Materials and Methods. The levels of GSH, CIST, NAC, MEA, I-152 were determined with HPLC by derivatization of the thiol species with DTNB [194]. The reported results come from a single experiment. Each value derives from the average of two technical replicates.

4.4.2.3 Modulation of LPS-induced cytokine production by I-152

The effects of I-152 on the modulation of cytokine production after stimulation with LPS were evaluated also on RAW 264.7 cells. The range of concentrations selected for I-152 is different from the previous one, going from 0.062 to 1 mM.

The mRNA expression of IL-10 seems to be not affected by I-152 treatment at the concentrations of 0.062 and 0.125 mM, while it is decreased by the concentrations 0.25 and 1 mM of the molecule (Figure 4.9a). The results regarding the production of the protein show no differences, except for a slight decrease with 1 mM of I-152 (Figure 4.9b).

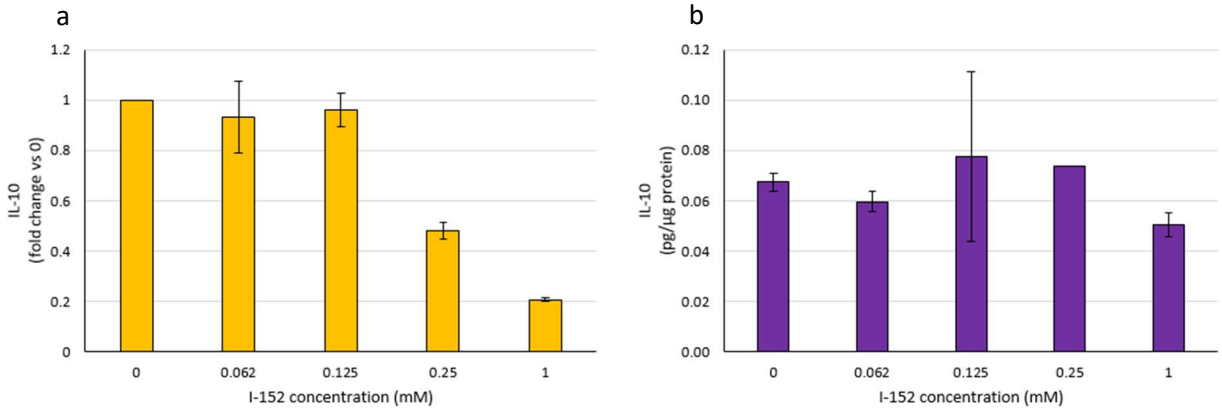

Figure 4.9 IL-10 levels in RAW 264.7 cells stimulated with *E. coli* LPS (10 µg/ml) for 1h and then treated for 6h with I-152 at the indicated concentrations. After cells were lysed, total RNA was extracted and retrotranscribed into cDNA. Relative mRNA expression was determined by real-time PCR technique and calculated with the ΔΔCt method using the 18s gene as housekeeping, as described in Materials and Methods (a). The concentration of IL-10 in the culture medium was determined by the ELISA method and was calculated using a standard curve, as described in Materials and Methods (b). Condition 0 represents cells stimulated with LPS for 1h, to which, after removal of the stimulus, a medium not containing I-152 was added. The values are the mean ± S.D. of two independent experiments.

The results obtained by the evaluation of IL-6 expression may indicate that a slight drop in mRNA levels is present with all I-152 concentrations used, although it appears to be more evident with 1 mM (Figure 4.10a), while a decrease of the secreted protein was observed starting from the 0.125 mM concentration, which may suggest a dose-dependent regulation (Figure 4.10b).

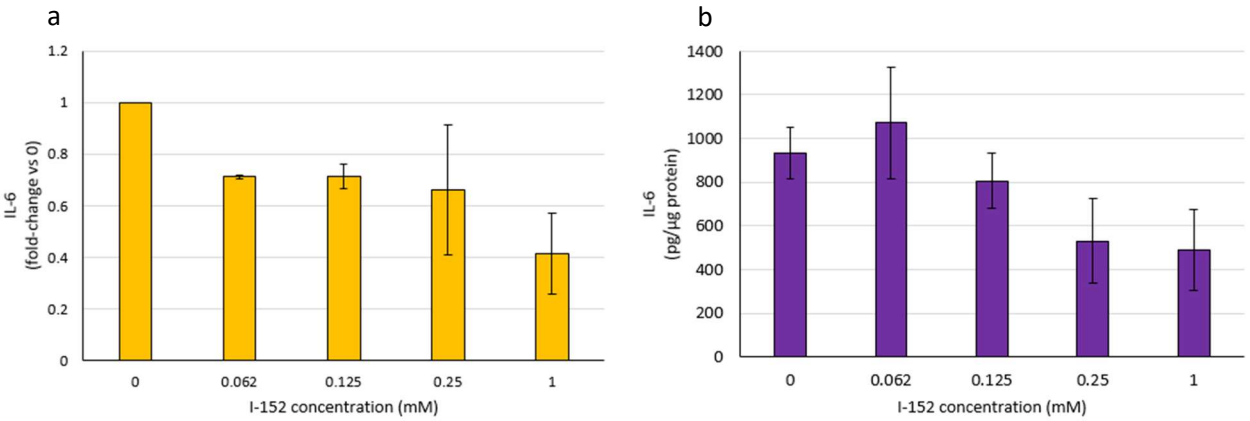

Figure 4.10 IL-6 levels in RAW 264.7 cells stimulated with *E. coli* LPS (10 µg/ml) for 1h and then treated for 6h with I-152 at the indicated concentrations. After cells were lysed, total RNA was extracted and retrotranscribed into cDNA. Relative mRNA expression was determined by real-time PCR technique and calculated with the ΔΔCt method using the 18s gene as housekeeping, as described in Materials and Methods (a). The concentration of IL-6 in the culture medium was determined by the ELISA method and was calculated using a standard curve, as described in Materials and Methods (b). Condition 0 represents cells stimulated with LPS for 1h, to which, after removal of the stimulus, a medium not containing I-152 was added. The values are the mean ± S.D. of two independent experiments.

Finally, there seem to be no overall differences in the mRNA expression of TNF-α after the I-152 treatments (Figure 4.11a), while a dose-dependent decrease in the protein may be observed at all concentrations of the molecule (Figure 4.11b).

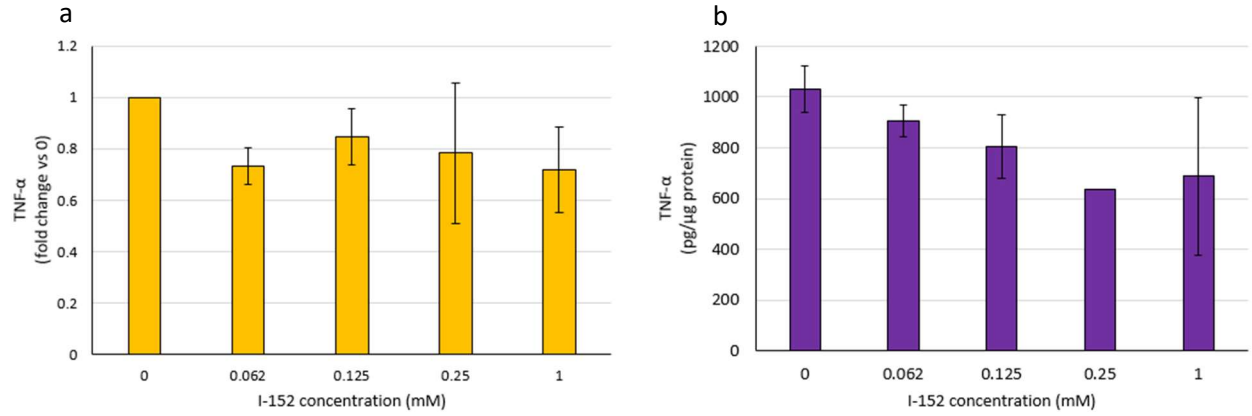

Figure 4.11 TNF-α levels in RAW 264.7 cells stimulated with *E. coli* LPS (10 µg/ml) for 1h and then treated for 6h with I-152 at the indicated concentrations. After cells were lysed, total RNA was extracted and retrotranscribed into cDNA. Relative mRNA expression was determined by real-time PCR technique and calculated with the ΔΔCt method using the 18s gene as housekeeping, as described in Materials and Methods (a). The concentration of TNF-α in the culture medium was determined by the ELISA method and was calculated using a standard curve, as described in Materials and Methods (b). Condition 0 represents cells stimulated with LPS for 1h, to which, after removal of the stimulus, a medium not containing I-152 was added. The values are the mean ± S.D. of two independent experiments.

4.5 Discussion

Many intracellular events involved in signal transduction, including those involved in the inflammatory response, are regulated by the intracellular redox state. In particular, LPS stimulation is able to activate the NF-kB pathway, which in turn leads to the degradation of IkB-α and the translocation of NF-kB to the nucleus [41]. Several studies show that both *E. coli* LPS and PA-LPS induce GSH depletion [201]; however, the data reported here appear to be not completely in agreement, because our findings may indicate a slight depletion of GSH only after a short time of exposure (30 minutes), while at longer times the level of the tripeptide seemed to be even higher than the one found in the controls. We can hypothesize that the cells can respond to this modest GSH alteration by activating antioxidant systems that induce the synthesis of GSH, which goes beyond the control values at longer times (Figure 4.7). Although the GSH decrease is modest, it seems sufficient to induce NF-kB activation and expression of some inflammatory cytokines which is not affected by the next increase of the tripeptide. It was already demonstrated that I-152 can be used to increase the intracellular GSH level [127]; our results seem to confirm these findings and show that I-152 can cross the cellular membrane quickly as indicated by the increased GSH content after 30 min-treatment with 1 mM I-152, suggesting that this molecule can be used to prevent/avoid the decline induced by LPS. This appear to be confirmed by the fact that I-152 was able to increase GSH levels in CF cells after stimulation with LPS. Moreover, I-152 provides high concentrations of other thiol species such as cysteine, NAC, and MEA; cysteine could derive from the deacetylation of NAC, or from the reduction of cystine reserves by MEA; MEA has always been quantized at lower concentrations than NAC, probably due to its oxidation into cystamine [202]. These thiol species, in particular cysteine, could be probably used by the cell to synthesize GSH, and at the same time, MEA can activate the transcription factors involved in the expression of the genes responsible for the GSH synthesis. More details about I-152 metabolism are present in the Chapter 5. Indeed, in the case of CF cells challenged with LPS, it seems that these cells can increase GSH levels by using cysteine which is the rate-limiting amino acid of the GSH synthesis. The data also indicate that the increase of the tripeptide levels and/or the presence of high concentrations of other thiol molecules (cysteine, NAC, MEA, and I-152) are useful to regulate the cytokine expression induced by LPS (IL-6, TNF- α and IL-10) in both cellular models considered. The results obtained suggest that I-152 may modulate IL-6 and IL-10 production by acting at the transcriptional level as demonstrated by. reduced mRNA levels, while for TNF-α, I-152 could act at a later stage by regulating either the synthesis of the protein or its degradation. The results obtained seem to suggest that I-152 is able to modulate the inflammatory response induced by stimulation with LPS by inhibiting the production of the cytokines IL-6 and TNF-α, thus showing to possess anti-inflammatory capabilities similar to other antioxidant molecules such as NAC [201]. Based on the capacity of both cellular models to cope with the LPS-induced GSH depletion, we can speculate that inhibition of inflammatory cytokines by I-152 treatment could be mainly linked to the high concentrations of thiol species provided by I-152; although further studies are needed to identify the exact mechanism of action. In this regard, it is well known that the canonical signaling pathway involved in the inflammatory response presupposes the activation of the transcription factor NF-kB [203], which is shown to be induced in the CF model after LPS stimulation. This transcription factor induces the

production of cytokines that modulate the immune response (such as TNF-alpha, IL-1, IL-6, and IL-8) as well as the production of adhesion molecules, which guide leukocytes to the sites of inflammation [204]. It has previously been shown that other molecules capable of increasing intracellular GSH inhibit the expression and release of inflammatory cytokines by blocking the activation of NF-kB [201] and presumably I-152 could also act similarly but whether high GSH concentration or high thiol species are responsible for the observed effect must be elucidated. Preliminary experiments conducted with high concentrations of I-152 have shown that the molecule can inhibit IkB-α phosphorylation by acting on the IKK kinase. While comparable results have been obtained in both models for IL-6 and TNF-α, different effects were observed in IL-10 production. IL-10 has been described as an anti-inflammatory defense mechanism developed by the immune system in order to control the excessive production of pro-inflammatory molecules and limit tissue damage as well as maintain or restore tissue homeostasis [205]. Indeed, an interplay and a mutual influence between IL-6 and IL-10 have been described in several pathologies suggesting a complex regulatory mechanism. It is therefore difficult to foresee the final effect of I-152 because it will likely differ according to the experimental conditions and it will depend on the presence of other cytokines.

4.6 Conclusions

In conclusion, our data show that the pathways that control the immune response are particularly sensitive to the intracellular redox state and that I-152 by increasing GSH and delivering a great amount of molecules carrying SH groups, could exert a specific anti-inflammatory action, suggesting a possible use in all those pathological and metabolic states characterized by excessive production of inflammatory cytokines. The data presented here are preliminary because the attention was mainly focused on the effects of I-152 on the inflammatory cytokines, so future studies will be needed to consolidate them and to identify the exact mechanism of action. It will also be interesting to investigate the effects of I-152 on *P. aeruginosa* as an antimicrobic, and biofilm breaker. Moreover, it would be interesting to study the interactions between I-152 and pyocyanin, a toxin produced by *P. aeruginosa* that reacts with GSH and consequently decreases its content in the lung of CF patients. [206].

CHAPTER 5

In this section, the results obtained from the study of I-152 metabolism are reported. To do that we examined how I-152 increases intracellular thiol species and how these modulate the pathways involved in the synthesis and degradation of GSH.

(Submitted paper)

5.1 Introduction

It was known that I-152 could efficiently boost GSH both *in vivo* and *in vitro*, under physiological and pathological conditions characterized by GSH depletion (i.e. viral infection) [126][130]. Although its capacity to increase intracellular GSH level has been attributed to its ability to provide cysteine precursors, the exact mechanism of action has not been yet elucidated. This study was aimed to further investigate whether I-152 was able to modulate the signaling pathways involved in GSH synthesis and/or degradation.

5.2 Materials and methods

5.2.1 Reagents

(See Paragraph 4.3.1 in Chapter 4).

5.2.2 RAW 264.7 cells: culture and treatments

RAW 264.7 cells, a murine macrophage cell line, were cultured in DMEM, supplemented with 10% heat-inactivated fetal bovine serum (FBS), 2 mM L-glutamine, 100 µg/ml streptomycin, and 100 U/ml penicillin (Sigma Aldrich, Milan, Italy). Cells were plated in 6-well plates (Ø35 mm dishes) (Greiner Bio-One, Germany) at an initial concentration of $1x10^5$ cells/ml in a volume of 2 ml of culture media and let to incubate at 37°C and 5% CO_2. After three days, when the cells had a confluence of 70-80%, two washes with physiological saline solution (NaCl 0.9%, K_2HPO_4, pH 7.4; PBS) were performed, and then we proceeded with the treatments.

To determine intracellular thiol species after treatment with I-152, RAW 264.7 cells were incubated with the molecule at different concentrations (0.062-1 mM) for 2, 6, and 24 h. Finally, they were washed with phosphate buffered saline (PBS), lysed, and processed for thiol analysis as described (paragraph 5.3.3).

5.2.3 Preparation of samples for the determination of GSH, cysteine, and other thiol species

(See Paragraph 4.3.4 in Chapter 4).

5.2.4 Spectrophotometric determination of proteins

(See Paragraph 4.3.5 in Chapter 4).

5.2.5 Determination of GSH and other thiol species by high-performance liquid chromatography (HPLC)

(See Paragraph 4.3.6 in Chapter 4).

5.2.6 Preparation of standard solutions for HPLC

(See Paragraph 4.3.7 in Chapter 4).

5.2.7 Western immunoblotting analysis

After the treatment described in paragraph 3.3.2, two washes with PBS were performed and cells were lysed for Western immunoblotting analysis on ice. To do that 100 µl of lysis buffer [50 mM Tris / HCl pH 8.0, 2% (w/v) SDS (Sodium dodecyl sulfate), 40 mM N-ethylmaleimide (NEM), 0.25 mM of sucrose supplemented with protease inhibitors] were put on each well, and whole-cell lysates were collected into 1.5 ml microtubes using a rubber scraper, and immediately put on ice. Next, the contents of the microtubes were boiled for 5 minutes, sonicated at 70W for 40 sec, and centrifuged 12000 rpm at RT. The protein content was determined in the supernatant according to the Lowry assay. Proteins were resolved by SDS polyacrylamide gel electrophoresis (SDS-PAGE) and electroblotted onto polyvinyldene difluoride (PVDF) membrane. Next, the membrane was blocked in 5% (w/v) nonfat dry milk powder (Cell Signaling Technologies) dissolved in TTBS (150 mM Tris-HCl pH 7.4; 150 mM NaCl; 0.1% (v/v) Tween-20) for 1h at RT. The membrane was then incubated overnight at 4°C with the following primary antibodies: NRF2 (Cell Signaling Technology, #D1Z9C), GCLm (ABclonal, A5314), ChaC1 (GeneTex, GTX120775), and β-ACTIN (Cell Signaling Technologies, #4967). The next morning, the primary antibodies were removed and incubation with horseradish peroxidase (HRP)-conjugated secondary antibody (Bio-Rad, Hercules, CA, USA) was performed for 1h at RT. Finally, the immunoreactive bands were visualized by the enhanced chemiluminescence detection kit WesternBright ECL (Advansta, Bering Dr, San Jose, CA USA); detection and quantification were performed by using the Image Lab software (Bio-Rad, Hercules, CA, USA).

5.3.8 Statistical analysis

The statistical analysis was performed using the t-test two groups of data, and one-way ANOVA to compare more than two groups. A Prism software version 5.0 was used (GraphPad, San Diego, CA, United States). p values ≤ 0.05 were considered significant.

5.3 Results

5.3.1 Determination of GSH and other thiol species in I-152-treated cells

The ability of I-152 to affect the redox state was evaluated in the mouse macrophage cell line RAW 264.7. Cells were treated with different concentrations of I-152 (0.062-1 mM) and thiol species (i.e. GSH, cysteine, NAC, MEA, and I-152) were determined after 2, 6, and 24h (Figure 5).

GSH quantification after 2h treatment with I-152 shows a dose-dependent increase up to the 0.25 mM concentration. At this concentration, it can be observed a significant increase of the tripeptide compared to the relative untreated control (0) (Figure 5.1a). In cells treated with 1 mM I-152, the increase of GSH was less evident compared to the relative untreated control (0). A similar trend can be noted also at 6 hours when the most significant increases of GSH content were registered in cells having received 0.125 and 0.25 mM of I-152. On the contrary, 1 mM I-152 caused a decrease in GSH content compared to the relative untreated control (0) (Figure 5.1a). At 24h higher levels of GSH were determined in the samples treated with the lower concentrations of I-152, while the higher concentrations lowered the tripeptide content (Figure 5.1a). Regarding the thiol species (Figure 5.1b), after the 2h-treatments, a dose-dependent increase of all the thiols is observed, except for the cysteine level in the cells treated with the highest concentration of I-152 (1 mM) which was found to be lower than all other conditions. A dose-dependent trend can be observed after 6h treatment, especially for I-152 and MEA. Finally, after 24h all the species are still detectable in all treatments.

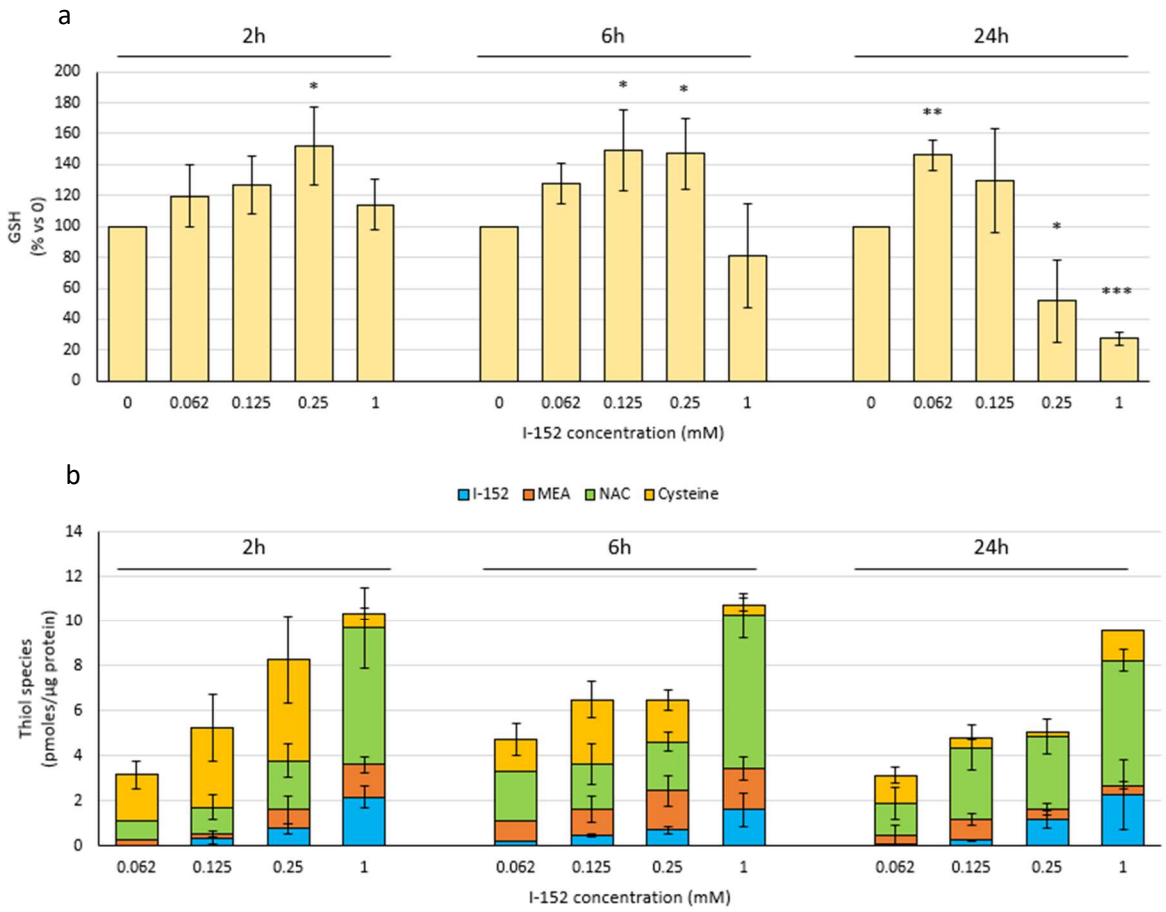

Figure 5.1 GSH (a) and other thiol species (b) content in RAW 264.7 cells treated with different concentrations of I-152 for 2, 6, and 24h. Cells were lysed with a solution containing Triton-X and the proteins precipitated with metaphosphoric acid as described in Materials and Methods. The levels of GSH and other thiol species were determined by HPLC by derivatizing thiol species with DTNB [194]. The values are the mean ± S.D. of five independent experiments. * $p < 0.05$, ** $p < 0.01$, *** $p < 0.001$.

5.3.2 Western immunoblotting analysis of Nfr2 and GCLm

The well-known GSH-boosting activity of I-152, previously demonstrated both *in vitro* and *in vivo*, is presumably due to its capacity to yield a high quantity of cysteine, as shown in Figure 5.2, that can be used for GSH synthesis. Indeed, we have investigated if I-152 could influence the expression of Nrf2, known to induce the expression of genes involved in GSH synthesis. To this aim, Nrf2 and GCLm protein expressions after the treatment with I-152 at different concentrations (0.062-1 mM) for 2, 6, and 24h were investigated. As shown in Figure 5.2a, I-152 treatment increased Nrf2 expression in a dose-dependent manner both after 2 and 24h of incubation. To assess whether the accumulation of Nrf2 resulted in overexpression of target genes, both GCLC and GCLM protein levels were determined. The results obtained show no changes in GCLC intracellular concentration (data not shown), while GCLM protein levels were significantly increased at 6h incubation and rose further at 24h (Figure 5.2b).

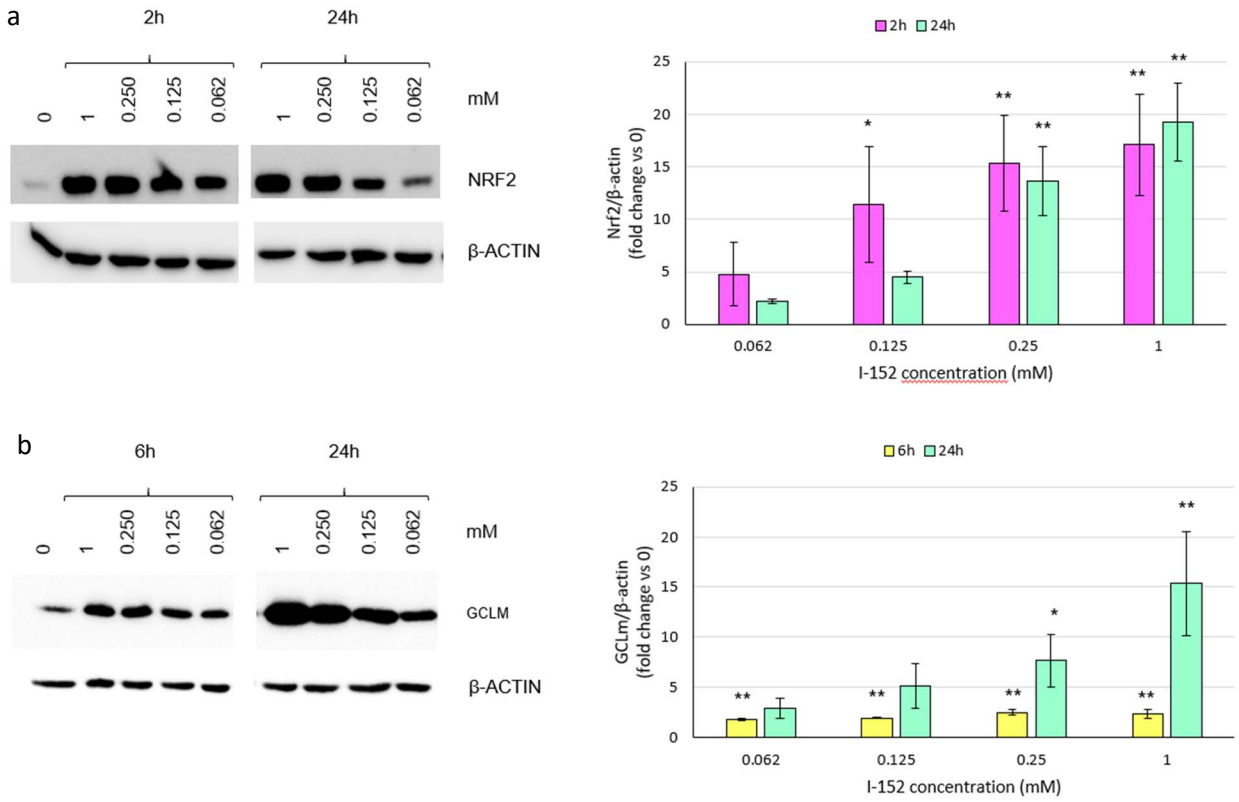

Figure 5.2 Western immunoblotting analysis of Nrf2 (a) and GCLm (b) expression in RAW 264.7 cells after incubation with I-152 at different concentrations (0.062-1 mM) at the time points shown in the figure (2 and 24h for Nrf2 expression; 6 and 24h for GCLm expression). Cells were lysed and the proteins were resolved by electrophoretic separation in SDS-PAGE, blotted onto a PVDF membrane, and probed with antibodies against Nrf2 and GCLm. Immunoreactive bands were quantified with the Image Lab software and normalized on actin. Values are the mean ± S.D. of at least three independent experiments. *p<0.05, **p<0.01.

5.3.3 Western immunoblotting analysis of ChaC1

Of course, GSH levels do not depend only on its rate of synthesis but also on its degradation. Thus, we reasoned that at the highest I-152 concentrations tested, GSH overproduction may lead to reductive stress and to the activation of degradative pathways to restore redox homeostasis [207]. Since GSH depletion has been often associated with ChaC1 expression, which controls intracellular GSH degradation under stressful conditions, ChaC1 levels were determined in cells treated with 1 mM I-152, but no significant differences with respect to the control were observed at all the times considered (Figure 5.3).

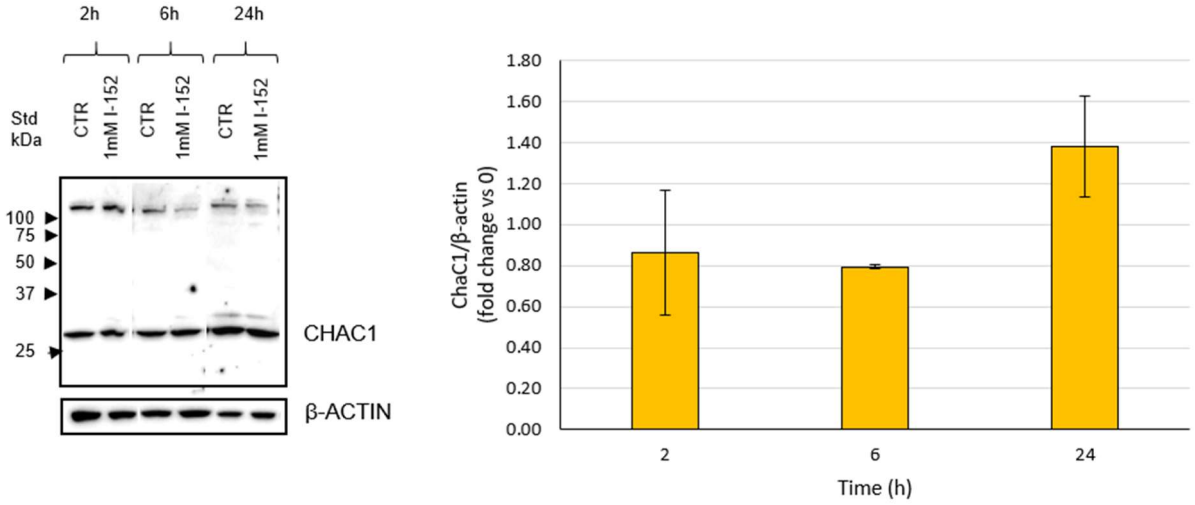

Figure 5.3 Western immunoblotting analysis of ChaC1 expression in RAW 264.7 cells after 1mM I-152 at the time points shown in the figure (2, 6, and 24h). Cells were lysed and the proteins were resolved by electrophoretic separation in SDS-PAGE, blotted onto a PVDF membrane, and probed with antibodies against Chac1. Immunoreactive bands were quantified with the Image Lab software and normalized on actin. Values are the mean ± S.D. of at least three independent experiments.

5.4 Discussion

The study of the mechanisms by which I-152 increases intracellular GSH levels showed that the molecule is a potentpro-GSH since it provides high levels of NAC as well as cysteine and, interestingly, favors the tripeptide production by inducing Nrf2 and, subsequently, GCLm protein expressions. The induction of GCLm is fundamental for GSH synthesis because it has been demonstrated that its presence alone is sufficient to increase GCLc activity. It has been demonstrated that GCLM levels are limiting within cells, thus up-regulation of GCLM alone is sufficient to increase GCL catalytic activity by increasing holoenzyme formation. The heterodimeric enzyme is more efficient in catalyzing the reaction and less sensitive to feedback inhibition by GSH [208][209].

The study of thiol species in cells treated with I-152 showed a high amount of NAC, which was still detectable when lower concentrations of the molecule were used; it is known that NAC can provide cysteine, the rate-limiting amino acid of the GSH synthesis. MEA quantification showed that its levels were markedly lower than those of NAC. This result was unexpected since I-152 releases equimolar amounts of NAC and MEA. It is possible that the MEA moiety, resulting from I-152 intracellular metabolization, could both be partly oxidized (MEA_{S-S}) and/or conjugated to other thiol species. Moreover, I-152 was still detectable, suggesting that the molecule enters into the cells as it is, and that is mostly metabolized intracellularly.

MEA is known to increase intracellular GSH content due to its ability to reduce cystine into cysteine [124]; moreover, recent evidence has shown that MEA_{S-S} is a strong activator of Nrf2, while the reduced form MEA is weaker, suggesting that it could be the oxidized form to activate the Nrf2 pathway [210].

The decreased GSH observed at the highest concentration of I-152 (1 mM) was thought to be due to the activation of GSH degradation mechanisms; however, ChaC1 was not induced. This aspect deserves further investigation and it can be speculated that the high amounts of thiol species provided by I-152 could induce reductive stress, thus inducing/enhancing mitochondrial oxidation and production of ROS [211].

5.5 Conclusions

The presented data show that I-152 can boost GSH not only delivering NAC and MEA inside the cells but inducing an accumulation of the main transcription factor involved in GSH synthesis. Hence, it can be considered a promising molecule to replenish GSH stores in all those pathologies characterized by GSH depletion. Further studies will be necessary to investigate what occurs when I-152 is administered at high concentrations.

FINAL CONCLUSIONS

Different redox-regulated pathways are involved in host responses towards several pathogens and alteration in redox balance, often characterized by GSH depletion, represents an exquisite strategy to evade or circumvent host innate immunity. These alterations can lead often to ineffective or exaggerated immune responses, which hamper the resolution of infections and are detrimental for the host. The data shown in this thesis suggest that the shift of the intracellular redox state towards a more reduced one could be a valid approach to influence and/or re-establish a balanced immune response and to interfere with the thiol-based redox metabolism which has a key role in vital processes for many pathogenic bacteria. Moreover, we can suggest that the idea of redox homeostasis involved in the management of oxidative stress is restrictive, and it should be considered as a fundamental metabolic and regulator key factor involved in several cellular functions, included the immune-associated ones.

REFERENCES

[1] Martinovich GG, Cherenkevich SN, Sauer H. Intracellular redox state: Towards quantitative description. Eur Biophys J 2005;34:937–42. https://doi.org/10.1007/s00249-005-0470-3.

[2] Schafer FQ, Buettner GR. Redox environment of the cell as viewed through the redox state of the glutathione disulfide/glutathione couple. Free Radic Biol Med 2001;30:1191–212. https://doi.org/10.1016/S0891-5849(01)00480-4.

[3] Trachootham D, Lu W, Ogasawara MA, Valle NR Del, Huang P. Redox regulation of cell survival. Antioxidants Redox Signal 2008;10:1343–74. https://doi.org/10.1089/ars.2007.1957.

[4] Wang X, Hai C. Novel insights into redox system and the mechanism of redox regulation. Mol Biol Rep 2016;43:607–28. https://doi.org/10.1007/s11033-016-4022-y.

[5] Thanan R, Oikawa S, Hiraku Y, Ohnishi S, Ma N, Pinlaor S, et al. Oxidative stress and its significant roles in neurodegenerative diseases and cancer. Int J Mol Sci 2014;16:193–217. https://doi.org/10.3390/ijms16010193.

[6] Oxidative Stress - 1st Edition n.d. https://www.elsevier.com/books/oxidative-stress/sies/978-0-12-642760-8 (accessed October 29, 2020).

[7] Giles GI, Tasker KM, Jacob C. Hypothesis: The role of reactive sulfur species in oxidative stress. Free Radic Biol Med 2001;31:1279–83. https://doi.org/10.1016/S0891-5849(01)00710-9.

[8] Sies H, Berndt C, Jones DP. Oxidative Stress. Annu Rev Biochem 2017;86:715–48. https://doi.org/10.1146/annurev-biochem-061516-045037.

[9] Finkel T. Signal transduction by reactive oxygen species. J Cell Biol 2011;194:7–15. https://doi.org/10.1083/jcb.201102095.

[10] Zhao RZ, Jiang S, Zhang L, Yu Z Bin. Mitochondrial electron transport chain, ROS generation and uncoupling (Review). Int J Mol Med 2019;44:3–15. https://doi.org/10.3892/ijmm.2019.4188.

[11] Takac I, Schröder K, Zhang L, Lardy B, Anilkumar N, Lambeth JD, et al. The E-loop is involved in hydrogen peroxide formation by the NADPH oxidase Nox4. J Biol Chem 2011;286:13304–13. https://doi.org/10.1074/jbc.M110.192138.

[12] Tu BP, Weissman JS. Oxidative protein folding in eukaryotes: Mechanisms and consequences. J Cell Biol 2004;164:341–6. https://doi.org/10.1083/jcb.200311055.

[13] Di Meo S, Reed TT, Venditti P, Victor VM. Role of ROS and RNS Sources in Physiological and Pathological Conditions. Oxid Med Cell Longev 2016;2016. https://doi.org/10.1155/2016/1245049.

[14] Moncada S, Palmer RMJ, Higgs EA. Nitric oxide: Physiology, pathophysiology, and pharmacology. Pharmacol Rev 1991;43:109–42.

[15] Förstermann U, Sessa WC. Nitric oxide synthases: Regulation and function. Eur Heart J 2012;33:829–37. https://doi.org/10.1093/eurheartj/ehr304.

[16] Šolc M. Kinetics of the reaction of nitric oxide with molecular oxygen [7]. Nature 1966;209:706. https://doi.org/10.1038/209706a0.

[17] Zegarska B, Pietkun K, Zegarski W, Bolibok P, Wisniewski M, Roszek K, et al. Air pollution, UV irradiation and skin carcinogenesis: What we know, where we stand and what is likely to happen in the future? Postep Dermatologii i Alergol 2017;34:6–14. https://doi.org/10.5114/ada.2017.65616.

[18] Ivanova IP. Initial Stage of Lipid Peroxidation with HO2• Radicals. Kinetic Study. Am J Phys Chem 2013;2:44. https://doi.org/10.11648/j.ajpc.20130202.13.

[19] Barrera G. Oxidative Stress and Lipid Peroxidation Products in Cancer Progression and Therapy. ISRN Oncol 2012;2012:1–21. https://doi.org/10.5402/2012/137289.

[20] Del Rio D, Stewart AJ, Pellegrini N. A review of recent studies on malondialdehyde as toxic molecule and biological marker of oxidative stress. Nutr Metab Cardiovasc Dis 2005;15:316–28.

https://doi.org/10.1016/j.numecd.2005.05.003.

[21] Jusakul A, Yongvanit P, Loilome W, Namwat N, Kuver R. Mechanisms of oxysterol-induced carcinogenesis. Lipids Health Dis 2011;10. https://doi.org/10.1186/1476-511X-10-44.

[22] Lemaire-Ewing S, Prunet C, Montange T, Vejux A, Berthier A, Bessède G, et al. Comparison of the cytotoxic, pro-oxidant and pro-inflammatory characteristics of different oxysterols. Cell Biol Toxicol 2005;21:97–114. https://doi.org/10.1007/s10565-005-0141-2.

[23] Nyström T. Role of oxidative carbonylation in protein quality control and senescence. EMBO J 2005;24:1311–7. https://doi.org/10.1038/sj.emboj.7600599.

[24] Dalle-Donne I, Aldini G, Carini M, Colombo R, Rossi R, Milzani A. Protein carbonylation, cellular dysfunction, and disease progression. J Cell Mol Med 2006;10:389–406. https://doi.org/10.1111/j.1582-4934.2006.tb00407.x.

[25] Cooke MS, Evans MD, Dizdaroglu M, Lunec J. Oxidative DNA damage: mechanisms, mutation, and disease. FASEB J 2003;17:1195–214. https://doi.org/10.1096/fj.02-0752rev.

[26] Wang JX, Gao J, Ding SL, Wang K, Jiao JQ, Wang Y, et al. Oxidative Modification of miR-184 Enables It to Target Bcl-xL and Bcl-w. Mol Cell 2015;59:50–61. https://doi.org/10.1016/j.molcel.2015.05.003.

[27] Faraci FM, Didion SP. Vascular protection: Superoxide dismutase isoforms in the vessel wall. Arterioscler Thromb Vasc Biol 2004;24:1367–73. https://doi.org/10.1161/01.ATV.0000133604.20182.cf.

[28] Glorieux C, Zamocky M, Sandoval JM, Verrax J, Calderon PB. Regulation of catalase expression in healthy and cancerous cells. Free Radic Biol Med 2015;87:84–97. https://doi.org/10.1016/j.freeradbiomed.2015.06.017.

[29] Toppo S, Vanin S, Bosello V, Tosatto SCE. Evolutionary and structural insights into the multifaceted glutathione peroxidase (Gpx) superfamily. Antioxidants Redox Signal 2008;10:1501–13. https://doi.org/10.1089/ars.2008.2057.

[30] Funato Y, Miki H. Nucleoredoxin, a novel thioredoxin family member involved in cell growth and differentiation. Antioxidants Redox Signal 2007;9:1035–57. https://doi.org/10.1089/ars.2007.1550.

[31] Holmgren A, Aslund F. [29] Glutaredoxin. Methods Enzymol 1995;252:264–74. https://doi.org/10.1016/0076-6879(95)52031-7.

[32] Groitl B, Jakob U. Thiol-based redox switches. Biochim Biophys Acta - Proteins Proteomics 2014;1844:1335–43. https://doi.org/10.1016/j.bbapap.2014.03.007.

[33] Ray PD, Huang BW, Tsuji Y. Reactive oxygen species (ROS) homeostasis and redox regulation in cellular signaling. Cell Signal 2012;24:981–90. https://doi.org/10.1016/j.cellsig.2012.01.008.

[34] Roos G, Messens J. Protein sulfenic acid formation: From cellular damage to redox regulation. Free Radic Biol Med 2011;51:314–26. https://doi.org/10.1016/j.freeradbiomed.2011.04.031.

[35] Casas AI, Dao VTV, Daiber A, Maghzal GJ, Di Lisa F, Kaludercic N, et al. Reactive Oxygen-Related Diseases: Therapeutic Targets and Emerging Clinical Indications. Antioxidants Redox Signal 2015;23:1171–85. https://doi.org/10.1089/ars.2015.6433.

[36] Jung KJ, Kim DH, Lee EK, Song CW, Yu BP, Chung HY. Oxidative stress induces inactivation of protein phosphatase 2A, promoting proinflammatory NF-κB in aged rat kidney. Free Radic Biol Med 2013;61:206–17. https://doi.org/10.1016/j.freeradbiomed.2013.04.005.

[37] Itoh K, Wakabayashi N, Katoh Y, Ishii T, Igarashi K, Engel JD, et al. Keap1 represses nuclear activation of antioxidant responsive elements by Nrf2 through binding to the amino-terminal Neh2 domain. Genes Dev 1999;13:76–86. https://doi.org/10.1101/gad.13.1.76.

[38] Kobayashi H, Kærn M, Araki M, Chung K, Gardner TS, Cantor CR, et al. Programmable cells: Interfacing natural and engineered gene networks. Proc Natl Acad Sci U S A 2004;101:8414–9. https://doi.org/10.1073/pnas.0402940101.

[39] Taguchi K, Motohashi H, Yamamoto M. Molecular mechanisms of the Keap1-Nrf2 pathway in stress response and cancer evolution. Genes to Cells 2011;16:123–40. https://doi.org/10.1111/j.1365-2443.2010.01473.x.

[40] Hayden MS, Ghosh S. Signaling to NF-κB. Genes Dev 2004;18:2195–224. https://doi.org/10.1101/gad.1228704.

[41] Kabe Y, Ando K, Hirao S, Yoshida M, Handa H. Redox regulation of NF-κB activation: Distinct redox regulation between the cytoplasm and the nucleus. Antioxidants Redox Signal 2005;7:395–403. https://doi.org/10.1089/ars.2005.7.395.

[42] Katsuyuki M, Kohzo N, Kotaro F, Xiangao S, Shuji S, Ken-ichi Y. Two different cellular redox systems regulate the DNA-binding activity of the p50 subunit of NF-κB in vitro. Gene 1994;145:197–203. https://doi.org/10.1016/0378-1119(94)90005-1.

[43] Matsuzawa D, Hashimoto K. Magnetic resonance spectroscopy study of the antioxidant defense system in Schizophrenia. Antioxidants Redox Signal 2011;15:2057–65. https://doi.org/10.1089/ars.2010.3453.

[44] Torres M. Mitogen-activated protein kinase pathways in redox signaling. Front Biosci 2003;8. https://doi.org/10.2741/999.

[45] Nakashima I, Takeda K, Kawamoto Y, Okuno Y, Kato M, Suzuki H. Redox control of catalytic activities of membrane-associated protein tyrosine kinases. Arch Biochem Biophys 2005;434:3–10. https://doi.org/10.1016/j.abb.2004.06.016.

[46] Balmanno K, Cook SJ. Tumour cell survival signalling by the ERK1/2 pathway. Cell Death Differ 2009;16:368–77. https://doi.org/10.1038/cdd.2008.148.

[47] Arthur JSC, Ley SC. Mitogen-activated protein kinases in innate immunity. Nat Rev Immunol 2013;13:679–92. https://doi.org/10.1038/nri3495.

[48] Son Y, Cheong Y-K, Kim N-H, Chung H-T, Kang DG, Pae H-O. Mitogen-Activated Protein Kinases and Reactive Oxygen Species: How Can ROS Activate MAPK Pathways? J Signal Transduct 2011;2011:1–6. https://doi.org/10.1155/2011/792639.

[49] Saitoh M, Nishitoh H, Fujii M, Takeda K, Tobiume K, Sawada Y, et al. Mammalian thioredoxin is a direct inhibitor of apoptosis signal-regulating kinase (ASK) 1. EMBO J 1998;17:2596–606. https://doi.org/10.1093/emboj/17.9.2596.

[50] Wang X, Martindale JL, Holbrook NJ. Requirement for ERK activation in cisplatin-induced apoptosis. J Biol Chem 2000;275:39435–43. https://doi.org/10.1074/jbc.M004583200.

[51] Cantrell DA. Phosphoinositide 3-kinase signalling pathways. J Cell Sci 2001;114:1439–45. https://doi.org/10.1142/p428.

[52] Sarbassov DD, Guertin DA, Ali SM, Sabatini DM. Phosphorylation and regulation of Akt/PKB by the rictor-mTOR complex. Science (80-) 2005;307:1098–101. https://doi.org/10.1126/science.1106148.

[53] Leslie NR, Downes CP. PTEN: The down side of PI 3-kinase signalling. Cell Signal 2002;14:285–95. https://doi.org/10.1016/S0898-6568(01)00234-0.

[54] Pelicano H, Xu RH, Du M, Feng L, Sasaki R, Carew JS, et al. Mitochondrial respiration defects in cancer cells cause activation of Akt survival pathway through a redox-mediated mechanism. J Cell Biol 2006;175:913–23. https://doi.org/10.1083/jcb.200512100.

[55] Wang Y, Zeigler MM, Lam GK, Hunter MC, Eubank TD, Khramtsov V V., et al. The role of the

NADPH oxidase complex, p38 MARK, and Akt in regulating human monocyte/macrophage survival. Am J Respir Cell Mol Biol 2007;36:68–77. https://doi.org/10.1165/rcmb.2006-0165OC.

[56] Kane LP, Shapiro VS, Stokoe D, Weiss A. Induction of NF-κB by the Akt/PKB kinase. Curr Biol 1999;9:601–4. https://doi.org/10.1016/S0960-9822(99)80265-6.

[57] Oestreicher J; Biochemistry and Cell Biology. n.d.

[58] Meister A. Glutathione metabolism and its selective modification. J Biol Chem 1988;263:17205–8.

[59] Ookhtens M, Kaplowitz N. Role of the liver in interorgan homeostasis of glutathione and cyst(e)ine. Semin Liver Dis 1998;18:313–29. https://doi.org/10.1055/s-2007-1007167.

[60] Lu SC. Regulation of glutathione synthesis. Mol Aspects Med 2009;30:42–59. https://doi.org/10.1016/j.mam.2008.05.005.

[61] Kaplowitz N, Aw TY, Ookhtens M. The Regulation of Hepatic Glutathione. Annu Rev Pharmacol Toxicol 1985;25:715–44. https://doi.org/10.1146/annurev.pa.25.040185.003435.

[62] Simoni R, Hill RL, Vaughan M. On glutathione. II. A thermostable oxidation-reduction system (Hopkins, F. G., and Dixon, M. (1922) J. Biol. Chem. 54, 527-563). Undefined 2002.

[63] Meister A, Tate SS. Glutathione and related gamma-glutamyl compounds: biosynthesis and utilization. Annu Rev Biochem 1976;45:559–604. https://doi.org/10.1146/annurev.bi.45.070176.003015.

[64] Meister A, Anderson ME. Glutathione. Annu Rev Biochem 1983;Vol. 52:711–60. https://doi.org/10.1146/annurev.bi.52.070183.003431.

[65] Huang C-S, Anderson ME, Meister A. THE JOURNAL OF BIOLOGICAL CHEMISTRY Amino Acid Sequence and Function of the Light Subunit of Rat Kidney y-Glutamylcysteine Synthetase*. vol. 268. 1993.

[66] Franklin CC, Backos DS, Mohar I, White CC, Forman HJ, Kavanagh TJ. Structure, function, and post-translational regulation of the catalytic and modifier subunits of glutamate cysteine ligase. Mol Aspects Med 2009;30:86–98. https://doi.org/10.1016/j.mam.2008.08.009.

[67] Meister A. [49] Glutathione synthetase from rat kidney. Methods Enzymol 1985;113:393–9. https://doi.org/10.1016/S0076-6879(85)13052-1.

[68] Grant CM, Maciver FH, Dawes IW. Glutathione Synthetase Is Dispensable for Growth under Both Normal and Oxidative Stress Conditions in the Yeast Saccharomyces cerevisiae Due to an Accumulation of the Dipeptide y-Glutamylcysteine. vol. 8. Meister; 1997.

[69] Lu SC. Glutathione synthesis. Biochim Biophys Acta - Gen Subj 2013;1830:3143–53. https://doi.org/10.1016/j.bbagen.2012.09.008.

[70] HANES CS, HIRD FJ, ISHERWOOD FA. Enzymic transpeptidation reactions involving gamma-glutamyl peptides and alpha-amino-acyl peptides. Biochem J 1952;51:25–35. https://doi.org/10.1042/bj0510025.

[71] Tate SS, Meister A. γ-Glutamyl transpeptidase: catalytic, structural and functional aspects. Mol Cell Biochem 1981;39:357–68. https://doi.org/10.1007/BF00232585.

[72] Kumar A, Tikoo S, Maity S, Sengupta S, Sengupta S, Kaur A, et al. Mammalian proapoptotic factor ChaC1 and its homologues function as γ-glutamyl cyclotransferases acting specifically on glutathione. EMBO Rep 2012;13:1095–101. https://doi.org/10.1038/embor.2012.156.

[73] Mungrue IN, Pagnon J, Kohannim O, Gargalovic PS, Lusis AJ. CHAC1/MGC4504 Is a Novel Proapoptotic Component of the Unfolded Protein Response, Downstream of the ATF4-ATF3-CHOP Cascade. J Immunol 2009;182:466–76. https://doi.org/10.4049/jimmunol.182.1.466.

[74] Tsunoda S, Avezov E, Zyryanova A, Konno T, Mendes-Silva L, Melo EP, et al. Intact protein folding

in the glutathione-depleted endoplasmic reticulum implicates alternative protein thiol reductants. Elife 2014;2014. https://doi.org/10.7554/eLife.03421.001.

[75] Forman HJ, Zhang H, Rinna A. Glutathione: Overview of its protective roles, measurement, and biosynthesis. Mol Aspects Med 2009;30:1–12. https://doi.org/10.1016/j.mam.2008.08.006.

[76] Deponte M. Glutathione catalysis and the reaction mechanisms of glutathione-dependent enzymes. Biochim Biophys Acta - Gen Subj 2013;1830:3217–66. https://doi.org/10.1016/j.bbagen.2012.09.018.

[77] Cheng S-B, Liu H-T, Chen S-Y, Lin P-T, Lai C-Y, Huang Y-C. Changes of Oxidative Stress, Glutathione, and Its Dependent Antioxidant Enzyme Activities in Patients with Hepatocellular Carcinoma before and after Tumor Resection. PLoS One 2017;12:e0170016. https://doi.org/10.1371/journal.pone.0170016.

[78] Meyer AJ, Hell R. Glutathione homeostasis and redox-regulation by sulfhydryl groups. Photosynth Res 2005;86:435–57. https://doi.org/10.1007/s11120-005-8425-1.

[79] Morris D, Khurasany M, Nguyen T, Kim J, Guilford F, Mehta R, et al. Glutathione and infection. Biochim Biophys Acta - Gen Subj 2013;1830:3329–49. https://doi.org/10.1016/j.bbagen.2012.10.012.

[80] Checconi P, Limongi D, Baldelli S, Ciriolo MR, Nencioni L, Palamara AT. Role of glutathionylation in infection and inflammation. Nutrients 2019;11. https://doi.org/10.3390/nu11081952.

[81] Fraternale A, Brundu S, Magnani M. Glutathione and glutathione derivatives in immunotherapy. Biol Chem 2017;398:261–75. https://doi.org/10.1515/hsz-2016-0202.

[82] Short S, Merkel BJ, Caffrey R, McCoy KL. Defective antigen processing correlates with a low level of intracellular glutathione. Eur J Immunol 1996;26:3015–20. https://doi.org/10.1002/eji.1830261229.

[83] Frosch S, Bonifas U, Eck H-P, Bockstette M, Droege W, Rüde E, et al. The efficient bovine insulin presentation capacity of bone marrow-derived macrophages activated by granulocyte-macrophage colony-stimulating factor correlates with a high level of intracellular reducing thiols. Eur J Immunol 1993;23:1430–4. https://doi.org/10.1002/eji.1830230704.

[84] Peterson JD, Herzenberg LA, Vasquez K, Waltenbaugh C. Glutathione levels in antigen-presenting cells modulate Th1 versus Th2 response patterns. Proc Natl Acad Sci U S A 1998;95:3071–6. https://doi.org/10.1073/pnas.95.6.3071.

[85] Fraternale A, Crinelli R, Casabianca A, Paoletti MF, Orlandi C, Carloni E, et al. Molecules Altering the Intracellular Thiol Content Modulate NF-kB and STAT-1/IRF-1 Signalling Pathways and IL-12 p40 and IL-27 p28 Production in Murine Macrophages. PLoS One 2013;8. https://doi.org/10.1371/journal.pone.0057866.

[86] Staal FJT, Roederer M, Herzenberg LA, Herzenberg LA. Intracellular thiols regulate activation of nuclear factor κB and transcription of human immunodeficiency virus. Proc Natl Acad Sci U S A 1990;87:9943–7. https://doi.org/10.1073/pnas.87.24.9943.

[87] Cai J, Chen Y, Seth S, Furukawa S, Compans RW, Jones DP. Inhibition of influenza infection by glutathione. Free Radic Biol Med 2003;34:928–36. https://doi.org/10.1016/S0891-5849(03)00023-6.

[88] Sgarbanti R, Nencioni L, Amatore D, Coluccio P, Fraternale A, Sale P, et al. Redox regulation of the influenza hemagglutinin maturation process: A new cell-mediated strategy for anti-influenza therapy. Antioxidants Redox Signal 2011;15:593–606. https://doi.org/10.1089/ars.2010.3512.

[89] Ravindran MS, Bagchi P, Cunningham CN, Tsai B. Opportunistic intruders: how viruses orchestrate ER functions to infect cells. Nat Rev Microbiol 2016;14:407–20. https://doi.org/10.1038/nrmicro.2016.60.

[90] Ellgaard L, Sevier CS, Bulleid NJ. How Are Proteins Reduced in the Endoplasmic Reticulum? Trends Biochem Sci 2018;43:32–43. https://doi.org/10.1016/j.tibs.2017.10.006.

[91] Wang L, Wang X, Wang CC. Protein disulfide-isomerase, a folding catalyst and a redox-regulated chaperone. Free Radic Biol Med 2015;83:305–13. https://doi.org/10.1016/j.freeradbiomed.2015.02.007.

[92] Hiscott J, Kwon H, Génin P. Hostile takeovers: Viral appropriation of the NF-κB pathway. J Clin Invest 2001;107:143–51. https://doi.org/10.1172/JCI11918.

[93] Le Negrate G. Viral interference with innate immunity by preventing NF-κB activity. Cell Microbiol 2012;14:168–81. https://doi.org/10.1111/j.1462-5822.2011.01720.x.

[94] Newton AH, Cardani A, Braciale TJ. The host immune response in respiratory virus infection: balancing virus clearance and immunopathology. Semin Immunopathol 2016;38:471–82. https://doi.org/10.1007/s00281-016-0558-0.

[95] Bhagirath AY, Li Y, Somayajula D, Dadashi M, Badr S, Duan K. Cystic fibrosis lung environment and Pseudomonas aeruginosa infection. BMC Pulm Med 2016;16. https://doi.org/10.1186/s12890-016-0339-5.

[96] Stoltz DA, Meyerholz DK, Welsh MJ. Origins of Cystic Fibrosis Lung Disease. N Engl J Med 2015;372:351–62. https://doi.org/10.1056/nejmra1300109.

[97] Cantin AM, Bégin R. Glutathione and inflammatory disorders of the lung. Lung 1991;169:123–38. https://doi.org/10.1007/BF02714149.

[98] Linsdell P, Hanrahan JW. Glutathione permeability of CFTR. Am J Physiol - Cell Physiol 1998;275. https://doi.org/10.1152/ajpcell.1998.275.1.c323.

[99] Boucher RC. Airway surface dehydration in cystic fibrosis: Pathogenesis and therapy. Annu Rev Med 2007;58:157–70. https://doi.org/10.1146/annurev.med.58.071905.105316.

[100] Liu T, Zhang L, Joo D, Sun SC. NF-κB signaling in inflammation. Signal Transduct Target Ther 2017;2:1–9. https://doi.org/10.1038/sigtrans.2017.23.

[101] Heijerman H. Infection and inflammation in cystic fibrosis: A short review. J Cyst Fibros 2005;4:3–5. https://doi.org/10.1016/j.jcf.2005.05.005.

[102] Hornef MW, Wick MJ, Rhen M, Normark S. Bacterial strategies for overcoming host innate and adaptive immune responses. Nat Immunol 2002;3:1033–40. https://doi.org/10.1038/ni1102-1033.

[103] Price J V., Vance RE. The Macrophage Paradox. Immunity 2014;41:685–93. https://doi.org/10.1016/j.immuni.2014.10.015.

[104] Podinovskaia M, Lee W, Caldwell S, Russell DG. Infection of macrophages with Mycobacterium tuberculosis induces global modifications to phagosomal function. Cell Microbiol 2013;15:843–59. https://doi.org/10.1111/cmi.12092.

[105] Anderberg SJ, Newton GL, Fahey RC. Mycothiol biosynthesis and metabolism: Cellular levels of potential intermediates in the biosynthesis and degradation of mycothiol in Mycobacterium smegmatis. J Biol Chem 1998;273:30391–7. https://doi.org/10.1074/jbc.273.46.30391.

[106] Pollock HM, Dahlgren BJ, Incze K, Farkas J, Mihalyi V, Zukal E. Antibacterial effect of cysteine-nitrosothiol and possible precursors thereof. Appl Microbiol 1974;27:442.

[107] Venketaraman V, Dayaram YK, Talaue MT, Connell ND. Glutathione and nitrosoglutathione in macrophage defense against Mycobacterium tuberculosis. Infect Immun 2005;73:1886–9. https://doi.org/10.1128/IAI.73.3.1886-1889.2005.

[108] Cacciatore I, Cornacchia C, Pinnen F, Mollica A, Di Stefano A. Prodrug approach for increasing cellular glutathione levels. Molecules 2010;15:1242–64. https://doi.org/10.3390/molecules15031242.

[109] Wendel A, Cikryt P. The level and half-life of glutathione in human plasma. FEBS Lett 1980;120:209–11. https://doi.org/10.1016/0014-5793(80)80299-7.

[110] Anderson ME, Powrie F, Puri RN, Meister A. Glutathione monoethyl ester: Preparation, uptake by tissues, and conversion to glutathione. Arch Biochem Biophys 1985;239:538–48. https://doi.org/10.1016/0003-9861(85)90723-4.

[111] De Vries N, De Flora S. N-acetyl-l-cysteine. J Cell Biochem 1993;53:270–7. https://doi.org/10.1002/jcb.240531040.

[112] Révész L, Modig H. Cysteamine-induced increase of cellular glutathione-level: A new hypothesis of the radioprotective mechanism [41]. Nature 1965;207:430–1. https://doi.org/10.1038/207430a0.

[113] Waring WS. Novel acetylcysteine regimens for treatment of paracetamol overdose. Ther Adv Drug Saf 2012;3:305–15. https://doi.org/10.1177/2042098612464265.

[114] Jargin S. On the use of acetylcysteine as a mucolytic drug. J Investig Biochem 2016;5:52. https://doi.org/10.5455/jib.20160929024258.

[115] Aldini G, Altomare A, Baron G, Vistoli G, Carini M, Borsani L, et al. N-Acetylcysteine as an antioxidant and disulphide breaking agent: the reasons why. Free Radic Res 2018;52:751–62. https://doi.org/10.1080/10715762.2018.1468564.

[116] Dodd S, Dean O, Copolov DL, Malhi GS, Berk M. N-acetylcysteine for antioxidant therapy: Pharmacology and clinical utility. Expert Opin Biol Ther 2008;8:1955–62. https://doi.org/10.1517/14728220802517901.

[117] Bavarsad Shahripour R, Harrigan MR, Alexandrov A V. N-acetylcysteine (NAC) in neurological disorders: Mechanisms of action and therapeutic opportunities. Brain Behav 2014;4:108–22. https://doi.org/10.1002/brb3.208.

[118] McClure EA, Gipson CD, Malcolm RJ, Kalivas PW, Gray KM. Potential role of N-acetylcysteine in the management of substance use disorders. CNS Drugs 2014;28:95–106. https://doi.org/10.1007/s40263-014-0142-x.

[119] Moreira PI, Harris PLR, Zhu X, Santos MS, Oliveira CR, Smith MA, et al. Lipoic acid and N-acetyl cysteine decrease mitochondrial-related oxidative stress in Alzheimer disease patient fibroblasts. J Alzheimer's Dis 2007;12:195–206. https://doi.org/10.3233/JAD-2007-12210.

[120] Blesa S, Cortijo J, Martinez-Losa M, Mata M, Seda E, Santangelo F, et al. Effectiveness of oral N-acetylcysteine in a rat experimental model of asthma. Pharmacol Res 2002;45:135–40. https://doi.org/10.1006/phrs.2001.0917.

[121] Ghezzi P, Ungheri D. Synergistic combination of n-acetylcysteine and ribavirin to protect from lethal influenza viral infection in a mouse model. Int J Immunopathol Pharmacol 2004;17:99–102. https://doi.org/10.1177/039463200401700114.

[122] Dinicola S, De Grazia S, Carlomagno G, Pintucci JP. N-acetylcysteine as powerful molecule to destroy bacterial biofilms. A systematic review. Eur Rev Med Pharmacol Sci 2014;18:2942–8.

[123] Levtchenko EN, de Graaf-Hess A, Wilmer M, van den Heuvel L, Monnens L, Blom H. Altered status of glutathione and its metabolites in cystinotic cells. Nephrol Dial Transplant 2005;20:1828–32. https://doi.org/10.1093/ndt/gfh932.

[124] Wilmer MJ, Kluijtmans LAJ, van der Velden TJ, Willems PH, Scheffer PG, Masereeuw R, et al. Cysteamine restores glutathione redox status in cultured cystinotic proximal tubular epithelial cells. Biochim Biophys Acta - Mol Basis Dis 2011;1812:643–51. https://doi.org/10.1016/j.bbadis.2011.02.010.

[125] Min-Oo G, Fortin A, Poulin JF, Gros P. Cysteamine, the molecule used to treat cystinosis, potentiates the antimalarial efficacy of artemisinin. Antimicrob Agents Chemother 2010;54:3262–70.

https://doi.org/10.1128/AAC.01719-09.

[126] Crinelli R, Zara C, Smietana M, Retini M, Magnani M, Fraternale A. Boosting GSH using the Co-drug approach: I-152, a conjugate of N-acetyl-cysteine and β-mercaptoethylamine. Nutrients 2019;11. https://doi.org/10.3390/nu11061291.

[127] Oiry J, Mialocq P, Puy JY, Fretier P, Clayette P, Dormont D, et al. NAC/MEA conjugate: A new potent antioxidant which increases the GSH level in various cell lines. Bioorganic Med Chem Lett 2001;11:1189–91. https://doi.org/10.1016/S0960-894X(01)00171-8.

[128] Fraternale A, Paoletti MF, Dominici S, Caputo A, Castaldello A, Millo E, et al. The increase in intra-macrophage thiols induced by new pro-GSH molecules directs the Th1 skewing in ovalbumin immunized mice. Vaccine 2010;28:7676–82. https://doi.org/10.1016/j.vaccine.2010.09.033.

[129] Fraternale A, Paoletti MF, Dominici S, Buondelmonte C, Caputo A, Castaldello A, et al. Modulation of Th1/Th2 immune responses to HIV-1 Tat by new pro-GSH molecules. Vaccine 2011;29:6823–9. https://doi.org/10.1016/j.vaccine.2011.07.101.

[130] Brundu S, Palma L, Picceri GG, Ligi D, Orlandi C, Galluzzi L, et al. Glutathione Depletion Is Linked with Th2 Polarization in Mice with a Retrovirus-Induced Immunodeficiency Syndrome, Murine AIDS: Role of Proglutathione Molecules as Immunotherapeutics. J Virol 2016;90:7118–30. https://doi.org/10.1128/jvi.00603-16.

[131] Hartley JW, Fredrickson TN, Yetter RA, Makino M, Morse HC. Retrovirus-induced murine acquired immunodeficiency syndrome: natural history of infection and differing susceptibility of inbred mouse strains. J Virol 1989;63.

[132] Klinken SP, Fredrickson TN, Hartley JW, Yetter RA, Morse HC. Evolution of B cell lineage lymphomas in mice with a retrovirus-induced immunodeficiency syndrome, MAIDS. J Immunol 1988;140.

[133] Mosier DE. Animal models for retrovirus-induced immunodeficiency disease. Immunol Invest 1986;15:233–61. https://doi.org/10.3109/08820138609026687.

[134] Mosier DE, Yetter RA, Morse HC. Retroviral induction of acute lymphoproliferative disease and profound immunosuppression in adult C57BL/6 mice. J Exp Med 1985;161:766–84. https://doi.org/10.1084/jem.161.4.766.

[135] Elborn JS. Cystic fibrosis. Lancet 2016;388:2519–31. https://doi.org/10.1016/S0140-6736(16)00576-6.

[136] Yoshimura K, Nakamura H, Trapnell BC, Chu C shyan, Dakemans W, Pavirani A, et al. Expression of the cystic fibrosis transmembrane conductance regulator gene in cells of non-epithelial origin. Nucleic Acids Res 1991;19:5417–23. https://doi.org/10.1093/nar/19.19.5417.

[137] Goss CH, Quittner AL. Patient-reported outcomes in cystic fibrosis. Proc. Am. Thorac. Soc., vol. 4, American Thoracic Society; 2007, p. 378–86. https://doi.org/10.1513/pats.200703-039BR.

[138] Bell SC, De Boeck K, Amaral MD. New pharmacological approaches for cystic fibrosis: Promises, progress, pitfalls. Pharmacol Ther 2015;145:19–34. https://doi.org/10.1016/j.pharmthera.2014.06.005.

[139] Lubamba B, Dhooghe B, Noel S, Leal T. Cystic fibrosis: Insight into CFTR pathophysiology and pharmacotherapy. Clin Biochem 2012;45:1132–44. https://doi.org/10.1016/j.clinbiochem.2012.05.034.

[140] Bobadilla JL, Macek M, Fine JP, Farrell PM. Cystic fibrosis: A worldwide analysis of CFTR mutations - Correlation with incidence data and application to screening. Hum Mutat 2002;19:575–606. https://doi.org/10.1002/humu.10041.

[141] Mall MA. Role of the amiloride-sensitive epithelial Na+ channel in the pathogenesis and as a

therapeutic target for cystic fibrosis lung disease: Experimental Physiology - Symposium Report. Exp. Physiol., vol. 94, Blackwell Publishing Ltd; 2009, p. 171–4. https://doi.org/10.1113/expphysiol.2008.042994.

[142] Donaldson SH, Boucher RC. Sodium channels and cystic fibrosis. Chest 2007;132:1631–6. https://doi.org/10.1378/chest.07-0288.

[143] Gustafsson JK, Ermund A, Ambort D, Johansson MEV, Nilsson HE, Thorell K, et al. Bicarbonate and functional CFTR channel are required for proper mucin secretion and link cystic fibrosis with its mucus phenotype. J Exp Med 2012;209:1263–72. https://doi.org/10.1084/jem.20120562.

[144] Pezzulo AA, Tang XX, Hoegger MJ, Abou Alaiwa MH, Ramachandran S, Moninger TO, et al. Reduced airway surface pH impairs bacterial killing in the porcine cystic fibrosis lung. Nature 2012;487:109–13. https://doi.org/10.1038/nature11130.

[145] Hartl D, Gaggar A, Bruscia E, Hector A, Marcos V, Jung A, et al. Innate immunity in cystic fibrosis lung disease. J Cyst Fibros 2012;11:363–82. https://doi.org/10.1016/j.jcf.2012.07.003.

[146] Nichols DP, Chmiel JF. Inflammation and its genesis in cystic fibrosis. Pediatr Pulmonol 2015;50:S39–56. https://doi.org/10.1002/ppul.23242.

[147] Lacy P. Mechanisms of Degranulation in Neutrophils. Allergy, Asthma Clin Immunol 2006;2:98. https://doi.org/10.1186/1710-1492-2-3-98.

[148] Sly PD, Gangell CL, Chen L, Ware RS, Ranganathan S, Mott LS, et al. Risk Factors for Bronchiectasis in Children with Cystic Fibrosis. N Engl J Med 2013;368:1963–70. https://doi.org/10.1056/nejmoa1301725.

[149] Brinkmann V, Reichard U, Goosmann C, Fauler B, Uhlemann Y, Weiss DS, et al. Neutrophil Extracellular Traps Kill Bacteria. Science (80-) 2004;303:1532–5. https://doi.org/10.1126/science.1092385.

[150] Gray RD, Hardisty G, Regan KH, Smith M, Robb CT, Duffin R, et al. Delayed neutrophil apoptosis enhances NET formation in cystic fibrosis. Thorax 2018;73:134–44. https://doi.org/10.1136/thoraxjnl-2017-210134.

[151] Painter RG, Bonvillain RW, Valentine VG, Lombard GA, LaPlace SG, Nauseef WM, et al. The role of chloride anion and CFTR in killing of Pseudomonas aeruginosa by normal and CF neutrophils. J Leukoc Biol 2008;83:1345–53. https://doi.org/10.1189/jlb.0907658.

[152] Bruscia EM, Bonfield TL. Innate and Adaptive Immunity in Cystic Fibrosis. Clin Chest Med 2016;37:17–29. https://doi.org/10.1016/j.ccm.2015.11.010.

[153] Roesch EA, Nichols DP, Chmiel JF. Inflammation in cystic fibrosis: An update. Pediatr Pulmonol 2018;53:S30–50. https://doi.org/10.1002/ppul.24129.

[154] Pandey S, Kawai T, Akira S. Microbial sensing by toll-like receptors and intracellular nucleic acid sensors. Cold Spring Harb Perspect Biol 2015;7. https://doi.org/10.1101/cshperspect.a016246.

[155] Amarante-Mendes GP, Adjemian S, Branco LM, Zanetti LC, Weinlich R, Bortoluci KR. Pattern recognition receptors and the host cell death molecular machinery. Front Immunol 2018;9:2379. https://doi.org/10.3389/fimmu.2018.02379.

[156] Dinarello CA. Overview of the IL-1 family in innate inflammation and acquired immunity. Immunol Rev 2018;281:8–27. https://doi.org/10.1111/imr.12621.

[157] Kaneko N, Kurata M, Yamamoto T, Morikawa S, Masumoto J. The role of interleukin-1 in general pathology. Inflamm Regen 2019;39:1–16. https://doi.org/10.1186/s41232-019-0101-5.

[158] Fraternale A, Brundu S, Magnani M. Polarization and Repolarization of Macrophages 2015. https://doi.org/10.4172/2155-9899.1000319.

[159] Tarique AA, Sly PD, Holt PG, Bosco A, Ware RS, Logan J, et al. CFTR-dependent defect in alternatively-activated macrophages in cystic fibrosis. J Cyst Fibros 2017;16:475–82. https://doi.org/10.1016/j.jcf.2017.03.011.

[160] Hussell T, Bell TJ. Alveolar macrophages: Plasticity in a tissue-specific context. Nat Rev Immunol 2014;14:81–93. https://doi.org/10.1038/nri3600.

[161] Bonfield TL, Hodges CA, Cotton CU, Drumm ML. Absence of the cystic fibrosis transmembrane regulator (Cftr) from myeloid-derived cells slows resolution of inflammation and infection . J Leukoc Biol 2012;92:1111–22. https://doi.org/10.1189/jlb.0412188.

[162] Bruscia EM, Zhang PX, Ferreira E, Caputo C, Emerson JW, Tuck D, et al. Macrophages directly contribute to the exaggerated inflammatory response in cystic fibrosis transmembrane conductance regulator-/-mice. Am J Respir Cell Mol Biol 2009;40:295–304. https://doi.org/10.1165/rcmb.2008-0170OC.

[163] Bruscia EM, Zhang P-X, Satoh A, Caputo C, Medzhitov R, Shenoy A, et al. Abnormal Trafficking and Degradation of TLR4 Underlie the Elevated Inflammatory Response in Cystic Fibrosis. J Immunol 2011;186:6990–8. https://doi.org/10.4049/jimmunol.1100396.

[164] Croasdell A, Duffney PF, Kim N, Lacy SH, Sime PJ, Phipps RP. PPAR γ and the Innate Immune System Mediate the Resolution of Inflammation. PPAR Res 2015;2015. https://doi.org/10.1155/2015/549691.

[165] Abdulrahman BA, Khweek AA, Akhter A, Caution K, Kotrange S, Abdelaziz DHA, et al. Autophagy stimulation by rapamycin suppresses lung inflammation and infection by Burkholderia cenocepacia in a model of cystic fibrosis. Autophagy 2011;7:1359–70. https://doi.org/10.4161/auto.7.11.17660.

[166] Cantin AM, Hartl D, Konstan MW, Chmiel JF. Inflammation in cystic fibrosis lung disease: Pathogenesis and therapy. J Cyst Fibros 2015;14:419–30. https://doi.org/10.1016/j.jcf.2015.03.003.

[167] Cowley EA, Linsdell P. Characterizatin of basolateral K+ channels underlying anion secretion in the human airway cell line Calu-3. J Physiol 2002;538:747–57. https://doi.org/10.1113/jphysiol.2001.013300.

[168] Takeyama K, Dabbagh K, Jeong Shim J, Dao-Pick T, Ueki IF, Nadel JA. Oxidative Stress Causes Mucin Synthesis Via Transactivation of Epidermal Growth Factor Receptor: Role of Neutrophils. J Immunol 2000;164:1546–52. https://doi.org/10.4049/jimmunol.164.3.1546.

[169] Roum JH, Buhl R, McElvaney NG, Borok Z, Crystal RG. Systemic deficiency of glutathione in cystic fibrosis. J Appl Physiol 1993;75:2419–24. https://doi.org/10.1152/jappl.1993.75.6.2419.

[170] van der Vliet A, Janssen-Heininger YMW, Anathy V. Oxidative stress in chronic lung disease: From mitochondrial dysfunction to dysregulated redox signaling. Mol Aspects Med 2018;63:59–69. https://doi.org/10.1016/j.mam.2018.08.001.

[171] Gao L, Kim KJ, Yankaskas JR, Forman HJ. Abnormal glutathione transport in cystic fibrosis airway epithelia. Am J Physiol - Lung Cell Mol Physiol 1999;277. https://doi.org/10.1152/ajplung.1999.277.1.l113.

[172] Winterbourn CC. Revisiting the reactions of superoxide with glutathione and other thiols. Arch Biochem Biophys 2016;595:68–71. https://doi.org/10.1016/j.abb.2015.11.028.

[173] Kettle AJ, Turner R, Gangell CL, Harwood DT, Khalilova IS, Chapman AL, et al. Oxidation contributes to low glutathione in the airways of children with cystic fibrosis. Eur Respir J 2014;44:122–9. https://doi.org/10.1183/09031936.00170213.

[174] Witschi A, Reddy S, Stofer B, Lauterburg BH. The systemic availability of oral glutathione. Eur J Clin Pharmacol 1992;43:667–9. https://doi.org/10.1007/BF02284971.

[175] Lands LC, Grey VL, Smountas AA. Effect of supplementation with a cysteine donor on muscular

performance. J Appl Physiol 1999;87:1381–5. https://doi.org/10.1152/jappl.1999.87.4.1381.

[176] Busse E, Zimmer G, Schopohl B, Kornhuber B. Influence of α-lipoic acid on intracellular glutathione in vitro and in vivo. Arzneimittel-Forschung/Drug Res 1992;42:829–31.

[177] Micke P, Beeh KM, Schlaak JF, Buhl R. Oral supplementation with whey proteins increases plasma glutathione levels of HIV-infected patients. Eur J Clin Invest 2001;31:171–8. https://doi.org/10.1046/j.1365-2362.2001.00781.x.

[178] Griese M, Ramakers J, Krasselt A, Starosta V, Van Koningsbruggen S, Fischer R, et al. Improvement of alveolar glutathione and lung function but not oxidative state in cystic fibrosis. Am J Respir Crit Care Med 2004;169:822–8. https://doi.org/10.1164/rccm.200308-1104oc.

[179] Visca A, Bishop CT, Hilton SC, Hudson VM. Case Study Improvement in clinical markers in CF patients using a reduced glutathione regimen: An uncontrolled, observational study 2008. https://doi.org/10.1016/j.jcf.2008.03.006.

[180] Grey V, Mohammed SR, Smountas AA, Bahlool R, Lands LC. Improved glutathione status in young adult patients with cystic fibrosis supplemented with whey protein. J Cyst Fibros 2003;2:195–8. https://doi.org/10.1016/S1569-1993(03)00097-3.

[181] Marrades RM, Roca J, Barberà JA, De Jover L, Macnee W, Rodriguez-Roisin R. Nebulized glutathione induces bronchoconstriction in patients with mild asthma. Am J Respir Crit Care Med 1997;156:425–30. https://doi.org/10.1164/ajrccm.156.2.9611001.

[182] Buhl R, Vogelmeier C, Critendent M, Hubbard RC, Hoyt RF, Wilson EM, et al. Augmentation of glutathione in the fluid lining the epithelium of the lower respiratory tract by directly administering glutathione aerosol (lung/antioxidant/therapy/bronchoalveolar lavage). vol. 87. 1990.

[183] Jonas CR, Gu LH, Nkabyo YS, Mannery YO, Avissar NE, Sax HC, et al. Glutamine and KGF each regulate extracellular thiol/disulfide redox and enhance proliferation in Caco-2 cells. Am J Physiol Integr Comp Physiol 2003;285:R1421–9. https://doi.org/10.1152/ajpregu.00702.2002.

[184] Duijvestijn Y, Brand P. Systematic review of N-acetylcysteine in cystic fibrosis. Acta Paediatr 2007;88:38–41. https://doi.org/10.1111/j.1651-2227.1999.tb01265.x.

[185] Cantin AM. Potential for antioxidant therapy of cystic fibrosis. Curr Opin Pulm Med 2004;10:531–6. https://doi.org/10.1097/01.mcp.0000138997.29276.a1.

[186] Tirouvanziam R, Conrad CK, Bottiglieri T, Herzenberg LA, Moss RB, Herzenberg LA. High-dose oral N-acetylcysteine, a glutathione prodrug, modulates inflammation in cystic fibrosis. Proc Natl Acad Sci U S A 2006;103:4628–33. https://doi.org/10.1073/pnas.0511304103.

[187] Conrad C, Lymp J, Thompson V, Dunn C, Davies Z, Chatfield B, et al. Long-term treatment with oral N-acetylcysteine: Affects lung function but not sputum inflammation in cystic fibrosis subjects. A phase II randomized placebo-controlled trial. J Cyst Fibros 2015;14:219–27. https://doi.org/10.1016/j.jcf.2014.08.008.

[188] Varelogianni G, Oliynyk I, Roomans GM, Johannesson M. The effect of N -acetylcysteine on chloride efflux from airway epithelial cells . Cell Biol Int 2010;34:245–52. https://doi.org/10.1042/cbi20090007.

[189] Chen J, Kinter M, Shank S, Cotton C, Kelley TJ, Ziady AG. Dysfunction of Nrf-2 in CF Epithelia Leads to Excess Intracellular H2O2 and Inflammatory Cytokine Production. PLoS One 2008;3:e3367. https://doi.org/10.1371/journal.pone.0003367.

[190] Devereux G, Steele S, Griffiths K, Devlin E, Fraser-Pitt D, Cotton S, et al. An Open-Label Investigation of the Pharmacokinetics and Tolerability of Oral Cysteamine in Adults with Cystic Fibrosis. Clin Drug Investig 2016;36:605–12. https://doi.org/10.1007/s40261-016-0405-z.

[191] De Stefano D, Maiuri MC. A Breathe in Cystic Fibrosis Therapy: A New Therapeutic Endeavor for

Cysteamine. EBioMedicine 2015;2:1306–7. https://doi.org/10.1016/j.ebiom.2015.09.038.

[192] Charrier C, Rodger C, Robertson J, Kowalczuk A, Shand N, Fraser-Pitt D, et al. Cysteamine (Lynovex®), a novel mucoactive antimicrobial & antibiofilm agent for the treatment of cystic fibrosis. Orphanet J Rare Dis 2014;9:189. https://doi.org/10.1186/s13023-014-0189-2.

[193] Ferrari E, Monzani R, Villella VR, Esposito S, Saluzzo F, Rossin F, et al. Cysteamine re-establishes the clearance of Pseudomonas aeruginosa by macrophages bearing the cystic fibrosis-relevant F508del-CFTR mutation. Cell Death Dis 2017;8:e2544. https://doi.org/10.1038/cddis.2016.476.

[194] Brundu S, Nencioni L, Celestino I, Coluccio P, Palamara AT, Magnani M, et al. Validation of a reversed-phase high performance liquid chromatography method for the simultaneous analysis of cysteine and reduced glutathione in mouse organs. Oxid Med Cell Longev 2016;2016. https://doi.org/10.1155/2016/1746985.

[195] Dorrington MG, Fraser IDC. NF-κB signaling in macrophages: Dynamics, crosstalk, and signal integration. Front Immunol 2019;10. https://doi.org/10.3389/fimmu.2019.00705.

[196] Kabe Y, Ando K, Hirao S, Yoshida M, Handa H. Redox regulation of NF-κB activation: Distinct redox regulation between the cytoplasm and the nucleus. Antioxidants Redox Signal 2005;7:395–403. https://doi.org/10.1089/ars.2005.7.395.

[197] Christian F, Smith E, Carmody R. The Regulation of NF-κB Subunits by Phosphorylation. Cells 2016;5:12. https://doi.org/10.3390/cells5010012.

[198] Lei Y, Wang K, Deng L, Chen Y, Nice EC, Huang C. Redox regulation of inflammation: Old elements, a new story. Med Res Rev 2015;35:306–40. https://doi.org/10.1002/med.21330.

[199] Tucureanu MM, Rebleanu D, Constantinescu CA, Deleanu M, Voicu G, Butoi E, et al. Lipopolysaccharide-induced inflammation in monocytes/macrophages is blocked by liposomal delivery of Gi-protein inhibitor. Int J Nanomedicine 2018;13:63–76. https://doi.org/10.2147/IJN.S150918.

[200] Droge W, Breitkreutz R. Glutathione and immune function. Proc Nutr Soc 2000;59:595–600. https://doi.org/10.1017/S0029665100000847.

[201] Limongi D, Baldelli S, Checconi P, Marcocci M, De Chiara G, Fraternale A, et al. GSH-C4 acts as anti-inflammatory drug in different models of canonical and cell autonomous inflammation through NFκB inhibition. Front Immunol 2019;10:155. https://doi.org/10.3389/fimmu.2019.00155.

[202] Turell L, Zeida A, Trujillo M. Mechanisms and consequences of protein cysteine oxidation: the role of the initial short-lived intermediates. Essays Biochem 2020;64:55–66. https://doi.org/10.1042/ebc20190053.

[203] Lawrence T. The nuclear factor NF-kappaB pathway in inflammation. Cold Spring Harb Perspect Biol 2009;1. https://doi.org/10.1101/cshperspect.a001651.

[204] Hoesel B, Schmid JA. The complexity of NF-κB signaling in inflammation and cancer. Mol Cancer 2013;12. https://doi.org/10.1186/1476-4598-12-86.

[205] Iyer SS, Cheng G. Role of interleukin 10 transcriptional regulation in inflammation and autoimmune disease. Crit Rev Immunol 2012;32:23–63. https://doi.org/10.1615/critrevimmunol.v32.i1.30.

[206] Cheluvappa R, Shimmon R, Dawson M, Hilmer SN, Le Couteur DG. Reactions of Pseudomonas aeruginosa pyocyanin with reduced glutathione. Acta Biochim Pol 2008;55:571–80. https://doi.org/10.18388/abp.2008_3063.

[207] Xiao W, Loscalzo J. Metabolic Responses to Reductive Stress. Antioxidants Redox Signal 2020;32:1330–47. https://doi.org/10.1089/ars.2019.7803.

[208] Lee JI, Kang J, Stipanuk MH. Differential regulation of glutamate-cysteine ligase subunit expression and increased holoenzyme formation in response to cysteine deprivation. Biochem J 2006;393:181–

90. https://doi.org/10.1042/BJ20051111.

[209] Chen Y, Shertzer HG, Schneider SN, Nebert DW, Dalton TP. Glutamate cysteine ligase catalysis: Dependence on ATP and modifier subunit for regulation of tissue glutathione levels. J Biol Chem 2005;280:33766–74. https://doi.org/10.1074/jbc.M504604200.

[210] Calkins MJ, Townsend JA, Johnson DA, Johnson JA. Cystamine protects from 3-nitropropionic acid lesioning via induction of nf-e2 related factor 2 mediated transcription. Exp Neurol 2010;224:307–17. https://doi.org/10.1016/j.expneurol.2010.04.008.

[211] Liu Y, Liu K, Wang N, Zhang H. N-acetylcysteine induces apoptosis via the mitochondria-dependent pathway but not via endoplasmic reticulum stress in H9c2 cells. Mol Med Rep 2017;16:6626–33. https://doi.org/10.3892/mmr.2017.7442.

ACKNOWLEDGEMENTS

First of all, I would like to express my sincere gratitude to my advisor Dr. Alessandra Fraternale for the continuous support during these years, and for transmitting me her knowledge and enthusiasm for research.

I would also like to thank Dr. Rita Crinelli for her important help and scientific support.

I also wish to express my gratitude to Professor Mauro Magnani and to all the people that I had the opportunity to work with at the University of Urbino.

Many thanks to Professor Emanuela Bruscia and Dr. Caterina Di Pietro from Yale University for helping, encouraging, and supporting me during my abroad experience.